FINAL REPORT

PROJECT A-858

INVESTIGATION TO IMPROVE VACUUM EVAPORATED THIN FILM RESISTORS

R. B. BEISER AND M. D. CARITHERS

Contract No. NAS8-20072

14 April 1965 to 13 December 1966

Prepared for
National Aeronautics and Space Administration
George C. Marshall Space Flight Center
Huntsville, Alabama

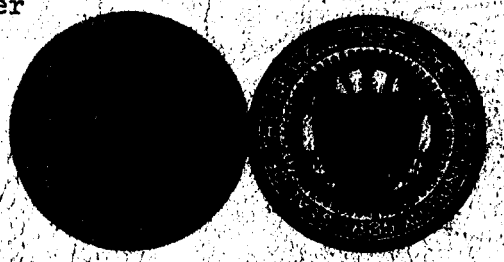

Engineering Experiment Station
GEORGIA INSTITUTE OF TECHNOLOGY
Atlanta, Georgia

GEORGIA INSTITUTE OF TECHNOLOGY
Engineering Experiment Station
Atlanta, Georgia

FINAL REPORT

PROJECT A-858

INVESTIGATION TO IMPROVE VACUUM EVAPORATED THIN FILM RESISTORS

By

R. B. BELSER AND M. D. CARITHERS

CONTRACT NO. NAS8-20072

14 APRIL 1965 to 13 DECEMBER 1966

Prepared for
NATIONAL AERONAUTICS AND SPACE ADMINISTRATION
GEORGE C. MARSHALL SPACE FLIGHT CENTER
HUNTSVILLE, ALABAMA

TABLE OF CONTENTS

TABLE OF CONTENTS (Continued)

LIST OF FIGURES

LIST OF FIGURES (Continued)

LIST OF FIGURES (Concluded)

LIST OF TABLES

ABSTRACT

The purpose of this research was to develop a stable thin film resistor material of high resistivity and low TCR, reproducibly depositable by vacuum evaporation methods. Films of the classes metal, metal-metal oxide, metal-silicon monoxide, metal nitrides, silicides, and borides have been prepared and examined for electrical and structural properties. Materials included have been Gd, Ti, Tm, V, and Zr; Al + SiO, Cr + SiO, Cu + SiO, and Mn + SiO; Ta_2O_5, TiO, TiO_2, V_2O_5, and ZrO_2; NbN and TiN; $CrSi_2$ and $TiSi_2$; B_4Si, NbB_2, Ni_2B, and TiB_2; and mixtures of $CrSi_2$ with $TiSi_2$ and with B_4Si. Some 758 films of the various materials were eximined with resistivities and TCR values respectively in the range 100 to 10^7 microhm-cm and 2200 x 10^{-6}/°C to -6000 x 10^{-6}/°C. Plots of TCR versus resistivity for the respective materials generally gave a straight line of steep slope through the region near zero TCR; and for most materials either resistivity or TCR values could be approximated from a known value of the other. Chromium + silicon monoxide proved to be the most desirable material examined from the standpoint of high resistivity (10,000 microhm-cm), low TCR (± 200 ppm/°C), and stability at 125°C (aging < 1% in 1000 hrs). Zirconium-zirconium oxide yielded about 2500 microhm-cm with low TCR but poorer aging qualities. $CrSi_2$ and ($CrSi_2$ + $TiSi_2$) yielded resistivities of about 1600 and 3600 microhm-cm, respectively, with low TCR (-440 ppm/°C) and good stability.

The principal fault with Cr + SiO is the difficulty in control of its co-evaporation with single or dual source arrangements. The greatest reproducibility was obtained with a dual source arrangement by manually controlling the current of each source. Satisfactory reproducibility can be expected with instrumented servo control of source temperatures and vapor outputs. With the dual source, a diaphragm was used to an advantage on one of the sources to decrease the dispersion of film resistivity to ± 10% over a 2" x 2" substrate area. Uniformity of substrate heating appeared as an additional variable affecting uniformity of film resistivity over large glass surfaces and suggests that suitable substrates of high heat conductivity may be used to an advantage to decrease variation in resistivity. The importance of the $CrSi_2$ is that it exhibits excellent stability and can be evaporated from a single source to produce films of greater resistivity than some currently used metal films. The resistivity of the zirconium-zirconium oxide combination and the stabilizing influence of SiO suggests that Zr + SiO would be a fruitful material to examine.

I. INTRODUCTION

The purpose of the research under Contract No. NAS8-20072 was to develop a resistor material of high resistance per square, low temperature coefficient of resistance, and high stability with respect to time and temperature. The desired material would be easily and reproducibly deposited by vacuum evaporation methods.

The use of thin films for forming passive elements in hybrid microelectronic circuits has lead to high reliability and greater flexibility in circuit design. Thin film resistive elements, for instance, provide a range of resistor values which exceeds that which can be achieved readily by doping of the semiconductor material used in integrated circuitry. In addition, the inter-element capacitance can be less in deposited circuitry than that in integrated circuitry where reverse-biased junctions provide the isolation between elements.

In the application of thin film resistive materials, one is most often confronted with problems in fabrication methods and in the reproducibility of these methods. Much of the difficulty can be attributed to minute details in the techniques which are not usually given proper attention. A rather complete description of the fabrication methods and procedures used during the contract is included as a major section of this report.

The exploration of materials for thin film resistive elements necessarily involved the examination of many metals, metal oxides and cermets. The selection of the deposition parameters for each material and the evaluation of the resultant films constituted the major part of the contract effort.

During the first three months of the contract a large number of films of titanium and zirconium deposited at various pressures of residual oxygen and at various evaporation rates were examined. These preliminary investigations which were conducted concurrently with the development of fabrication techniques indicated the feasibility of obtaining high resistance per square and low temperature coefficient of resistance. The evaporation of titanium in oxygen at a pressure of 10^{-3} torr and at a rate of 2 angstroms per second produced a value of 1655 ohms/square. Zirconium films deposited in a residual gas pressure of 2×10^{-6} Torr gave a high R/sq. of 905 ohms per square and a change in resistance of $< 1\%$ after heating to 125°C in air for about 30 minutes. A resistivity of 2400 microhm-cm was obtained for a zirconium - zirconium oxide film having a TCR < 100 ppm/°C.

In the next quarter the properties of films formed by the co-deposition of chromium and silicon monoxide from a common source were examined along with studies on vanadium and zirconium. The chromium-silicon monoxide system appeared to be quite promising as a high resistivity material of low TCR and high stability so that more emphasis was placed on this combination than on some of the other materials. Resistivities of the Cr + SiO films ranged from 1000 to 10,000 microhm-cm with TCR values of $\pm$ 1 x $10^{-4}/^{\circ}C$. It was difficult to control the evaporation of the two materials from the common source used because of their differing vapor pressures. One neighboring element in the periodic table to chromium, that is, manganese, was selected for a study of its co-deposition with silicon monoxide from a common source because it appeared the resultant films might have similar properties to the Cr + SiO mixtures; and, since the vapor pressures of Mn and SiO are reported to be approximately the same, easier control of the process might be accomplished. The latter hypotheses was not borne out in the experiments due to the fact that the manganese vaporized at a much higher rate than did the SiO. Electrical properties of the two species were similar but the Cr + SiO films displayed higher resistivity at a given TCR value and exhibited superior aging. Other materials were co-deposited with SiO and examined subsequently.

During the third quarter some film specimens of titanium nitride and niobium nitride were examined. The titanium nitride films exhibited resistivities too low to meet the desired specifications and both materials were difficult to evaporate from refractory metal boats; the niobium nitride required the use of electron beam bombardment techniques. Other materials studied during this quarter included Al + SiO, Cu + SiO, Sn + SiO, and Mn + SiO. Aging studies of the films were begun to determine the stability of the resistance at 125° C for unprotected and SiO-protected films.

During the next quarter the aging studies were continued along with the fabrication of additional Cr + SiO and Mn + SiO films. In general, the aging of SiO-protected resistors is far less than that of unprotected resistors. Post-deposition baking techniques were initiated.

The final periods were devoted to extensive aging studies of the most promising films, exploratory studies on other materials, notably borides and silicides, and the examination of films by electron and x-ray diffraction, electron microscopy and other analytical techniques.

The sections which follow give a detailed description of the film fabrication and measurements procedures (Section II-A) and the results

obtained on the various materials studies (Section II-B). Particular emphasis is placed on the chromium-silicon monoxide films and the boride and silicide films. Further discussion of these results is included in Section III and a summary of the main results and suggestions for future studies are included in Section IV. The appendix consists of tables which contain detailed data on most of the films studied and summary data on certain parameters.

II. EXPERIMENTAL WORK

A. FILM FABRICATION AND MEASUREMENTS

1. Vacuum Deposition Procedures and Apparatus

Of the several possible methods for fabricating thin film resistors, the one used in this study was deposition by evaporation in high vacuum as specified in the contract. A detailed description of the various evaporation apparatus and the procedures used is included in this section. Such detail is considered necessary since differences in fabrication methods not adequately described in the published literature make it difficult to compare or duplicate results obtained in separate laboratories on similar type films. The other reason for extensive detail is that procedures are then well documented for future use.

A total of seven hundred fifty-eight film specimens were fabricated for the various studies. An additional representative number of comparative film specimens were prepared on electron microscope grids for analytical studies. The films fall into seven major classes of materials as follows: pure metals, metal-silicon monoxide cermets, metal-metal oxide as a result of evaporating pure metals in partial pressures of oxygen, metal-metal oxides as a result of evaporating metal oxide compounds, metal-metal nitrides from the evaporation of metal nitride compounds, silicides, and borides. The metal-silicon monoxide systems studies were Al-SiO, Cr-SiO, Cu-SiO, and Mn-SiO. The metals Gd, Ti, Tm, V, and Zr were prepared. Metal compounds evaporated in high vacuum included Ta_2O_5, TiO, TiO_2, V_2O_5, ZrO_2, NbN, TiN, $CrSi_2$, mixtures of $CrSi_2$ and $TiSi_2$, mixtures of $CrSi_2$ and B_4Si, B_4Si, NbB_2, Ni_2B, and TiB_2. Film resistors were prepared on three different substrate materials, Corning #7059 glass, soft glass microscope slides, and fused quartz. Significant fabrication details are given in Table I for most of the films fabricated, and these data are summarized in Table V.

The principal apparatus employed in the fabrication of these specimens included substrate cleaning equipment, four high vacuum systems, two substrate changers, and an electron beam evaporation system. Other small accessories and instrumentation necessary for establishing processing parameters and control were utilized.

1.1 Vacuum Deposition Apparatus and Techniques. The basic deposition apparatus consisted of four high vacuum systems. These were equipped

with versatile chambers and base plates and instrumentation for the measurement of various parameters during deposition. They were designated systems A, B, C, and D and are described subsequently.

Vacuum System "A": System "A" was constructed at Georgia Tech. Basic components are a forepump with a pumping speed of 5 cubic feet per minute, an oil diffusion pump 4 inches in diameter, a liquid nitrogen cold trap, appropriate valves, gauges, and two a. c. power supplies rated at 2 KVA each. Pressure measurements are made with a Veeco vacuum gauge, type RG-3A. An ionization gauge tube, Veeco type RG-75, is installed between the bell jar and cold trap for pressure measurements below 1×10^{-4} Torr. Argon and other gases are admitted to the system through bleeder valves located in the exhaust pipe to the base plate and chamber.

For the work under the contract, a straight section of Pyres Brand "Double Tough" pipe six inches in diameter and 12 inches in length was used as a chamber (the pipe is manufactured by Corning Glass Works). An overall view of the chamber arrangement is shown in Figure 1. Upward evaporations were made from refractory filaments, boats, or crucible sources connected to current feedthroughs at the base of the chamber. A top cover plate was adapted with a substrate holder, heater, and shutter, as shown in Figure 2. The shutter mechanism permitted shielding of the substrate during premelting and outgassing of the evaporant.

The heater enclosure was constructed of stainless steel shim stock and served as a radiation shield for a graphite cloth heating element. The graphite heating element was a 1-inch wide x 3-inch long piece of graphite tape stretched parallel to the substrate. The substrate holder was attached to the open side of the heater enclosure with screws and doubled as a contact mask for the substrate. It was machined from 12 gauge stainless steel, type 304. The mask supported substrates measured up to 1 x 3 x 1/16 inches.

The fixture was calibrated for substrate temperature versus heater current. To accomplish this, a platinum film resistance thermometer on a 1 x 3 inch microscope slide was placed in the substrate position, and its temperature was measured at the end of 1/2 and 1 hour heating intervals for a given heater current. The temperature within the enclosure represented an average temperature for the substrate under these conditions.

The mask was machined to enable the deposition of four parallel film resistors across a 1 x 3 inch substrate. Terminal areas were enlarged so that the shape of the deposit pattern resembled that of a dumbell. Initially

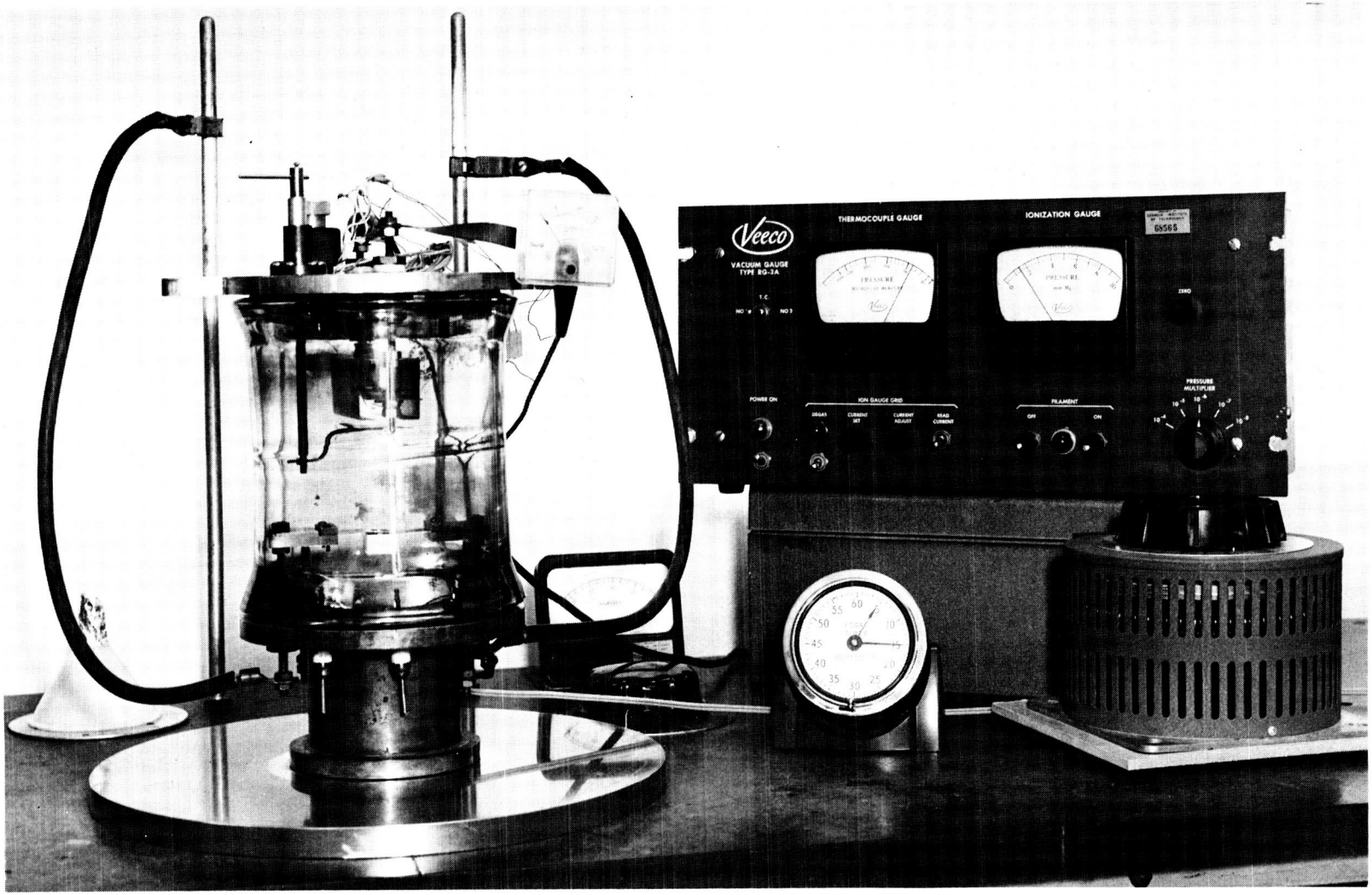

Figure 1. Vacuum System A.

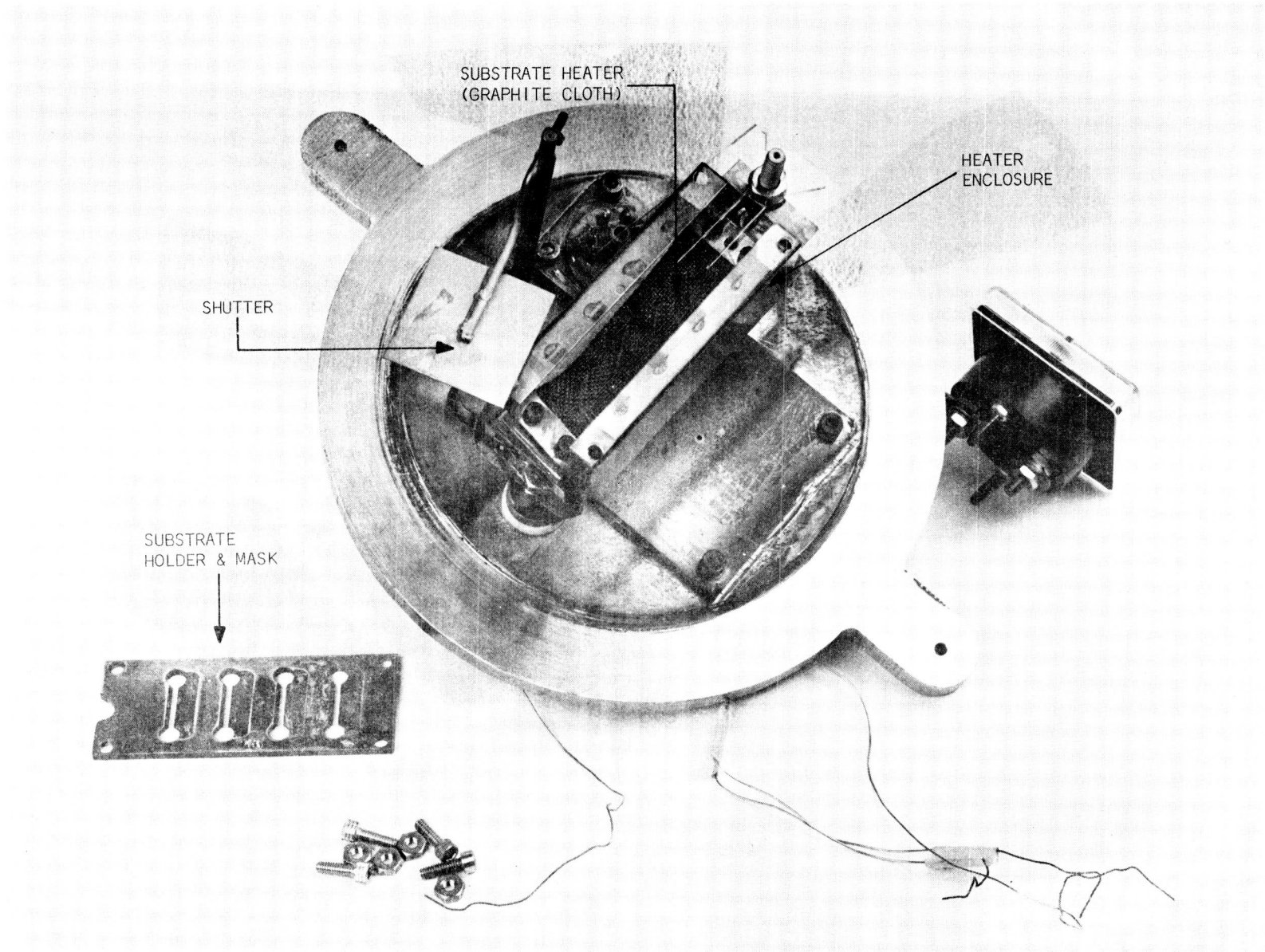

Figure 2. Substrate Support and Heating Assembly for Vacuum System A.

the substrate assembly was fixed to the heater so that the substrate was at an angle of 45 degrees with the horizontal plane including the source. Thus, each of the four resistor deposits were at a different distance from the source. To record this the resistors were labeled A, B, C, and D in going from the substrate end closest to the source to the end farthest from the source. The median source-to-substrate-distance was about five inches. During deposition, the A end was exposed to proportionately greater radiation intensity from the evaporation source. No attempt was made to measure the actual temperature gradient across the substrate during deposition. Resistors of several materials* were deposited with this arrangement. It will be noted that the A section is thickest with the thickness decreasing in the order of the B, C, and D sections. Usually, the specific resistivity of the films increased with the order of the sections.

The heater and substrate assembly was then modified so that the substrate was parallel with the heating element and the horizontal plane of the source. The previous mask was used in this arrangement, also. In addition, a second mask was machined for depositing a film resistor pattern measuring 1/2 x 1/2 inches on a pre-terminated 1 x 1 inch substrate centered over the evaporation source at a distance of about 5 inches.

Vacuum System "B": Constructed at Georgia Tech, vacuum system "B" is similar to that of vacuum system "A" described above. The major differences are an oil diffusion pump of six inches in diameter instead of four inches and a water baffle instead of a LN_2 cold trap. Otherwise, the systems were equipped similarly.

The chamber and header assembly was similar to that of system "A" as shown in Figure 2. A substrate mask-holder was machined to enable the deposition of three resistors in a 1/2 x 1/2 inch area on pre-terminated substrates. It could support either three 1 x 1 inch substrates or one 1 x 3 inch substrate at a distance of about 5 inches above the evaporation source.

A V-trough and slider was attached to the header for dropping powder mixtures onto a heated filament for flash evaporations. This was used to deposit a few chromium-silicon monoxide resistors by flash evaporation of the respective powder mixture of chromium and silicon monoxide.

* including Ti + O_2.

Vacuum System "C": This vacuum system is a standard Veeco model of the VE-400 series. It consists of a forepump with a pumping speed of 5 cubic feet per minute, an oil diffusion pump 4 inches in diameter, a water baffle, a liquid nitrogen cold trap, manually operated valves, thermocouple and ionization gauges, a glass bell jar 18 inches in diameter, and two a. c. power supplies rated at 2 KVA. All pressure measurements were made with the standard ionization gauge supplied with the system. The gauge tube is located near the cold trap and in the basic piping immediately between the diffusion pump and base plate. Thus, the pressures recorded are probably lower than the actual bell jar pressures. This difference, however, was probably less than one order of magnitude during evaporations, especially, when a Meissner cold trap inside the bell jar was operated.

A stainless steel collar was added to the system to provide for extra feedthroughs for electrical apparatus and rotary shafting to operate the substrate changer discussed subsequently. Also, a Meissner cold trap was constructed and located in the bell jar. The trap was constructed of one-half inch diameter copper tubing, coiled to form a helix of six turns and approximately 6 inches in diameter and 6 inches in length. Liquid nitrogen was passed through the tubing by "Monel" alloy feedthroughs mounted in the stainless steel collar. The Meissner trap was operated immediately before and during. the deposition of the films to give a lower pressure inside the bell jar during the critical period of film deposition.

A substrate changer constructed at Georgia Tech was installed on this system and is illustrated in Figure 3. The changer is constructed of nonmagnetic materials free of low vapor pressure constituents, particularly zinc. Major components are fabricated of types 303 and 304 stainless steel. Bearings and thrust washers are fabricated of a zinc free bronze alloy impregnated with about 1.5 percent graphite. Mica, boron nitride, and alumina are used for electrical insulators. Adequate pump-out features such as grooves or channels are machined on mating surfaces. Screws are center drilled for screw holes that bottom-out. Where possible bottomless holes are used for screws. Top and bottom support plates are secured to the three legs by nuts and are adjustable in the vertical direction. The substrate carrier plate is fixed to a bronze bearing fitted and supported in the center of the top support plate. A pitch chain sprocket is secured to the top of the bearing for rotation of the substrate carrier plate about a centrally located axle. The central axle extends through the bottom plate and is supported by a precision collar that rides on top of the bottom support plate; the sub-

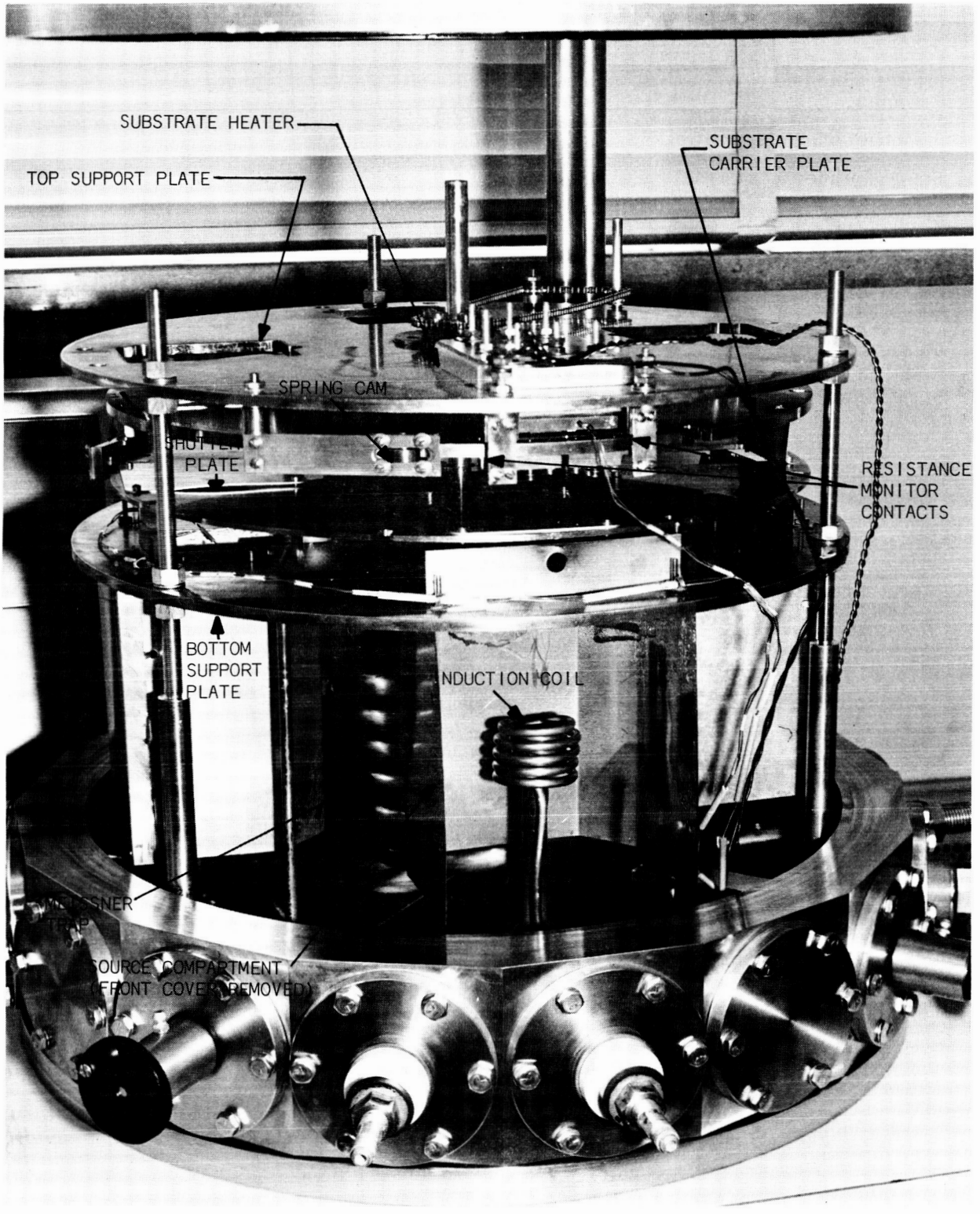

Figure 3. Substrate Changer Used with Vacuum System C.

strate carrier bearing locates the axle centrally at the top end. The shutter plate is fixed to a bronze bearing that rotates freely about the center axle while a pitch chain sprocket secured to the bearing permits turning of the shutter. Miniature stainless steel pitch chains, universal joints, gears, and shafting are connected to rotary feedthroughs installed in the stainless steel collar to independently rotate the substrate carrier and shutter plates from outside the bell jar. Adjustable spring cams ride on the perimeters of the shutter and substrate carrier plates. The cams engage with notches in the respective plates to obtain independent registration of the plates with respect to each other and the various source compartments. Independent substrate holders are positioned in the substrate carrier plate. Four positions will accommodate substrates with a maximum size of 2 1/2 x 3 1/8 inches. Holes in the top support plate permit access to the substrate carrier plate.

The substrate holder served also as the mask for these studies. Four ports or vapor windows are located ninety degrees apart in the bottom plate. Evaporation filaments or sources are located below the windows. The stainless steel forms secured to the bottom side of the bottom plate are source enclosures which provide shielding of the sources from each other. Also, the shields prevent undesired vapor condensation on the bell jar and changer. Each source compartment has a quick-release front cover plate for ready access to the interior. An adjustable frame for holding a 1 inch x 1.5 inch microscope slide is mounted on top of the bottom plate at each of the vapor windows to serve as a front surface mirror for viewing each source from the exterior of the bell jar during evaporation.

Radiant substrate heater assemblies and a resistance monitor are the major accessories incorporated into the changer. The heaters rest in any of the four holes in the top plate directly above a substrate or substrates to be coated and can be readily transferred from one position to another or removed for access to the substrate carrier plate. Figure 3 shows a heater installed in the changer. Major construction details are illustrated in Figure 4. The graphite cloth element provides heating over the entire substrate holder and is very efficient. For example, the cloth barely reaches the color temperature range to obtain substrate temperatures of 500° C. (The method of establishing substrate temperature is discussed subsequently). For this work, the graphite cloth was folded to form two closely spaced layers in series. The layers were insulated by a thin sheet of mica. The heater also

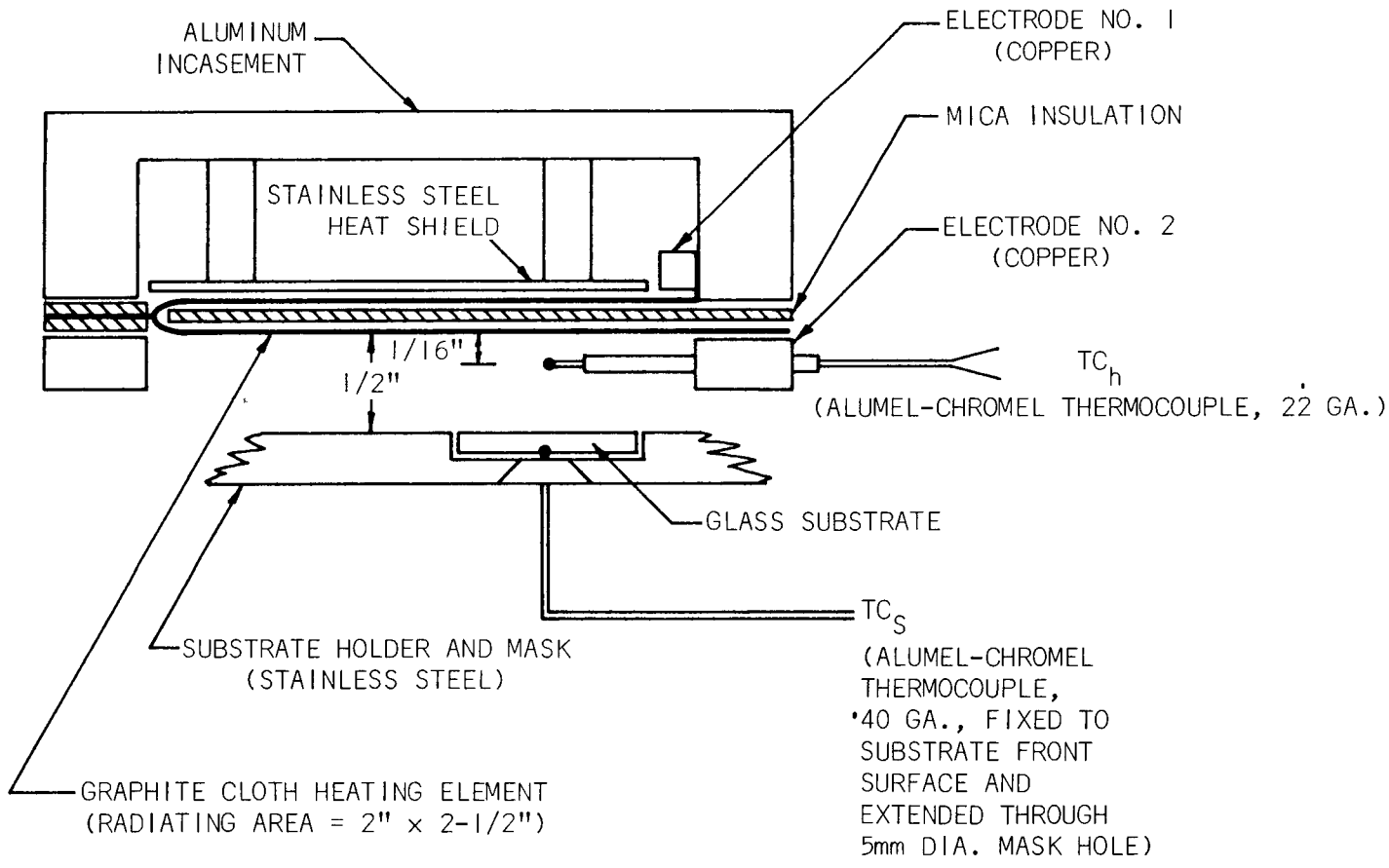

Figure 4. Substrate Heater Assembly Showing Relative Positions of Substrate and Thermocouples for Determination of Substrate Temperature.

operates quite satisfactorily with a single layer of graphite cloth; however, a greater current is required for a single layer element to obtain a given substrate temperature.

Substrate temperature was indicated by a 22 gauge chromel-alumel thermocouple, TC_h, positioned between the graphite cloth heating element of the substrate heater and the substrate holder. TC_h was calibrated against a 40 gauge chromel-alumel thermocouple, TC_s, fixed to the front surface of a substrate. A loop of nichrome wire was heated by resistance heating and was employed to embed the thermocouple in the substrate surface. Figure 4 illustrates the arrangement of the thermocouples for calibration of TC_h. The temperatures indicated by both thermocouples were measured versus time for one hour and one-half hour heating periods and various variac settings of the heater power supply. Data obtained for one hour heating periods are plotted in Figure 5. The thermocouple fixed to the substrate, TC_s, indicated higher temperatures than TC_h for temperatures below 425° C and lower values for temperatures above 425° C. Heater currents at the end of the heating periods ranged from 5 amperes for a substrate temperature of 200° C to 14.1 amperes for a substrate temperature of 500° C. These data were used to determine substrate temperatures from measurements with TC_h during the fabrication of film resistors.

As discussed subsequently, Cr-SiO films deposited on substrates measuring 2 x 2 inches were non-uniform in resistivity over the surface area. Much of the non-uniformity was attributed to non-uniform heating of the substrate with the graphite heating element. The area of the graphite element was 2" x 2.5". This is approximately equal to the area of the substrates. The element sagged with extended use, also. More uniform heating of substrates can possibly be had by making the area of the heating element somewhat larger than the area of the substrate and by preventing the cloth from sagging. In this work, improved uniformity was obtained by placing a metal block on the substrate. The substrate was heated by the block which was equal in area to the substrate and was heated by the graphite heater.

Two sets of substrate masks were used with the changer. These are illustrated in Figure 6. Each set of masks consisted of a mask for predepositing gold over chromium terminations and a mask for deposition of the resistive film. Both masks were machined from type 304 stainless steel. The masks at the left sides of Figures 6a and 6b are the termination masks for the respective resistive film masks shown to the right. The slotted

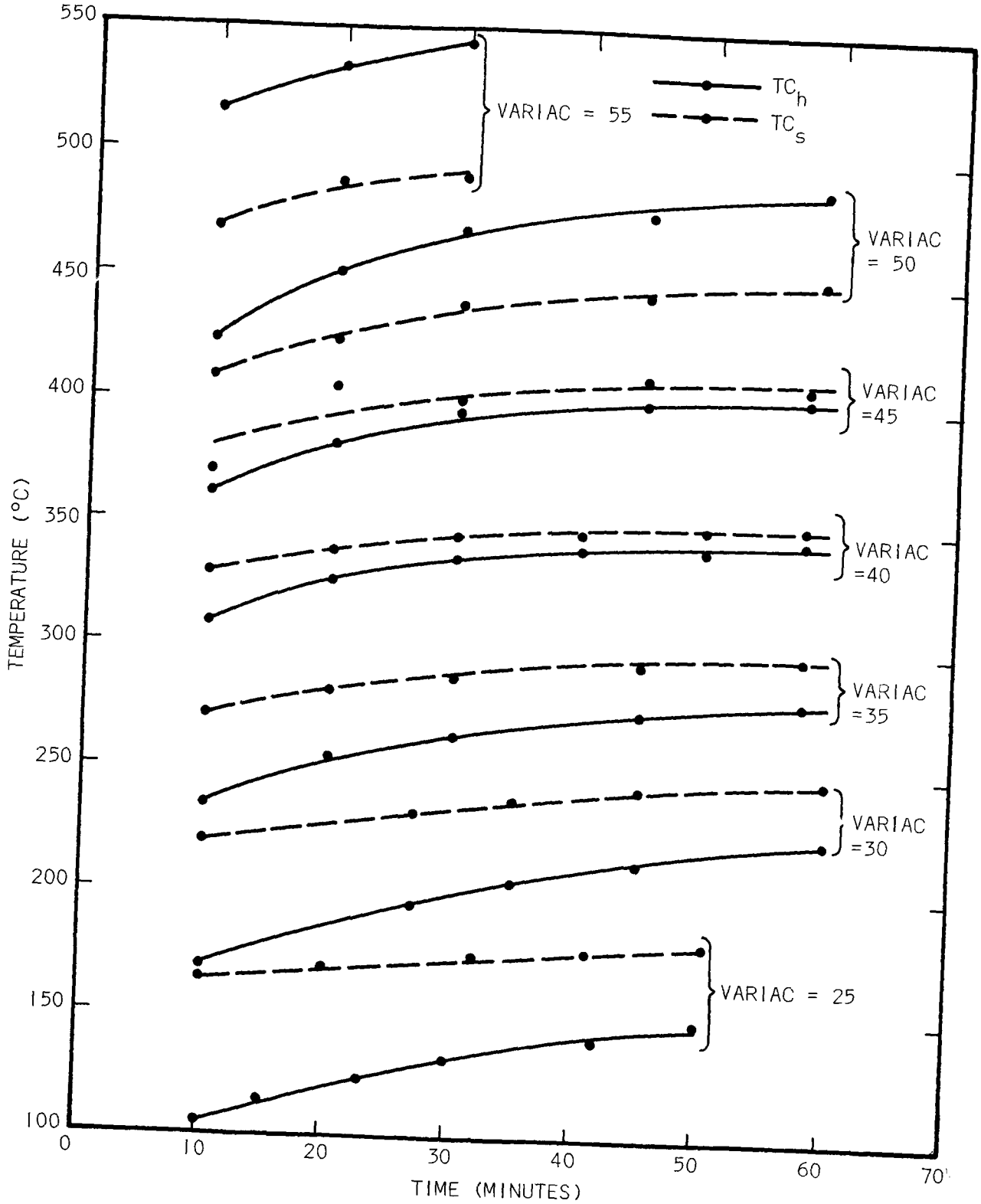

Figure 5. Substrate Temperature vs Time and Variac Setting for Heater Assembly of Substrate Changer on Vacuum System C.

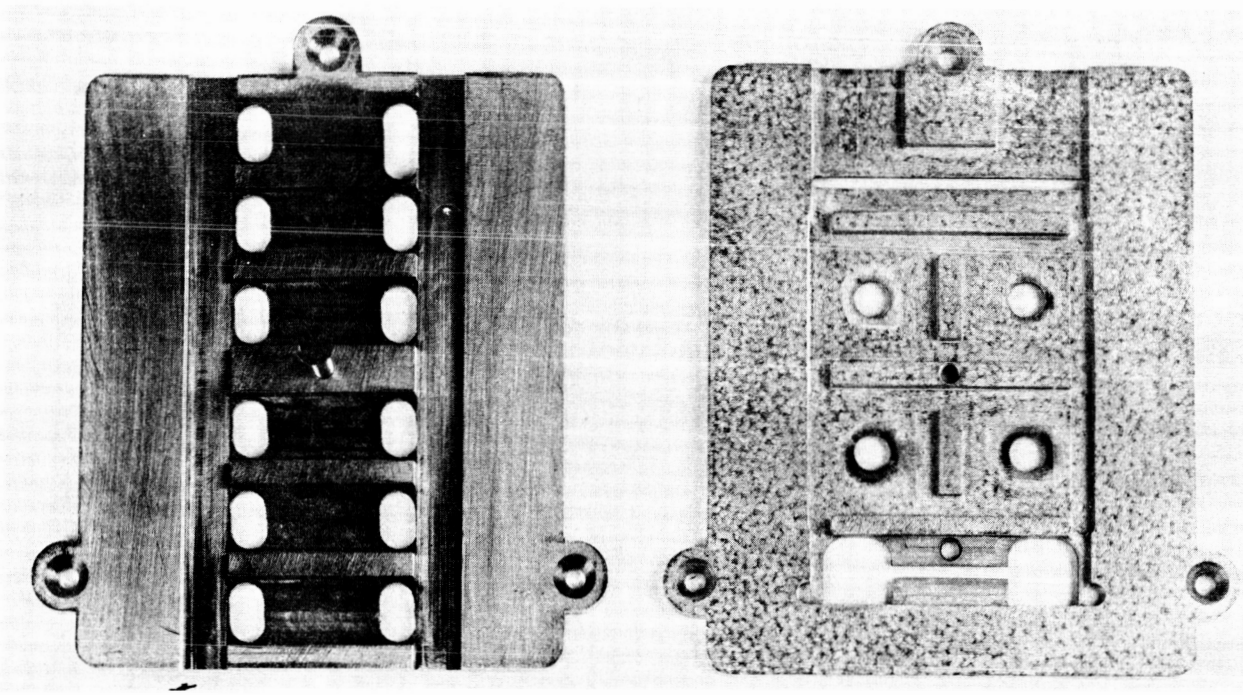

(a) MASKS FOR DEPOSITION OF RESISTORS 5/8-INCHES LONG × 1/16-INCHES WIDE

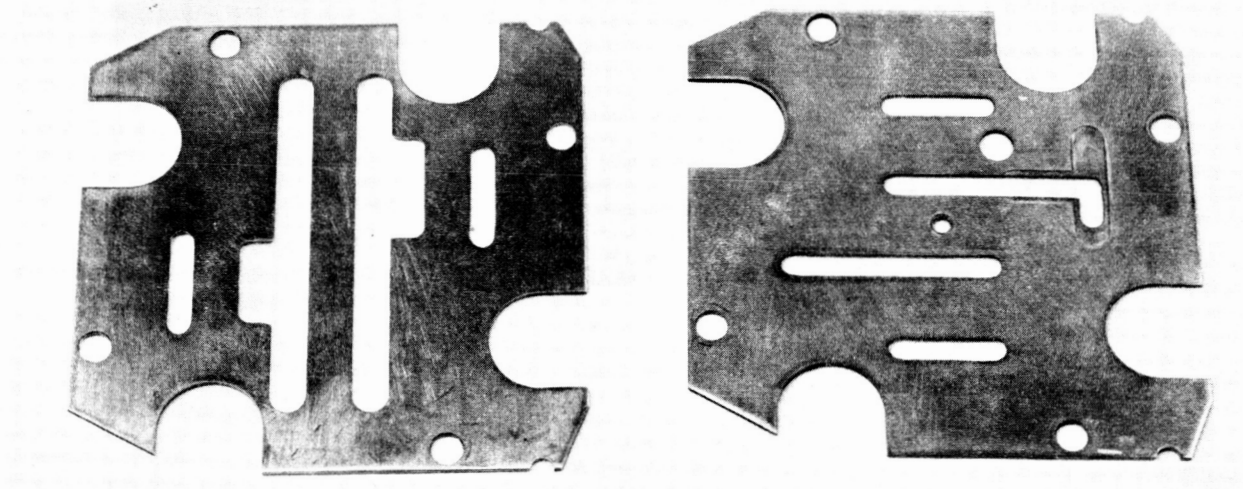

(b) MASKS FOR DEPOSITION OF 6 RESISTORS ON A 2 × 2-INCHES SUBSTRATE

Figure 6. Substrate Masks.

holes at the top and bottom ends of the mask to the right in Figure 6a were used for depositing the resistive films. Between the terminals each resistor was 5/8 inch long and 1/16 inch wide. The resistor deposited at the slotted hole with the dumbell shaped ends was monitored during deposition. The small round hole near the center of the slot was for holding an electron microscope grid. The mask to the right in Figure 6b was used to deposit six resistors in a single evaporation on a 2 x 2 inch substrate.

A tantalum grain box, R. D. Mathis type ME-1, was used to co-evaporate Cr-SiO and Mn-SiO. The source was in the position of the induction coil shown in Figure 3. The source temperature was calibrated against source current to obtain the source temperature values by the method indicated in Figure 7.

The resistance monitor on the changer consists of a set of stationary spring contacts mounted in the top support plate that engage with a set of contacts fixed to the substrate carrier plate at each of the four substrate positions. By connecting leads from the contact on the substrate carrier plate to pre-deposited terminations on a substrate, the resistance of conductive films can be measured during the deposition process. This feature permitted deposition of resistive films to a given resistance value. During deposition of films in this report, the film resistance was monitored with an impedance bridge, General Radio type 1650-A. After removal from the vacuum chamber, the resistance of the film was measured at room temperature with a wheatstone bridge, Rubicon Instruments model 1071.

Vacuum System "D": Vacuum system "D" was set up primarily for electron beam evaporations. The system is a Veeco model VE-775 automatic evaporator. It is equipped with a modified Edwards microcircuit jig or substrate changer and a Veeco VE-B6 electron beam gun system. Electron beam evaporations were made from a massive copper crucible. Apparatus within the bell jar is shown in Figure 8. The bell jar of this system is constructed of stainless steel and is 26 inches in diameter.

Evaporation of metal films onto room temperature substrates with the electron gun resulted in film deposits of non-uniform thickness. The non-uniformity was noted for a number of metals evaporated with the electron gun on substrates at temperatures up to 250° C. The non-uniformity resulted from electron and/or ionic charges arriving at the substrate and possibly the charge build-up that occurred on the substrate surface. Film deposits on glass substrates heated to 400° C and above appeared uniform. At 400° C, the substrates are slightly conducting and apparently this prevents the surface

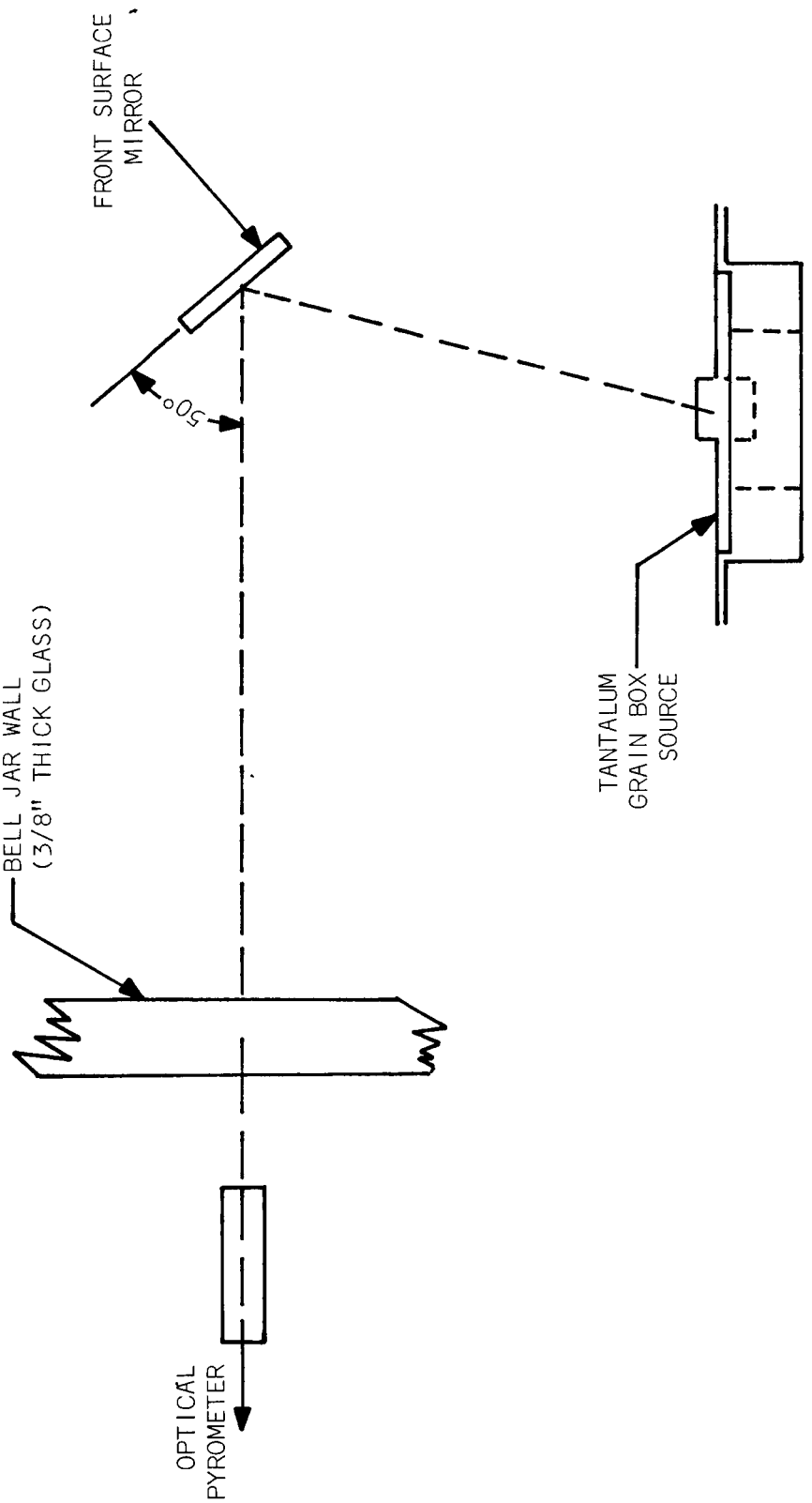

Figure 7. Method of Measuring Source Temperature.

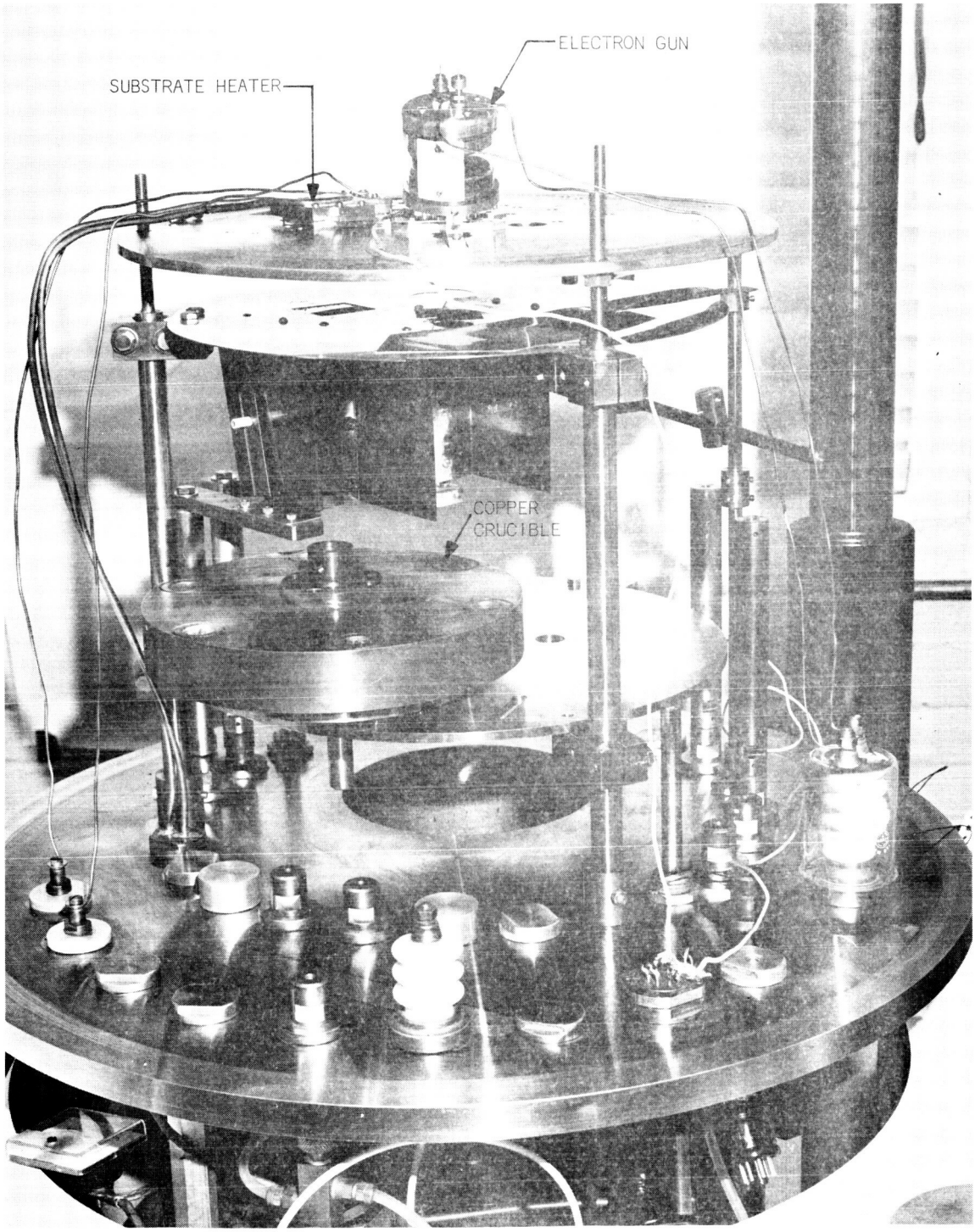

Figure 8. Deposition Apparatus of Vacuum System D.

from becoming charged during the deposition. Thus, it is believed that the surface charge that can occur effects primarily the non-uniformity observed on the cooler and non-conducting substrates. A collector ring installed in front of the substrate and biased at plus 300 to 600 vdc with respect to the substrate holder and baseplate eliminated the non-uniformity in film deposits on cool substrates; on the other hand, the non-uniformity persisted with the ring biased negatively; hence, it appears that the ring prevented the arrival of electrons at the substrate surface which interfered with obtaining uniform deposits. Even though uniform film deposits were obtained on hot substrates, bombardment of the film by charges during build-up obviously continued in the absence of the collector ring. Hence, it is quite possible that film purity or characteristics are affected by such bombardment.

As a result of the high pumping speed of this system, most evaporations were made in the low 10^{-6} Torr range.

1.2 Substrate Selection. Corning Type 7059 glass was selected as one of the primary substrate materials. It is a barium alumino-silicate with compositions of extremely low alkali content. Because of the latter, it has found frequent use in the electronic industry as a substitute for the more common glasses where migration of alkali ions with applied electric fields caused instability in film components. The surface of this glass is quite wavy; however, the smoothness is equal to or better than one micro-inch, according to the manufacturer. The glass was obtained in dimensions of 1 x 1 x 0.32 inches from Corning Glass Works, Electronic Components Department, Raleigh, N. C. Soft glass microscope slides of the non-corrosive varieties were used extensively, also.

During efforts to evaporate some refractory materials with the electron beam apparatus, the soft glass substrates were heated to the softening point in certain instances. Hence, polished fused quartz substances were obtained for electron beam evaporations of refractory materials. The dimensions of these were 1 x 1 x 0.030 inches. These were purchased with the trade name "Micro-fused Quartz" from Dell Optics Company, Ltd., North Bergen, N. J. (Between the glasses and fused quartz substrates, no difference in film parameters were noted that could be attributed to the substrate material.)

Conventional copper grids overcoated with carbon films were utilized for supplemental analytical studies with the electron microscope.

1.3 Substrate Cleaning and Apparatus. Two substrate cleaning methods were used during the program. Method number 1 was employed for all of the

specimens fabricated with vacuum systems A and B, and Method 2 was used with vacuum systems C and D. In both methods reagent grade chemicals were employed.

Cleaning Method 1. Concentrated chromic acid was poured into a cleaned beaker or petri dish. A few drops of distilled water were carefully added to the acid. With addition of the water, the acid became hot. The substrate was placed in the hot acid for 3 to 5 minutes. The substrate was then removed from the acid with tweezers and successively rinsed with distilled water and methanol. After the methanol rinse the substrate was dried with a hot air blower.

Cleaning Method 2. For Method 2, special cleaning and handling apparatus including a demineralized water rinse, vapor degreaser, and rack for supporting a batch of substrates were employed.

The filtered demineralized water rinse depicted in Figure 9 was used initially. It provided a temporary and useful water rinse facility for the initiation of this work. The throw-away demineralizing cartridge employed was the Research Model manufactured by the Illinois Water Treatment Company. The filter was fabricated by packing a filtering grade of glass wool into a 5/8 inch diameter x 4 inches long polyethylene tube (calcium chloride drying tube.) The covered polyethylene dish used for the water bath is 3 inches wide x 9 inches long x 3 inches deep. A water flow rate of approximately 350 cc per minute was maintained during rinsing.

During the latter part of the program, a Barnstead demineralizing loop, Model PL-1-C, was obtained for final water rinsing. The PL-1-C loop was equipped with a submicron filter, one mixed bed demineralizing cartridge, one organic removal cartridge, resistivity metering, and appropriate valving. To this a centrifugal water pump was added to recirculate a supply of water through a stainless steel rinse tank. The system was charged with distilled water, U.S.P. grade. This was added to the system as the water level dropped with normal evaporation from the tank. The rinsing tank was installed in a clean box and was covered with a lid when not is use. After operating for a few minutes, the resistivity of the water reached a level of 15 to 18 megohms. This level of resistivity was used as a standard for rinsing the substrates; i.e., after placing a batch of substrates in the rinse tank, they were not removed until the resistivity of the water returned to the normal maximum value. The substrates were cleaned in acid before rinsing in water. After installation of the high purity loop, gross acid was rinsed from the racked substrates

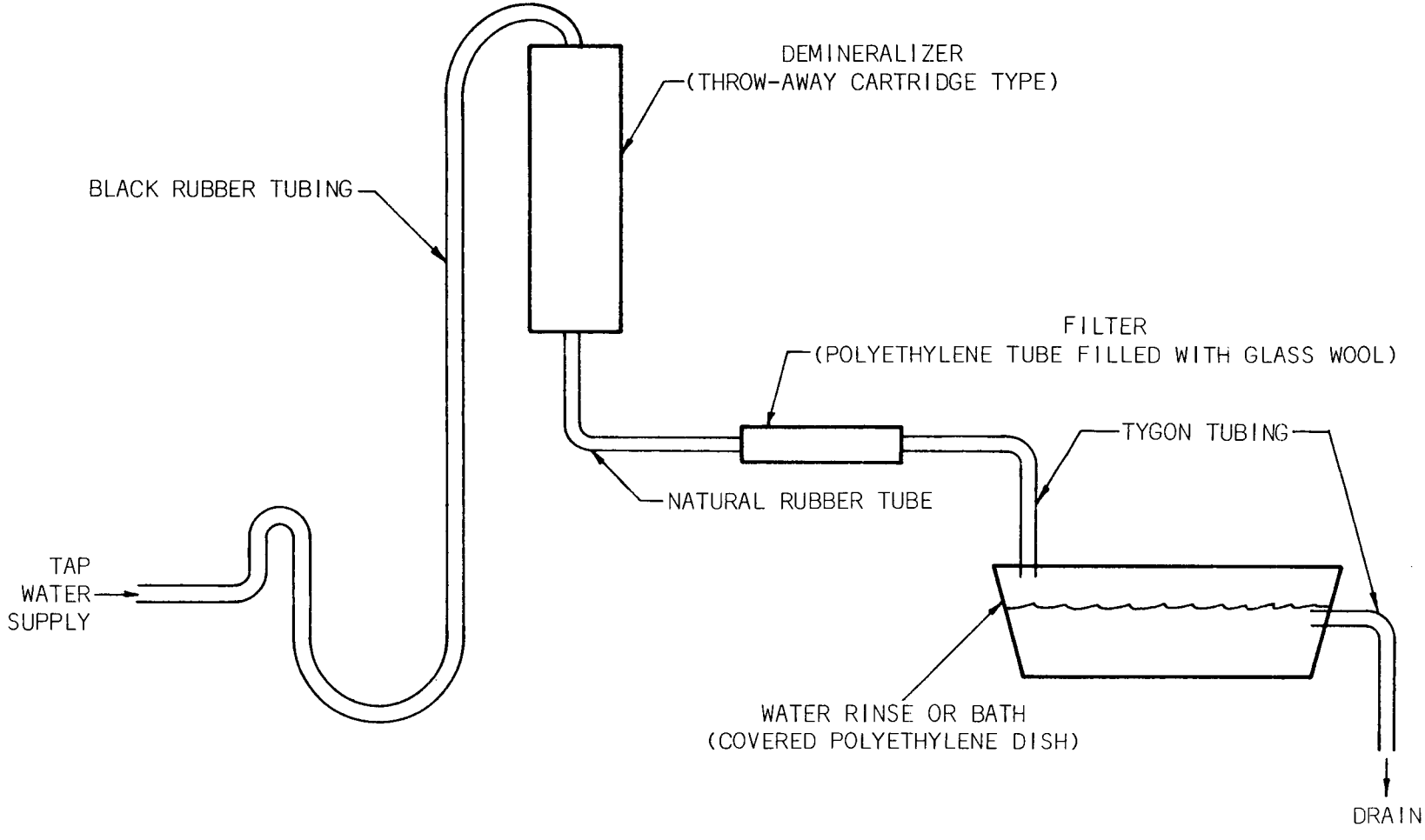

Figure 9. Demineralized Water Rinse for Substrate Cleaning.

with the initial water rinse of Figure 9 immediately before placing them in the high purity rinse tank.

A vapor degreasing chamber constructed from stainless steel was employed during the final stage of substrate cleaning. The top of the container was closed with an aluminum plate. The container was partially filled with the liquid trichloroethylene and specimens were supported on a rack above the liquid. When the liquid was heated to the boiling point by an electric hot plate, it vaporized and condensed on the substrates. A continuous washing action occurred as the condensed droplets were returned by gravity to the liquid below. The degreaser was very useful in obtaining smear-free surfaces.

A special rack was constructed from type 304 stainless steel to support substrates during cleaning. Figure 10 illustrates the general construction of the rack which holds sixteen substrates for batch cleaning of rectangular substrates. The rack is milled from a solid piece of stainless steel to eliminate deep holes and screw threads that tend to hold solution between successive baths or rinses. It is cleaned with the substrates, and the substrates are supported so as to provide for adequate drainage of liquids from the substrate corners and edges. The latter feature eliminates the gross formation of so-called water marks or smears that occur if droplets of liquid collect along the edges or corners during final drying of a substrate. The hook type handle is constructed from a stainless steel rod and is used to transport the rack.

Figure 11 shows the final cleaning station for substrate cleaning method 2. The following is a stepwise description of the cleaning procedure.

(1) Scribe code numbers on back of substrates and arrange in deposition order in substrate cleaning rack,

(2) Place racked substrates in a fresh hot chromic acid bath, about 100° C, for 5 minutes (chromic acid formed by saturating concentrated sulfuric acid with chromium trioxide at room temperature -- keep acid dish covered to minimize oxidation at elevated temperatures),

(3) Remove from the chromic acid and rinse away gross acid with flowing demineralized water from drain tube of Figure 9,

(4) Dip racked substrates in tank rinse of Figure 9,

(5) Submerge racked substrates in high purity water rinse, Figure 11, leave in recirculating bath a minimum of 10 minutes after resistivity returns to a minimum of 15 megohms,

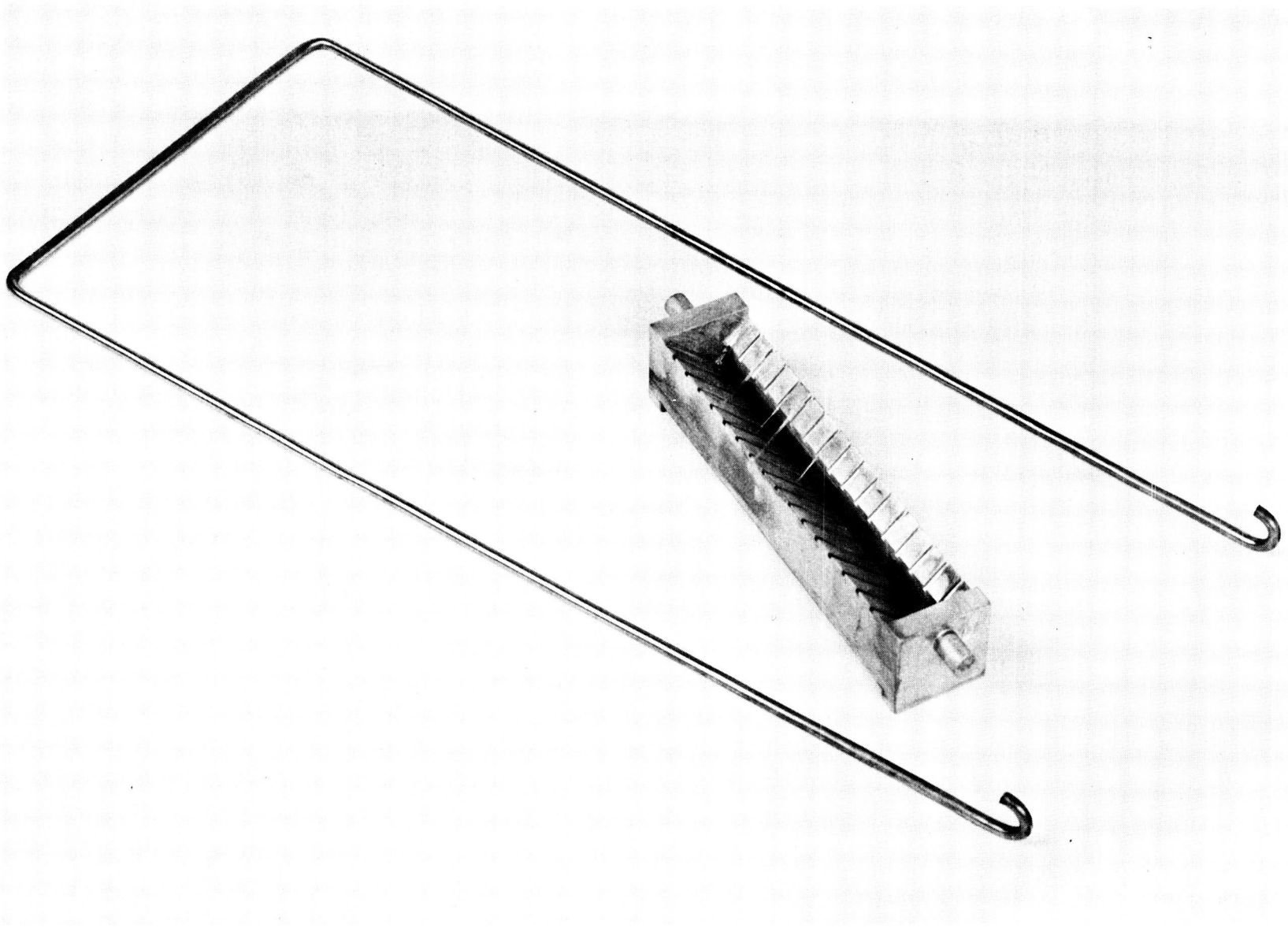

Figure 10. Substrate Cleaning Rack.

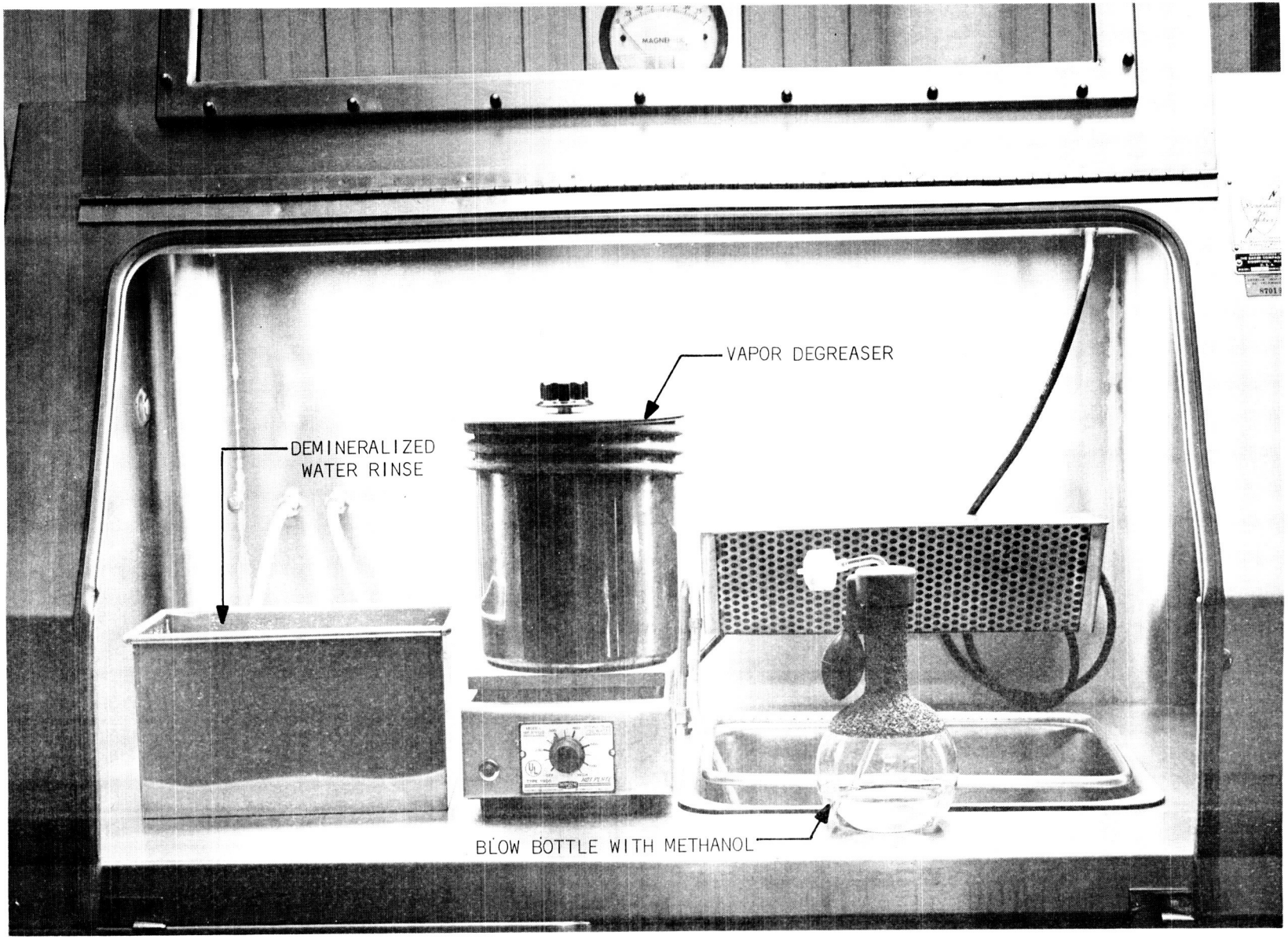

Figure 11. High Purity Water Rinse and Final Cleaning Station for Substrate Cleaning Method 2.

(6) Remove racked specimens from water rinse and rinse with methanol from a blow flask,

(7) Place racked substrates in trichloroethylene degreaser for a minimum of 10 minutes or until ready to place in vacuum deposition apparatus,

(8) Carefully remove substrates from degreaser,

(9) Use cleaned tweezers to remove substrates from cleaning rack and position in holders in the vacuum deposition apparatus.

In the performance of the above cleaning procedures, the substrates were not allowed to dry between successive baths. The methanol rinse was used primarily to remove water from the substrates and rack before degreasing since water and trichloroethylene do not mix very well. The trichloroethylene degreaser was used primarily as a storage point immediately before film deposition and as a technique of drying the substrates to obtain a streak-free surface rather than for any unique cleaning or degreasing property of the trichloroethylene vapor.

1.4 Film Thickness Measurement Apparatus. A constant deviation spectrometer, Hilger and Watts model D 186, was used in conjunction with an interferometer to measure film thickness. The interferometer is equipped with a white light source and operates on the principle of multiple beam interferometry[1] to produce fringes of equal chromatic order. The interferometer was constructed under a previous project funded by the Engineering Experiment Station of Georgia Tech. Design was based on that described by Scott, McLauchlan and Sennett.[2]

1.5 Other Fabrication Apparatus. A stereomicroscope with a magnification range from 0.7X to 60X, an optical pyrometer, wheatstone resistance bridge, thermocouple potentiometers, multimeters, and ultrasonic bonding apparatus were available for routine measurements examination, and preparation of specimens during fabrication.

1.6 General Fabrication Procedure. Common procedures and precautions followed to fabricate film resistors are discussed. Details particular to a specific species of films are given later.

Preparation of Substrates for the Resistive Films: Immediately following cleaning by one of the two previously discussed cleaning methods, the substrates were appropriately masked and placed in a vacuum system for evaporation of film terminations. Upon evacuation of the bell jar to the low 10^{-5} Torr range or lower, the substrates were heated to about 300° C

and the terminal films were evaporated. The terminals were deposited in successive evaporation of chromium and gold. First, chromium was evaporated to a thickness of 300 to 1000 angstroms. This was followed immediately with the evaporation of an overlayer of gold. The thickness of the gold overlayer was from 2000 to 3000 angstroms. After cooling, the substrates were removed from the vacuum chamber, placed in a cleaned petri dish, and stored in a desiccator until ready for deposition of the resistive films.

The chromium underlayer was employed to obtain strong adherence of the gold film. Gold terminals were selected to provide a low resistance contact to the resistive films. The terminals were deposited before the resistive films to eliminate the possibility of contact resistance that can result from surface oxides between terminals and resistive films. The latter will occur if the initial film deposited forms a surface oxide before the second film is deposited. A minimum gold thickness of 2000 angstroms was necessary for subsequent bonding of gold foil leads to the terminals by thermal compression or ultrasonic bonding techniques.

Immediately before evaporation of the resistive films, the pre-terminated substrates were removed from the desiccator and loaded into masks. Gold leads were bonded to the terminals of those substrates to be monitored during deposition; otherwise, the leads were attached after deposition of the resistive films. All of the substrates were pre-terminated, except for a few films fabricated early in the program. For the latter films, leads were soldered to the resistive films with indium after deposition.

General Evaporation Procedure for the Resistive Films: After the substrates were installed in the deposition apparatus and the source was filled with evaporant, the following general procedure was followed for the evaporation of the resistive films:

(1) Fill LN_2 trap at beginning of pump-down, except for vacuum system B,
(2) Evacuate to high vacuum range,
(3) Turn on substrate heater for desired temperature,
(4) Outgas evaporant and source by pre-heating or melting the evaporant with the substrate shutter closed,
(5) After 30 minutes of substrate heating, record substrate temperature and high vacuum pressure,
(6) Open shutter and evaporate resistive film, record pressure during evaporation, and record monitor resistance at the end of the evaporation,

(7) Turn substrate heater off and cool substrates to 100° C or less,

(8) Open vacuum chamber, remove specimens and store in a desiccator.

Attachment of Leads: Typically, gold ribbon leads (0.001 x 0.005 inches) were bonded to the gold film terminals of each resistor. Thermal compression bonding was used in most of the bonding; however, ultrasonic welding apparatus was available and used when convenient. Typical specimens with leads attached are shown in Figure 12.

2. Measurements of Resistive Parameters

Measurements of resistance, temperature coefficient of resistance (TCR), and thickness were made to determine the relationship between specific resistivity and TCR of each film species. Representative specimens were then selected for aging and passivation studies. Initial parameters for the individual specimens are listed in Table I and summarized in Table V.

2.1 Resistance Measurements: Resistance measurements were made with a wheatstone bridge, Rubicon Instruments model 1071. After leads were fixed to the resistors, resistance was measured to four significant figures at room temperature. From the total resistance and known length to width ratio of the film, the resistance per square was calculated. During subsequent aging studies resistors were removed from the oven and returned after measurement at room temperature.

2.2 Measurement of Temperature Coefficient of Resistance: To determine the TCR, the films were placed in a tube furnace and cycled to 125° C in air. Initially, the resistors were cycled to this temperature in 5 to 10 minutes. Later in the program a different oven was used, and the time was increased to 20 to 30 minutes. The TCR values were calculated from the relationship:

$$TCR = \frac{R_T - R_o}{R_o(T - T_o)}$$

where R_T was the resistance value at 125° C, R_o was the room temperature resistance after cycling, and $T - T_o$ was the difference in temperature, in degrees centigrade, at room temperature (T_o) and 125° C(T).

Some films changed in resistance during heating to 125° C; hence, after the measurements at 125° C were made, the resistors were rapidly removed from the oven and cooled to room temperature. By using the latter room temperature value, oxidation and annealing effects were minimized in the calculated TCR

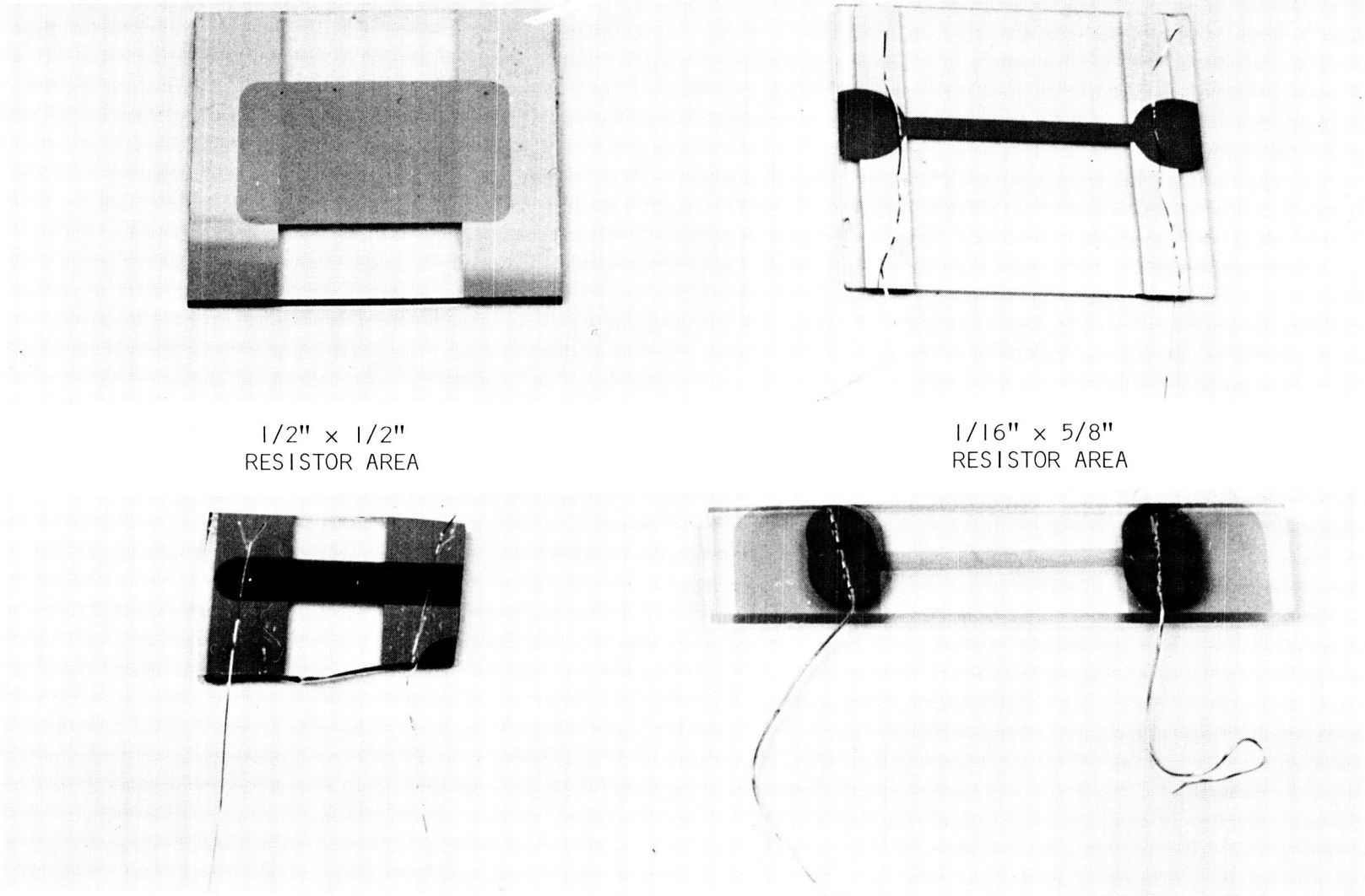

Figure 12. Typical Resistors with Leads Attached.

values. Table III† shows the changes in resistance experienced during TCR measurements. Thinner films, less than 500 angstroms in thickness, usually increased in resistance by a greater percentage than did substantially thicker films during the TCR measurements. This is to be expected since an oxidized layer of given thickness is a proportionately greater fraction of the thickness of thinner films.

2.3 Determination of Specific Resistivity. Specimens with TCR values representative of the TCR range obtained for each species of films were selected for thickness measurements so that the relationship between specific resistivity (ρ) and TCR could be established. Typically, two measurements of thickness were made at different points on each film, and the average value was taken as the film thickness. Thickness measurements were made with the apparatus discussed in section 1.4. The specific resistivity was then calculated from the relationship:

$$\rho = \text{Resistance per square} \times \text{film thickness};$$

where the resistance per square is in ohms and the thickness is in centimeters. Specific resistivity values are listed in the tables in units of microhm-cm.

After the characteristic relation between resistivity and TCR was established for a species and a given fabrication procedure, subsequent resistivity values were estimated from a plot of resistivity versus TCR.*

3. Passivation and Stabilization of Films

Two techniques of passivating and annealing films to enhance stability were examined. These were overcoating with SiO and post-deposition baking in air at elevated temperatures. These measures were taken after the resistive parameters were determined.

Some films of the Mn + SiO and Cr + SiO series were overcoated with SiO by evaporation techniques in high vacuum. The SiO was deposited to a thickness of about 6,000 Angstroms. During overcoating, the films were heated to about 300° C in 30 minutes in the vacuum environment. Subsequent aging of these films was then compared to that of similar films baked in air and to that of unprotected films.

---

* A typical example for zirconium-zirconium oxide films is given in Figure 13.

† in the Appendix

Post-deposition baking in air was studied more extensively as a means of stabilizing the films. Selected specimens of the various species were baked in air for 3 to 16 hours at temperatures ranging from 200° C to 300° C. Subsequent aging of the films were compared to similar films overcoated with SiO and to unprotected films.

4. Extended Aging Studies

Selected specimens from most of the species fabricated were stored in a convection oven at 125° C. Changes in the resistive parameters with time were recorded. Typically, the study was conducted for 1000 hours. Both protected and unprotected films were studied for a no-load condition.

During the aging period, resistance measurements were made about once a week. For each measurement, the specimens were removed from the oven, and their resistance values at room temperature were recorded. Thus, each resistor received a mild temperature shock upon removal and return to the oven. A graph of resistance change with time was prepared for each resistor placed on aging.

5. Other Analytical Measurements

Electron microscope and electron diffraction studies of grids coated during the evaporation of the various specimens were made. Film compositions were obtained primarily from the electron diffraction studies although electron microprobe and x-ray diffraction techniques were also used.

6. Use of Microprobe to Analyze Thin Films

The specimens prepared for examination with the electron microprobe were deposited on carbon film substrates supported by electron microscope grids. These specimens, when submitted for examination, were quite wrinkled and wavy. With a specimen of this nature, the analyzing crystal in the microprobe "sees" a different input angle for each different area to be analyzed. X-ray counts thus vary greatly as a result of this difference in the angle and because of variance of absorption of the emitted radiation in paths of different lengths through the specimen. Variances of 30% from one grid opening to the next opening on the same grid were not uncommon; thus, no quantitative data could be obtained.

Two methods that may overcome these difficulties are:

(1) To float the deposited films off the substrates and deposit them on fine mesh grids; or

(2) To deposit the films on polished solid substrats of different elements than those in the film.

These methods should be considered for any future investigations of materials exhibiting wrinkling due to internal stresses or to other causes.

B. ELECTRICAL PARAMETERS OF EVAPORATED FIIMS EXAMINED

1. Introduction

As stated previously 758 films in seven categories of metal or metal compound films were examined. Measurements of electrical resistance, thickness, specific resistivity, and temperature coefficients of resistance (TCR) were made for most of these. In addition, structures of selected films were examined by electron and x-ray diffraction and by electron microscopy.

These categories of films will be discussed in order of the simplicity of the preparation of the films; i.e., metal films, metal-metal oxide films, metal-silicon monoxide films, and films formed by evaporation of the more exotic compounds such as borides, nitrides, silicides, or combinations of these compounds. This order of presentation proceeds from the commonly positive temperature coefficient of resistance of metal films to the nearly zero or highly negative one of some of the materials examined.

2. Metal Films

Although the preparation of resistors of metal films was not a part of the program due to the known low resistivities of the metals in their pure state, incidental to the program some evaporations of metals were carried out in order to establish a starting point from which to examine the effects of evaporation of selected metals in oxygen at low pressure (10^{-5} to 10^{-3} Torr). Films of chromium, gadolinium, manganese, titanium, thulium, vanadium and zirconium were examined. It will be noted also by examination of the literature that little has been reported previously concerning the electrical properties of films of gadolinium, manganese, thulium or vanadium. This fact is a second reason for including in this report measurements of the parameters of the metal films examined.

Most of the films were deposited on glass substrates at temperatures near 400° C. The exact conditions for the preparation of each film are noted in Table I (Appendix). The TCR values of all except the very thinnest films, or some of the slowly evaporated ones, were positive; the highest value obtained was 0.0021/° C, 2100 x 10^{-6}/° C, or (2100 ppm/° C). Selected examples of values determined for the films are shown in Table IA and exact details of preparation and measurements for each film are shown in Table I.

It will be noted that the TCR values for these films varied from -900 x 10^{-6}/° C for the very thinnest films to +2100 x 10^{-6}/° C for relatively thick and more pure ones. Thickness ranges were approximately 100Å to 5000Å,

TABLE I-A

RESISTANCE PARAMETERS OF TYPICAL METAL FILMS
EVAPORATED IN HIGH VACUUM

Metal	Thickness (Angstroms)	R/sq (ohms)	Resistivity (Microhm-cm)	TCR (10^{-4}°C)	ρ/ρ_b (*)
Chromium		1.8		+14	
		31.5		+ 6	
Manganese		6		+ 1.4	
	730	29	210	+ 1.5	1.14
Vanadium	920	9.8	90	+ 9.3	3.6
	very thin (<100)	3,295.	> 3,295	- 9.4	>130.
Titanium		13		+21	
Zirconium	1,125	15.6	174	+ 5	3.96
	869	2,106	18,300	- 4.3	420
Gadolinum	2,485	5.3	132	+ 6.7	0.99
	5,890	5.64	332	+ 5.96	2.48
Thulium		4.6		+13.8	
	Examples of Metal Films Evaporated in Partial Pressure of Argon Mixed with Oxygen at about 10^{-4} torr with little, if any, oxygen present.				
Vanadium	590	16.5	97.4	+14	3.8
Titanium	700 (Estimated)	10.7	≈75	+21	≈1.8
	767	35.2	270	+ 1.95	6.4
Zirconium	1,280	7.7	99	+18	2.3
Gadolinium	1,369	15.7	214	+ 6.2	1.6
Thulium	743	31.6	235	+ 9.5	2.6

* ρ/ρ_b is the ratio of the specific resistivity of the metal film to that of the respective bulk metal. ρ_b values from Metals Handbook, American Society for Metals, Cleveland, Ohio, 1961.

and R/sq. values were 1 to 3300 ohms giving resistivities in the range of approximately 30 to 18,300 microhm-cm. The highest resistivity value was obtained for a zirconium film having a thickness of 869Å and a TCR of $-430 \times 10^{-6}/°C$. It was deposited at a slow rate of about 1 Å/sec. in three successive intervals of 5 minutes at a substrate temperature of 360° C.

The value of $2100 \times 10^{-6}/°C$ is only approximately one half the TCR of a pure metal film and the one of -430×10^{-6} is obviously one for a very impure film. Impurities present at the substrate interface and at the exterior one pollute the film in all instances except those employing the very best vacua obtainable and meticulous substrate cleaning. In addition, molecules of the residual atmosphere are occluded in the film. Hence, virtually no evaporated film is a pure one and we only prepare metal films under most conditions which include varying degrees of impurities. The effects of impurity content may be enhanced by employment of a highly active metal, slow evaporation rates, increased pressures, and control of residual atmosphere in the vacuum chamber.

Of the metal films examined only the ones of zirconium gave resistivities in the range of 10,000 microhm-cm desired; and the TCR of these was approximately $-400 \times 10^{-6}/°C$. These values were obtained at deposition rates of a few angstroms per second with substrate temperatures of 350 to 450° C and bell jar pressures in the 10^{-5} and 10^{-6} torr ranges. A much lower bulk resistivity (ρ_b) of 44 microhm-cm is reported[6] for zirconium.

3. Films Prepared by Evaporation of Metals in Oxygen at Low Pressure

As noted in the preceding section, resistivities of deposited films were increased by slow evaporation rates indicating combination of the atoms of the deposited film with atoms of the residual atmosphere and probably at the substrate surface. Thus, by increasing the oxygen content of the residual atmosphere one would expect to further increase the resistivities of the films. Hence, gadolinium, titanium, thulium, vanadium, and zirconium were evaporated in this manner. In the early experiments, failure to flush entirely the inlet hose of argon resulted in evaporation conducted in a residual atmosphere of argon; this action, in turn, resulted in TCR values for the films as high as those obtained under the best vacuum conditions in the systems employed, and in some cases higher.*

---

* This result suggested that evaporations in residual argon pressures of about 10^{-4} torr would give TCR values higher than normally obtained for films of metals evaporated in vacua of about 10^{-6} torr.

Correction of the oxygen inlet procedure resulted in films of the expected TCR and resistivity values. Table IB gives examples of films of vanadium, titanium, and zirconium prepared in this manner. These films were selected because they show the general range of resistivities for the various materials having near zero TCR. The resistivities of vanadium and titanium films prepared by this manner were about 300 microhm-cm, and a zirconium film possessed a value of about 2400 microhm-cm. A total of some 85 zirconium films were prepared; these had a resistivity range of 99 to approximately 6×10^7 microhm-cm and a TCR range of $(+ 1800 \text{ to } - 6200) \times 10^{-6}/^\circ C$. It is evident that the higher positive TCR value represents that of an essentially metallic film and the low negative one that of a zirconium film composed largely of zirconium oxide or suboxides. The highest resistivity within the $\pm 200 \times 10^{-6}/^\circ C$ range was the 2420 microhm-cm previously noted.

It is possible to plot the resistivities obtained for a series of films of this type against the TCR values and obtain a curve such as that displayed in Figure 13 for zirconium-zirconium oxide films. This curve illustrates a considerable scatter of the data and a very steep slope of the curve in the vicinity of zero TCR. This behavior implies difficulty will be encountered in obtaining a repeatable TCR, and, in general, agrees with experience during this research.

Similar data plotted for titanium and vanadium films deposited by evaporation in oxygen enriched residual atmospheres are exhibited in Figures 14 and 15. Although the slope of the respective curves is much less in the vicinity of zero TCR than for the zirconium, the much lower resistivity values obtainable are obvious.

The few efforts with gadolinium and thulium were non-productive. Data for all the films discussed are given in detail in Table I (Appendix).

It is evident again that zirconium alone of these materials gives promise of high resistivity at low TCR values. However, large variations and the steep slope of the TCR versus resistivity curve near zero TCR indicate a high probability that difficulty encountered in reproducibility of a desired TCR will discount any advantage to be gained by the generally higher resistivity of this material. Although higher in resistivity than the other materials by a factor of 8 or more, it still falls considerably short of the specified value of 10^4 microhm-cm at a TCR of $\pm 200 \times 10^{-6}/^\circ C$.

TABLE I-B

RESISTANCE PARAMETERS OF TYPICAL FILMS PREPARED BY EVAPORATION OF METALS IN OXYGEN AT LOW PRESSURE

(Films were selected with TCR values near zero)

	Thickness (Angstroms)	R/sq (ohms)	Microhm-cm	TCR (10^{-4}/°C)
Vanadium	509	53.6	273	+ 0.07
	237	132.5	314	- 1.66
Titanium	767	35.2	270	+ 1.95
	504	51.6	260	- 0.18
Zirconium	726	84	604	+ 0.01
	1050	230	2420	- 0.88

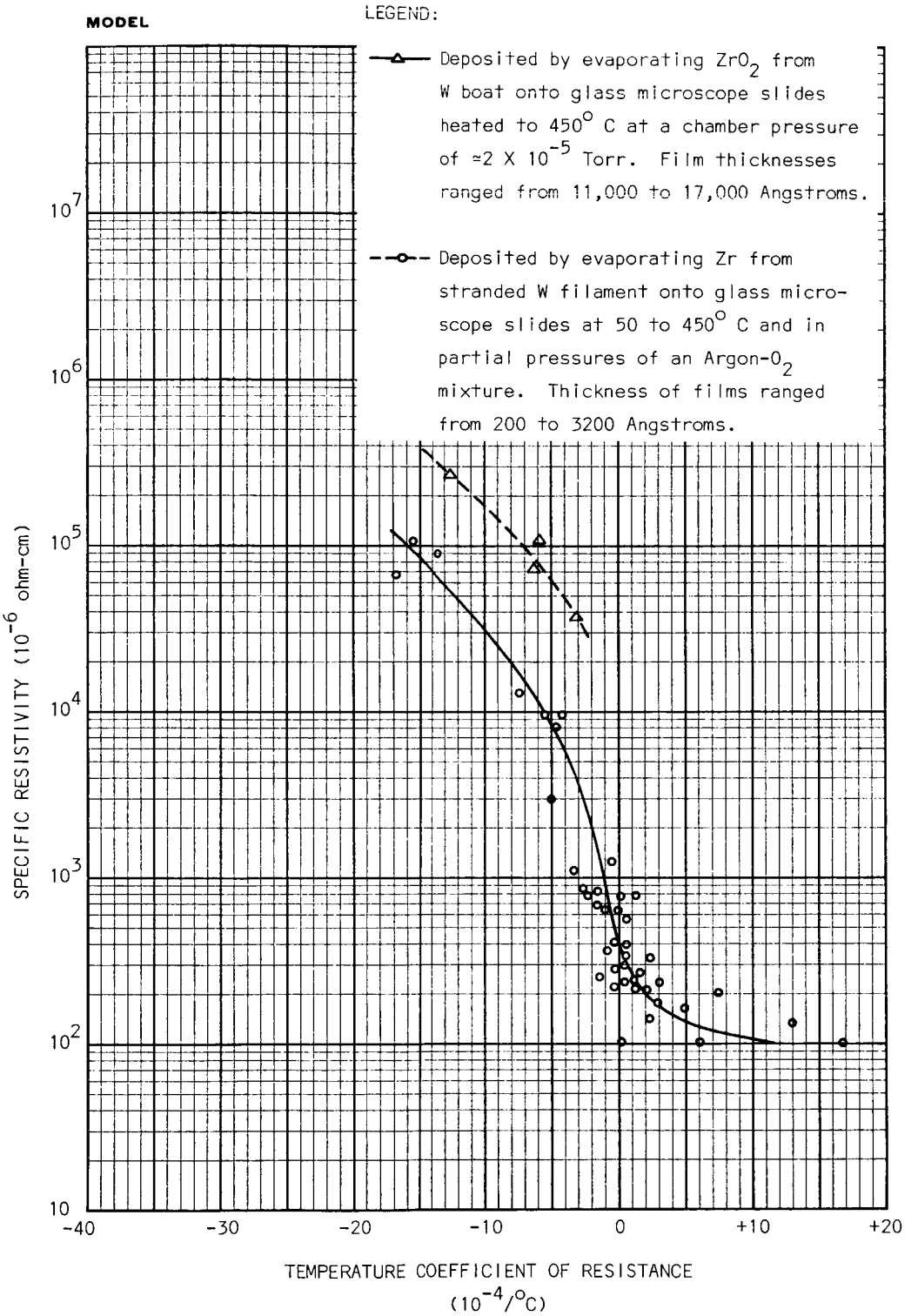

Figure 13. Specific Resistivity vs TCR of Zirconium-Zirconium Oxide Films.

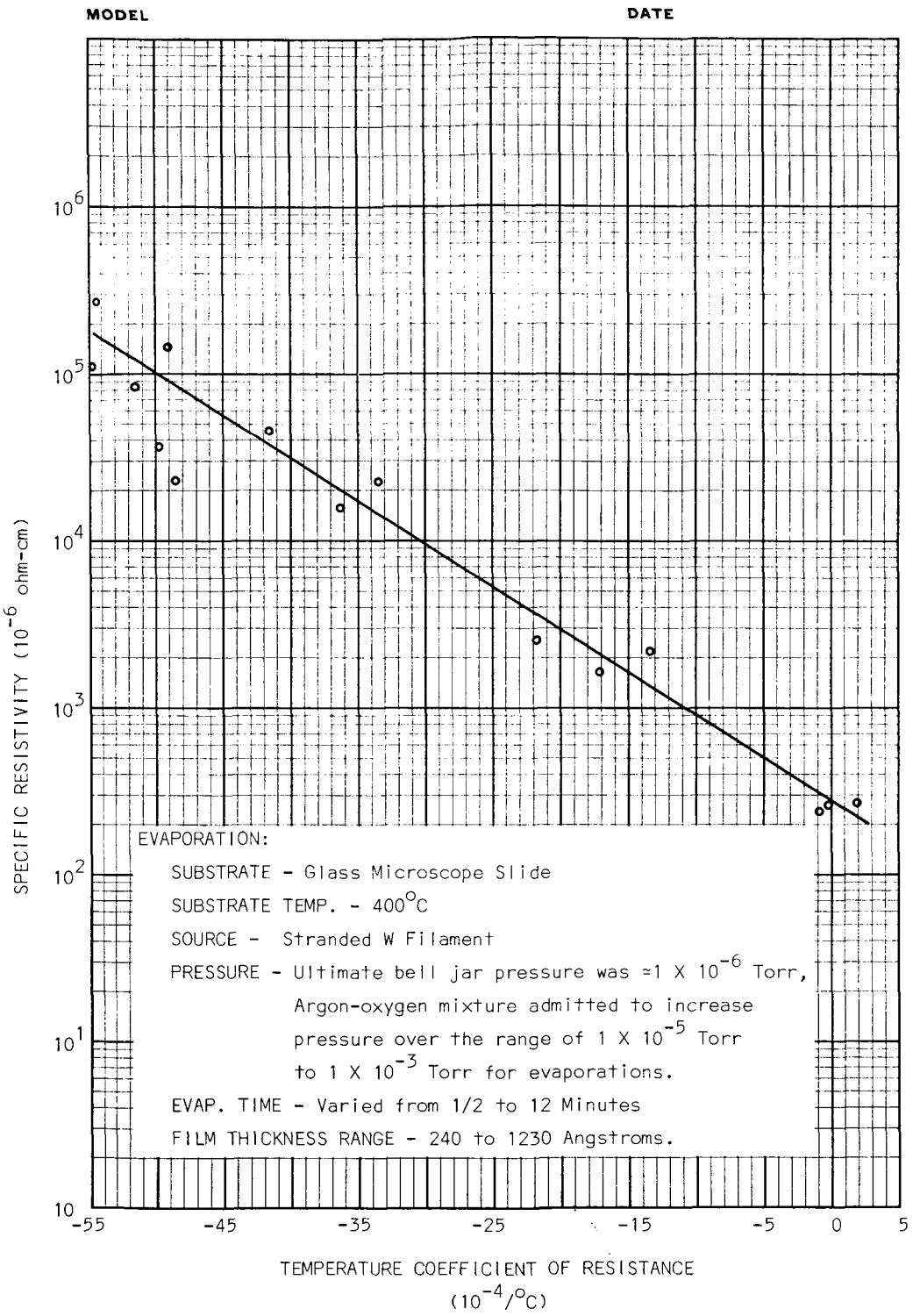

Figure 14. Specific Resistivity vs TCR of Titanium Films Evaporated in Oxygen at Low Pressure.

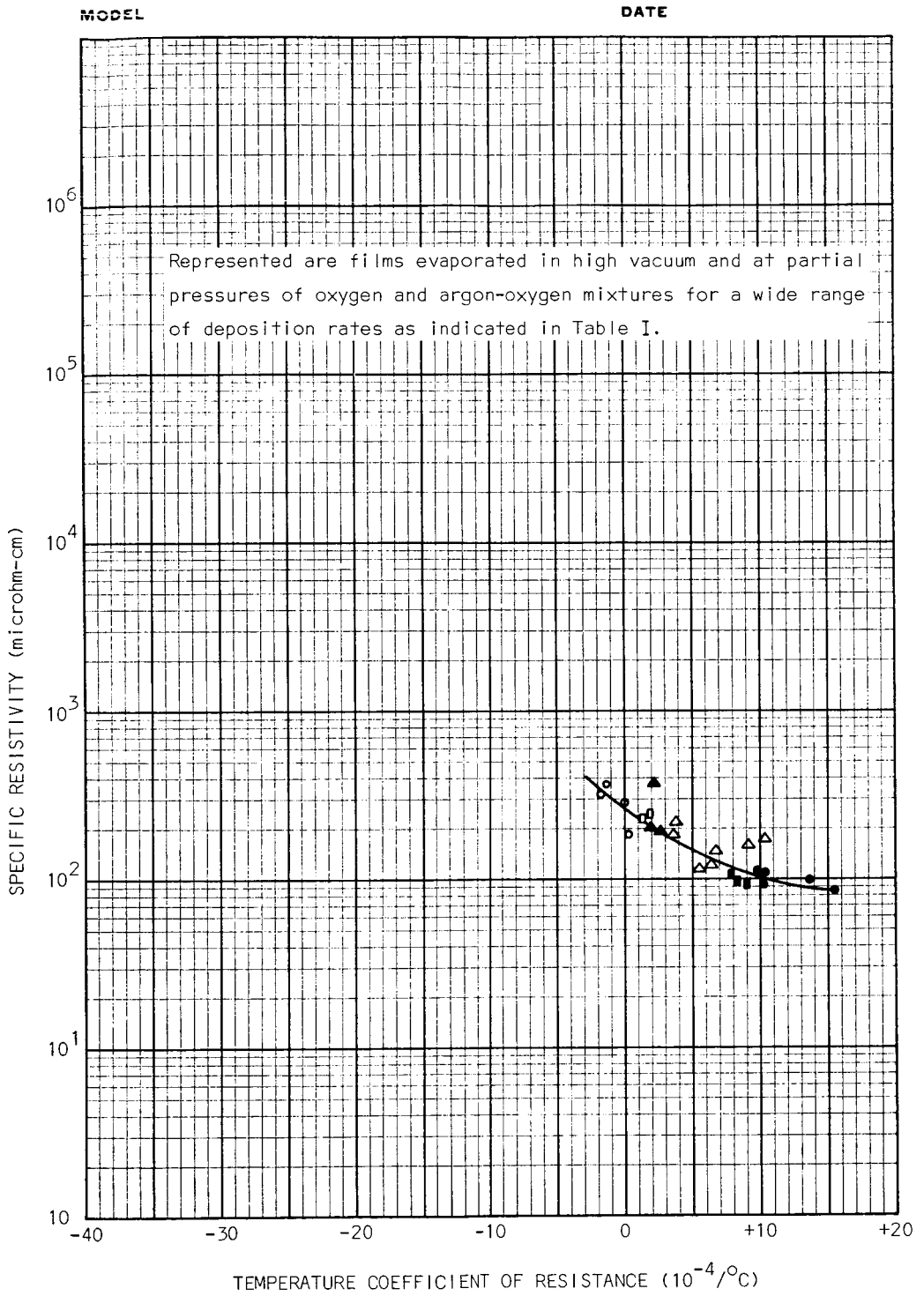

Figure 15. Specific Resistivity vs TCR of Vanadium Films.

4. Films Prepared by Evaporation of Oxides or Suboxides

Films were also prepared by the evaporation of selected metal oxides or suboxides in vacua. These included oxides of tantalum, titanium, vanadium, and zirconium. The data for these films are reported in Table I (Appendix). Although very high resistivities were common, high negative TCR values accompanied the high resistivity values. No indications again were obtained that this procedure was a fruitful course with the single exception that a zirconium oxide film was prepared having a resistivity of 3.82×10^4 microhm-cm and a TCR of $-291 \times 10^{-6}/°C$. The data for the zirconium oxide evaporations are also included in Figure 13. These data indicated that the desired resistor parameters can be met with zirconium compounds of some form (without considering any stability or aging requirements).

5. Films of Metal-Silicon Monoxide

5.1 Introduction: The foregoing experiments did not appear to present fruitful methods of obtaining high resistivity films of low TCR; whereas, experience by others[3, 4, 5] had indicated that metals co-evaporated with silicon monoxide were a possible alternative, presenting, of course, the difficulties in rate control of the dual evaporation sources or the rate control of two materials from a single source.

Although chromium-silicon monoxide was known to be a desirable pair, an interpretative study required the employment of more than one metal-silicon monoxide pair, and studies of films of aluminum, copper, and manganese co-evaporated with silicon monoxide were made. Of these, the chromium-silicon monoxide pair gave resistivity and TCR results more nearly in the range desired and data concerning it will be presented next.

5.2 Films of Chromium-Silicon Monoxide: Some 45 films of chromium-silicon monoxide films were prepared by co-evaporating the materials from a common source in the manner described in Section II-A 1.1, Vacuum System C and in Table I.* The TCR values of these films as shown in Tables I and V** varied over the range $(-3800 \text{ to } +283) \times 10^{-6}/°C$ and the resistivities from about 10^3 to 10^7 microhm-cm. Of particular interest was the fact that thick films with a resistivity of about 10^4 microhm-cm possessed TCR values consistently within the limit $\pm 200 \times 10^{-6}/°C$.

* A discussion of film uniformity and reproducibility control appears in Section II B, 11.

** See appendix for Tables I and V.

Figure 16 displays the general variation of TCR with resistivity for these films. Data on their aging and reliability are presented in Section II B, 8.

5.3 Films of Aluminum-Silicon Monoxide. Sixteen films of aluminum and silicon monoxide were deposited by co-evaporation of the materials and were measured for their electrical properties. The general distribution of the resistivity versus TCR data are shown in Figure 17 and in Tables I and V. Here it will be noted that here is a considerable gap in which no measurements fall between positive and negative TCR values. No attempt was made to obtain points within the gap since the films were generally softer and were less adherent compared to the Cr-SiO films. Only one film with a low absolute TCR was obtained, giving a TCR value of +158 x 10^{-6} at a resistivity of 326 microhm-cm. Hence, this pair did not appear to be a fruitful one to investigate further.

5.4 Films of Copper-Silicon Monoxide. Thirty nine films of copper-silicon monoxide were prepared and examined. Data concerning these are reported in Tables I and V and in Figure 18. An unusual behavior occurred in which there is a gap in the data between relatively highly positive and negative TCR values. Apparently this is a characteristic of the species; for a series of attempts were made to produce films that would give data to fill the gap; and did not appear to be possible. Of those films for which thicknesses were measured, the lowest absolute TCR value obtained was 276 x 10^{-6}/°C. This film had a resistivity of 42 microhm-cm. These films generally exhibited a most singular behavior in that some of them displayed very high resistivities and a positive TCR. In Table I it may be seen that a resistivity of 192,000 microhm-cm was recorded for a film (Cu + SiO-7B-A) possessing a TCR of + 407 x 10^{-6}/°C and one with a resistivity of 13,600 microhm-cm exhibited a TCR of +1100 x 10^{-6}/°C. This anomalous behavior should probably be studied further as to the reason for it and as to its possible usefulness. Both high and low resistivity values were obtained for nearly equal positive TCR values. A wide variation in resistivity was also obtained for negative TCR values. Thus, for the purpose of resistors copper-silicon monoxide films do not fulfill the desired requirements.

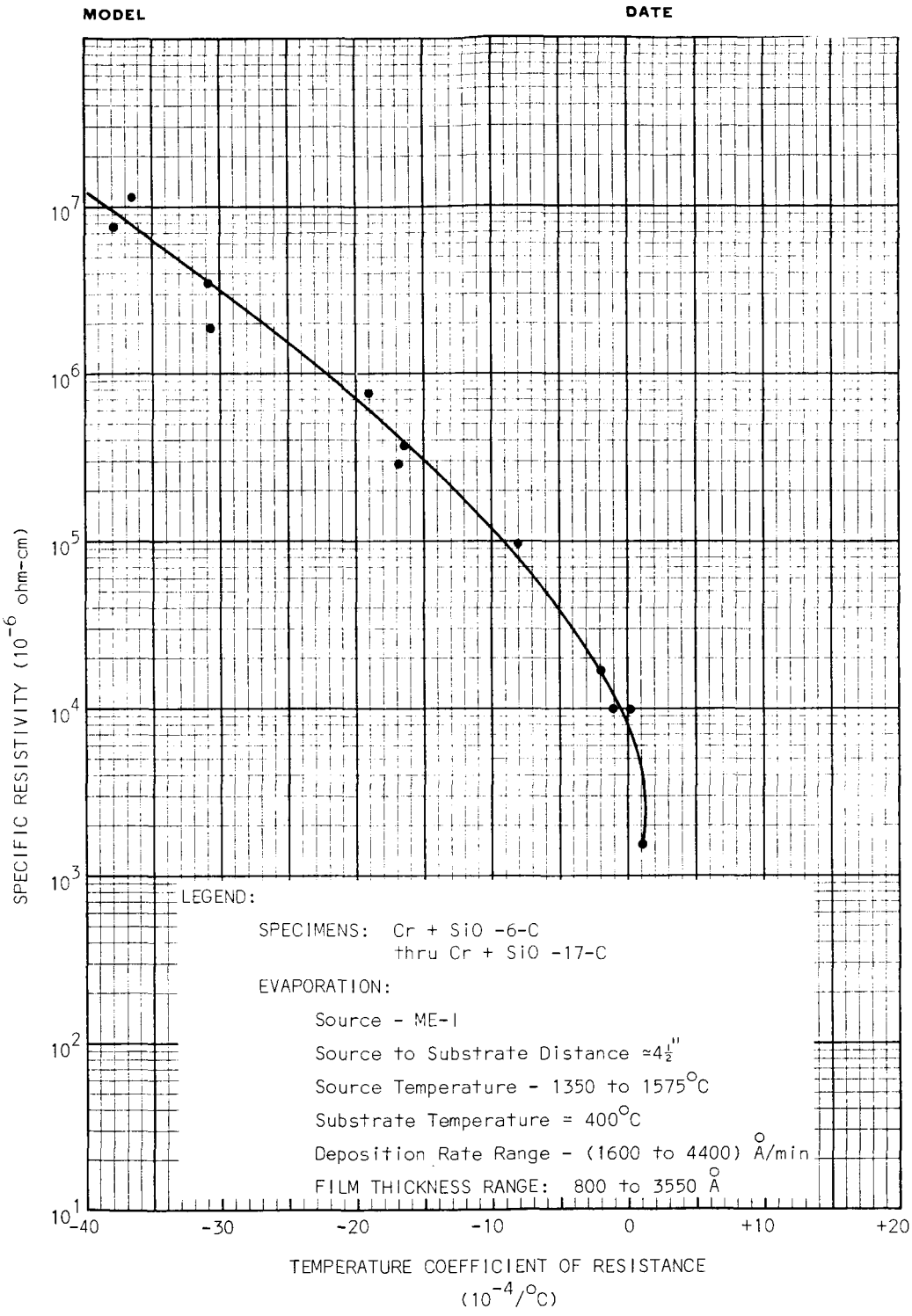

Figure 16. Specific Resistivity vs TCR of Cr + SiO Films.

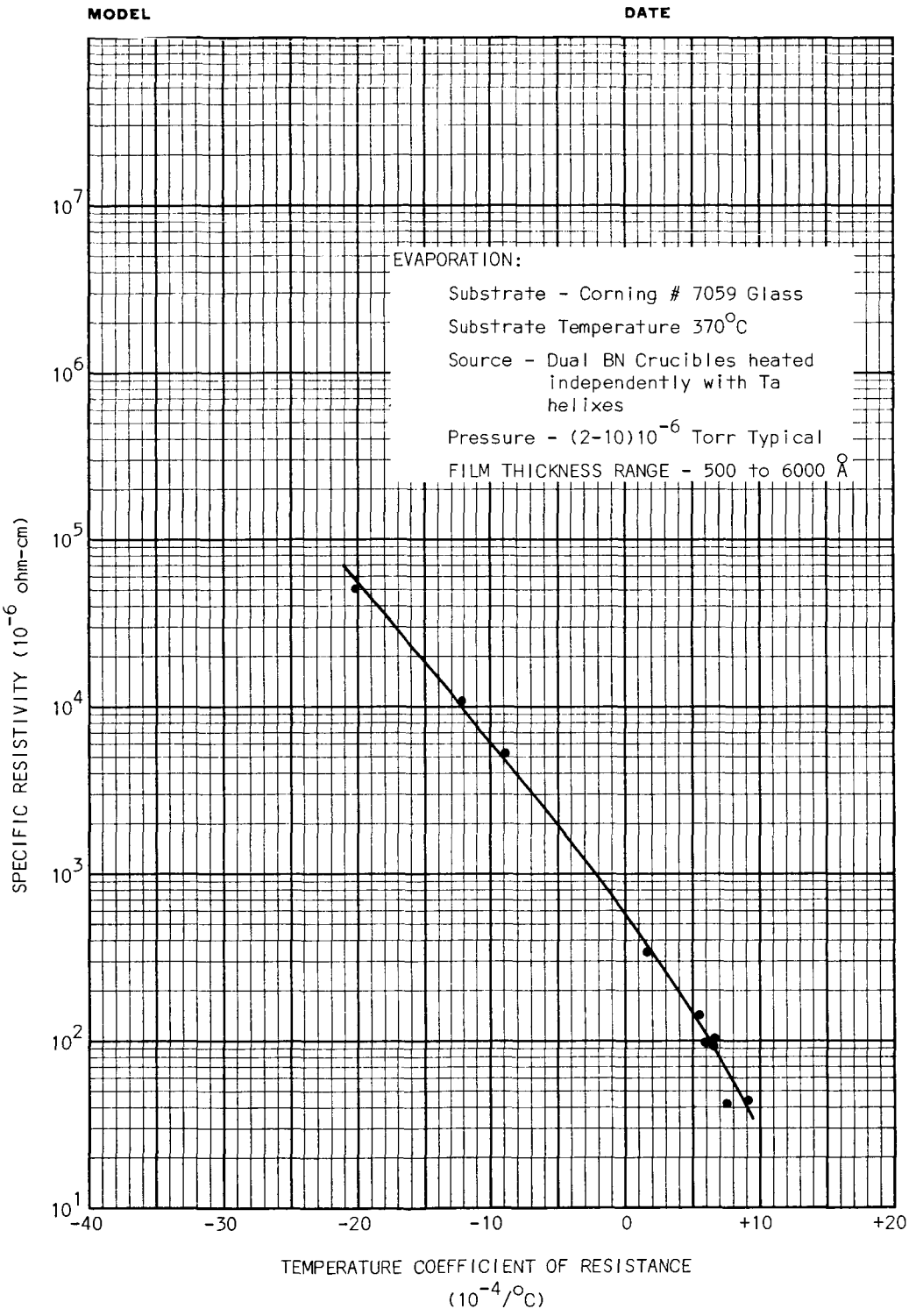

Figure 17. Specific Resistivity vs TCR of Al + SiO Films.

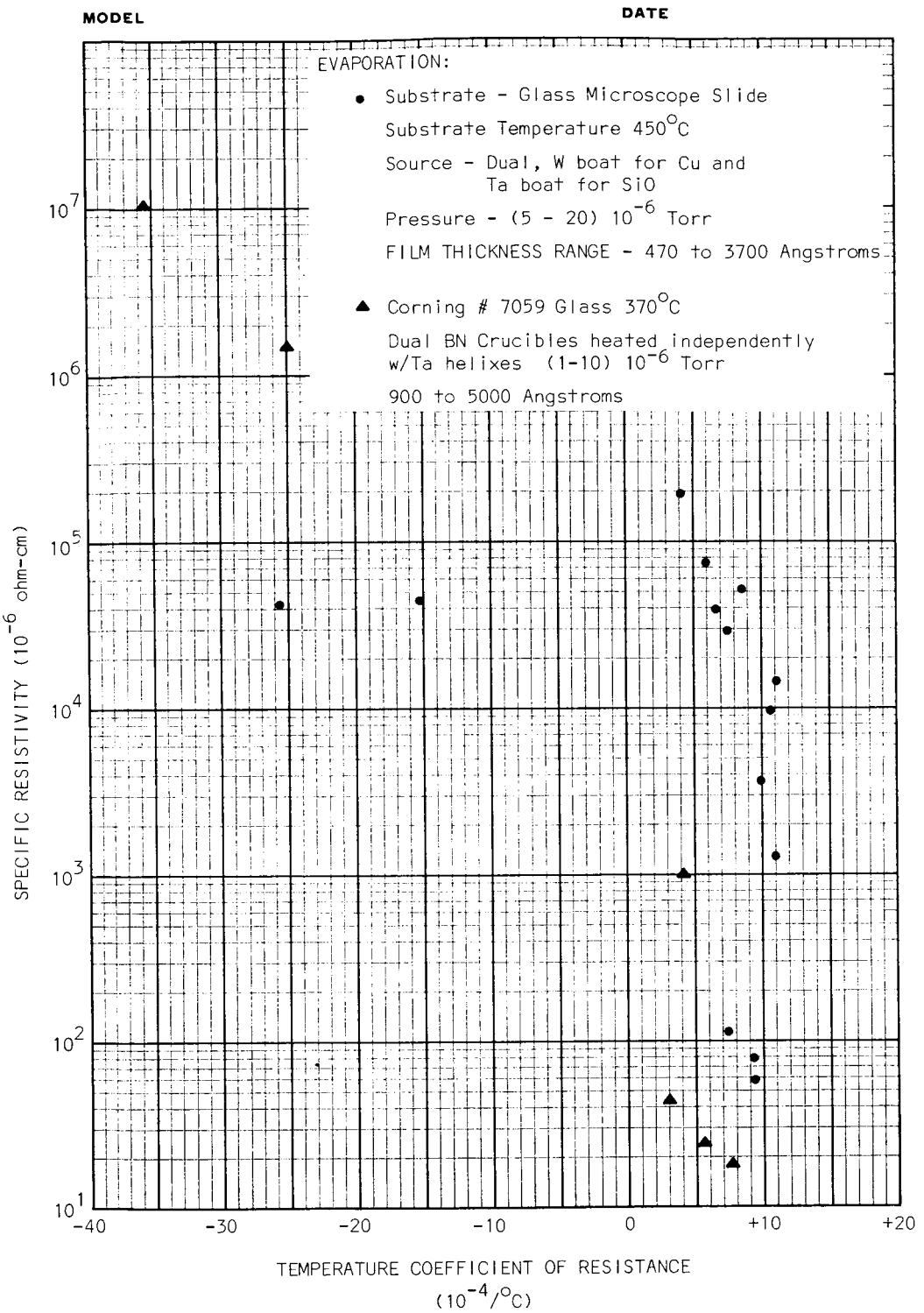

Figure 18. Specific Resistivity vs TCR of Cu + SiO Films.

5.5 Films of Maganese-Silicon Monoxide. Manganese is a near neighbor of chromium in the Periodic Table. It was therefore considered as a suitable metal to co-evaporate with silicon monoxide, especially, since it and SiO sublimate over a common temperature range. Thirty-one films of this mixture were prepared by evaporations from a common source. The parameters of the films are given in Table I (Appendix) and summarized in Table V. Here again both resistivity and TCR varied over large ranges. The highest resistivity at low TCR was 3800 microhm-cm at $-46 \times 10^{-6}/°C$. Data plotted in Figure 19 indicate that resistivities near 10^4 microhm-cm should be obtainable at a TCR of about $-200 \times 10^{-6}/°C$. However, in the aging tests conducted subsequently the Mn+SiO films were less stable than Cr+SiO. In addition, the hardness of the films was inferior to Cr+SiO films.

6. Films of Borides and Silicides of Selected Metals

6.1 Introduction. A literature survey was made on the properties of metal borides and silicides. These materials are refractory and highly resistant to corrosion. The literature search revealed little information on films formed by evaporating the compounds. On the other hand, considerable information is available on the compounds and on films formed by vapor-pyrolysis techniques (references 6, 7, 8, and 9). The borides are metallic in nature and have low electrical resistivities and positive temperature coefficients of electrical resistance.[7] Several compounds of the borides and silicides exhibit semiconducting properties. In general, however, most of the metal borides and silicides are metallic conductors with room temperature resistivities in the range 6-200 microhm-cm.[9] The metal borides of the group IV metals are better electrical conductors than their respective components[6] in most cases. The electrical properties of several of these compounds are listed in references 7, 8, and 9.

The compounds silicon boride (B_4Si), niobium boride (NbB_2), nickel boride (NiB) titanium boride (TiB_2), chromium silicide ($CrSi_2$), and titanium silicide ($TiSi_2$) were obtained from commercial sources. Minimum purity of the materials was 98 percent. The selection of these materials was based on availability from stock and on reported vapor pressure characteristics of the respective constituents, among other properties. Figure 20 shows the vapor

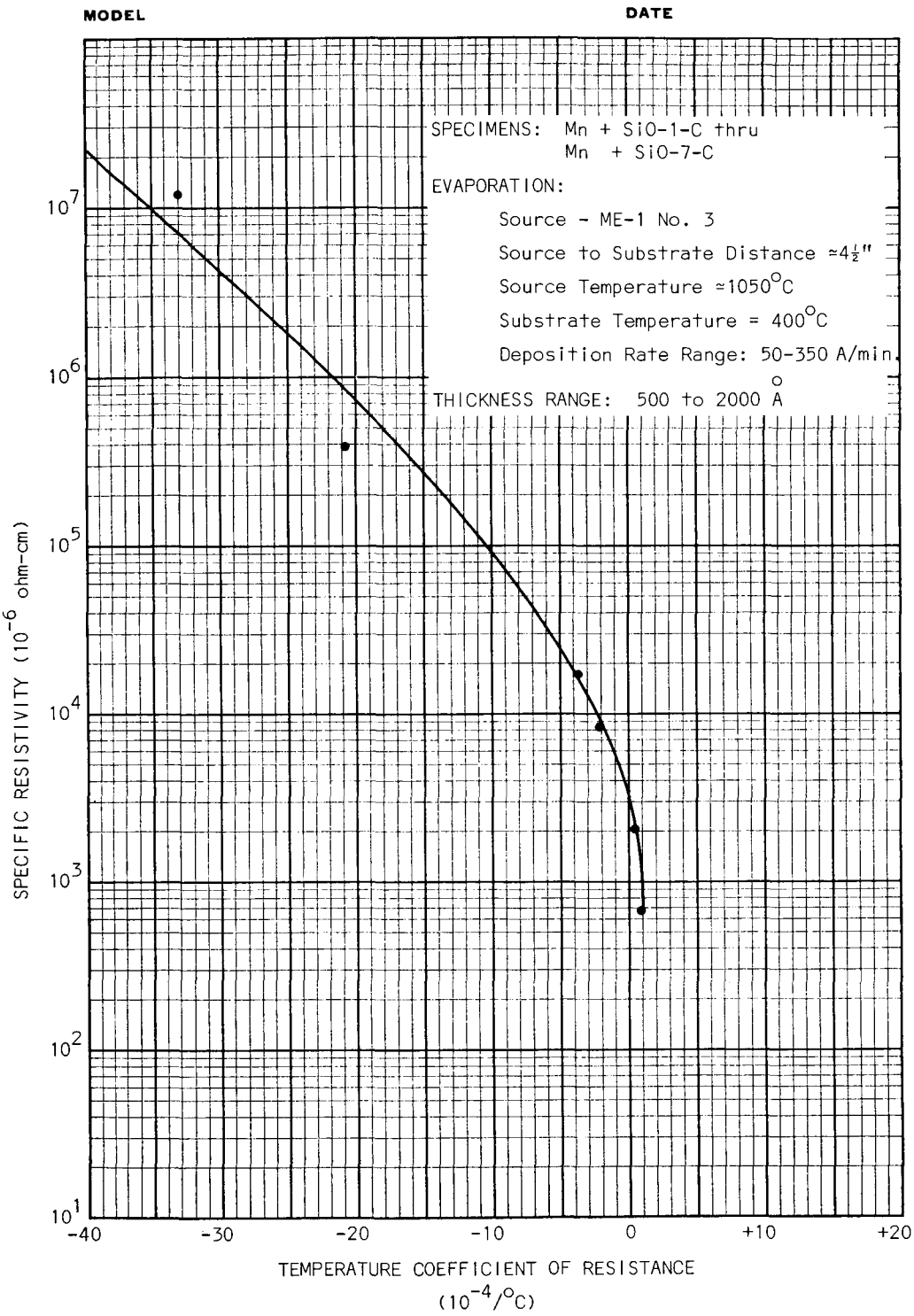

Figure 19. Specific Resistivity vs TCR of Mn + SiO Films.

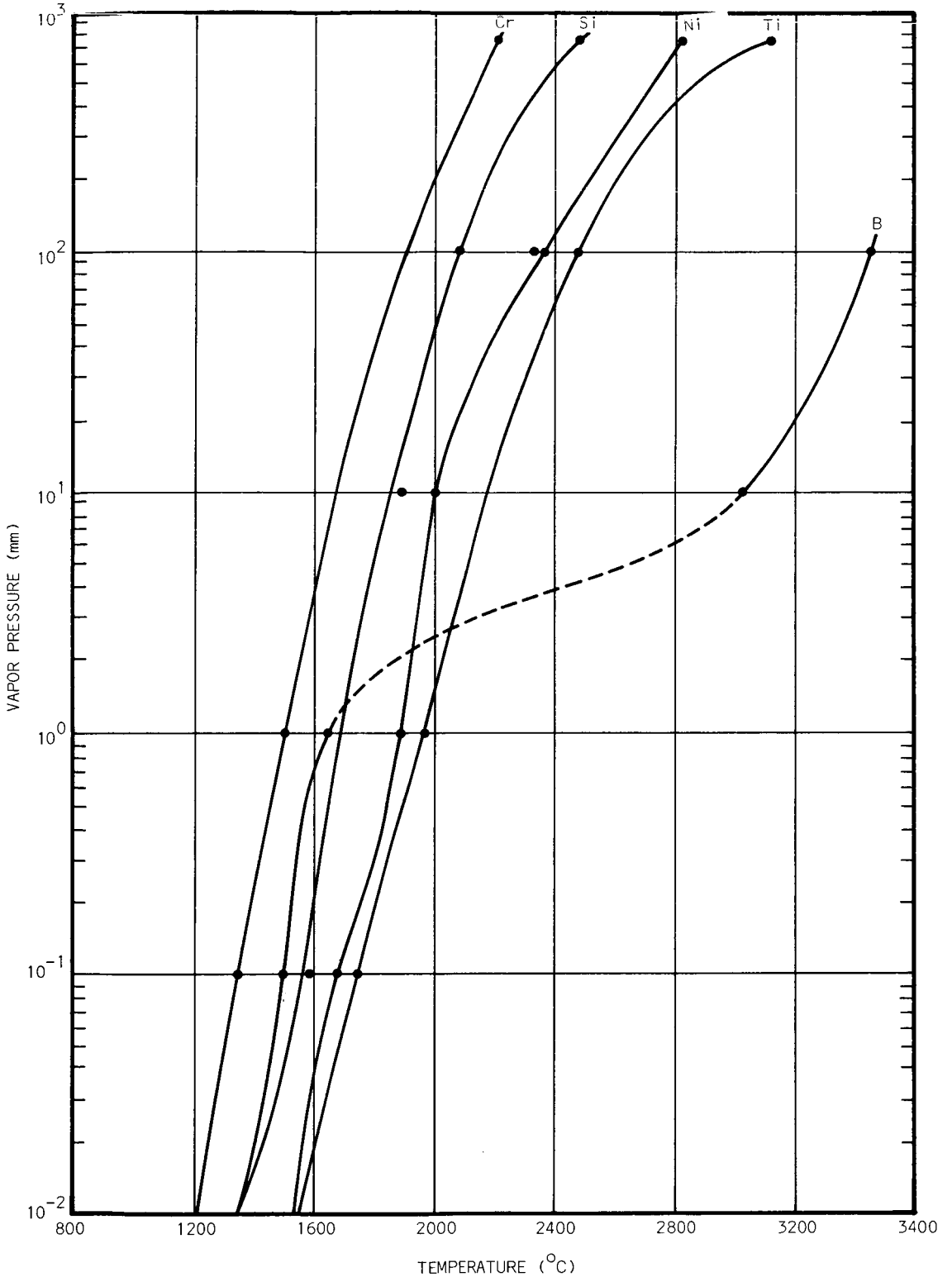

Figure 20. Vapor Pressure vs Temperature for Cr, B, Si, Ni, and Ti.

pressure of Cr, B, Si, Ni and Ti for the temperature range of 1200 to 3400 degrees Centigrade. The figure was prepared from a table of density and vapor pressure of common elements by R. P. Riegert and distributed by Sloan Instruments, Santa Barbara, California. NiB_2 was obtained in lump form from Alfa Inorganics, Inc. The remaining compounds were obtained from A. D. MacKay, Inc., New York City.

At temperatures between 1200 and 1700°C, vapor pressures of Si and B are nearly equal and of a magnitude for practical evaporation in this temperature range; hence, silicon boride should be vaporized with little change in composition. The vapor pressures of Cr, Ti, Ni, and Nb differ considerably from that of Si and B. Thus, considerable partial distillation of these would be expected during evaporations where sufficient disassociation of the compounds occurred. The vapor pressure curve of Boron is quite different from the other elements in the range for practical evaporations, in that, it flattens out in the temperature range of about 1700 to 2800°C. The melting point of 2300°C occurs near the center of the range. The vapor pressure curves of Ni and Ti cross that of Boron near 2000°C. Thus, at the points of intersections stoichiometric evaporations of the compounds should be possible; on the other hand, departure from stoichiometry would probably occur at temperatures above and below the points of intersection. It appeared feasible that the latter feature could be employed to produce high resistivity films of the boride materials by evaporating at temperatures which would result in boron enriched films. A number of elements with vapor pressure curves that intersect the boron curve in the region of low slope of the vapor pressure versus temperature plot are Pd, Y, V, and Zr. In general, the silicides are less refractory than the borides; therefore, materials of this species with relatively low melting points can be more readily evaporated. Also, silicide film resistors were expected to be more stable than the others because of the protective features of silicon oxide. Though a very limited number of films were prepared of the compounds, most of the discussed effects were observed to some degree.

6.2 Preparation of the Films. Electron beam apparatus was used to evaporate the compounds $CrSi_2$, B_4Si, NbB_2 and TiB_2. In addition, evaporations of $CrSi_2$ - $TiSi_2$ and $CrSi_2$ - B_4Si mixtures were made by electron beam techniques.

$CrSi_2$ and $TiSi_2$ were evaporated from resistively heated tungsten boats; similarly, Ni_2B was evaporated from tungsten baskets. Stable high resistivity films were prepared from most of the materials, and in general, the stability was enhanced by post-deposition baking of the films at elevated temperatures in air.

The electron beam evaporations were made with a Veeco Ve-B6C system. Evaporant charges were placed in a massive copper crucible. The electron gun was spaced at a distance of 10 inches from the crucible. At this distance, the beam diameter was about 1/2 to 3/4 inches with maximum electron density over a 3/8 inch diameter spot at the center of the beam The broadness of the beam aided in outgassing and melting powdered charges; however, due to the beam dispersion, the power density available at the crucible was diminished. The relatively large gun to evaporant distance minimized contamination of the gun from evaporant vapors. Contamination was minimized further by having a large metal plate with a small exit hole for the beam between the crucible and gun to shield the gun from evaporant vapor. These measures eliminated the need of frequent cleaning of the gun. The substrate to crucible distance was 8 inches for all of the electron beam evaporations. Figure 3 illustrates the arrangement of the apparatus in the bell jar. Upward evaporations were made with the tungsten sources at a substrate to source distance of about 4 inches.

Soon after deposition, the resistive parameters (resistance, R per square, and TCR) of the films were determined. Typical specimens were then selected for aging studies. To complete extended aging studies, measurements were continued for about two months beyond the originally specified contract period. The effects of post deposition baking on the films and subsequent stability were examined, also. Detailed fabrication and resistive parameter are given in Table I and summarized in Table V. Effects of post-deposition baking are shown in Tables II and II A.* A summary of aging results is given in Table III. The more pertinent aspects are discussed subsequently. In these studies no evaluations were made of noise characteristics or of thermoelectric potentials. The latter behavior should be examined, in particular, for boride films. In general, the films were not examined for semiconductor

* For Table IIA - see Appendix.

TABLE II

SUMMARY OF RESULTS OF POST-DEPOSITION BAKING OF FILMS

Specific Resistivity (microhm-Cm)	Resistor Series	No. Of Specimens	ΔR (%)			ΔTCR (%)			Remarks
			Lo	Avg	Hi	Lo	Avg	Hi	
			Baked at 200°C 6 3/4 hours						
$(.5 < 1 \leq 5)10^2$	Mn + SiO	2	14	14.5	15	24.9	20		
$(.5 < 1 \leq 5)10^3$	Mn + SiO	2	12	13	14	24.9	66.4	108	
			Baked at 250°C for 6 1/2 & 10 1/2 hours						
$(.5 < 1 \leq 5)10^2$	Cr + SiO	1		0			32		
	Mn + SiO	1		47			31		
$(.5 < 1 \leq 5)10^3$	Cr + SiO	1		0.3			8		
	Mn + SiO	2	66	68	70	17.2	26.1	35	
			Baked at 300°C ± 25°C for 3 to 16 hours						
$(.5 < 1 \leq 5)10^2$	Cr + SiO	2	0.0	0.02	0.04	0	10	19	At 325°C - 7 Hrs.
	$CrSi_2$	2	0.47	2.34	4.2				At 300°C - 5 Hrs.
	V	2	698.	5,210.	9,720.	4600	7000	9500	At 325°C - 10 Hrs.
$(.5 < 1 \leq 5)10^3$	$CrSi_2$	1	15.						At 300°C - 5 Hrs.
	$CrSi_2 + TiSi_2$	2	2.29	5.2	8.1				At 300°C - 4 1/2 Hrs.
	$TiSi_2$	2	27.	28.	29.				At 300°C - 7 Hrs.

(Continued)

TABLE II (Continued)

SUMMARY OF RESULTS OF POST-DEPOSITION BAKING OF FILMS

Specific Resistivity (microhm-Cm)	Resistor Series	No. of Specimens	ΔR (%)			ΔTCR (%)			Remarks
			Lo	Avg	Hi	Lo	Avg	Hi	
$(.5 < 1 \leq 5)10^4$	Cr + SiO	2	25	33	41	81	81	81	At 325°C - 7 Hrs.
$(.5 < 1 \leq 5)10^5$	$CrSi_2 + B_4Si$	1	0.71						At 300°C - 4 1/2 Hrs.
	NbB_2	1	170.						At 300°C - 3 Hrs.
$(.5 < 1 \leq 5)10^6$	Cr + SiO	4	0.7	5.5	13	20	370	1350	At 275°C - 16 Hrs.

properties. These are not likely to exist in films with TCR values of low magnitude but would be suspected to occur in films of highly negative TCR or those having resistivities approaching that of semiconductors.

6.3 Silicon Boride Films. The electron beam apparatus was employed to evaporate silicon boride (B_4Si). A relatively thick film was deposited; it was transparent and had a yellowish to brownish appearance. An infinite resistance was obtained with ohmmeter probes applied to the film surface. Hence, this material alone is not believed to be a likely one for resistor fabrication. The film showed considerable resistance to scratching with a steel point; however, the hardness and adherence were not as good as that usually experienced with SiO films.

6.4 Niobium Boride Films. Niobium boride film resistors were deposited by evaporating the compound NbB_2 from a massive cooper crucible using an electron beam gun to heat the evaporant. Fifteen resistors NbB_2 -1 thru 15 were fabricated by this method of evaporation. Glass substrates, Corning type 7059, were used for specimens 1 and 2. Polished quartz substrates were used for specimens 3 thru 14, and a glass microscope slide was used for 15. The substrates were heated to 250°C before initiating the evaporation process. Deposition periods of 10 minutes in length were used for the first eight specimens in the series. The remaining specimens were deposited in one to three minute intervals. According to reference (7), the resistivity of NbB_2 is 65.5 microhm-cm, and the compound has a positive temperature coefficient of resistance. Except for specimen NbB_2 -9, resistivity of the niobium boride films ranged from 1.03×10^5 to 1×10^6 microhm-cm with highly negative temperature coefficients of resistance, see Tables I and V. A much lower TCR value of -4.76×10^{-4}/°C was obtained for NbB_2 -9; during this evaporation, the stainless steel shutter did not clear the path of the electron beam, and a portion of it was melted. Evidently, this accounted for the lower TCR value obtained.

In Table I, it can be seen that the TCR values shifted in a positive direction with increasing evaporant temperature corresponding to increasing electron beam power used to heat the evaporant. To obtain niobium boride films with small TCR values by this technique of evaporation, it is indicated that evaporant temperatures exceeding 2300°C will be required. The electron

beam power fluctuated considerably during these evaporations. To obtain control over the resistivity of films deposited by this method, precise control of the electron beam power will be necessary. A plot of specific resistivity versus TCR for this species is shown in Figure 21.

From the variations in TCR and resistivity with beam power, it is apparent that distillation effects resulted in varying degrees of boron enrichment of the films compared to the compound formulation of the evaporant. This could not be verified by electron diffraction measurements. The electron diffraction patterns indicated that the films were amorphous.

Aging studies of specimens selected from the niobium boride series were conducted. Unprotected resistors and resistors baked in air at 300°C were stored in a 125°C oven to observe subsequent stability with time. The films have aged relatively poorly. The resistance of films with resistivities in the range of 10^5 to 10^6 microhm-cm increased an average of 125 percent during post-deposition baking at 300°C for 3 hours in air, and subsequent increases in value of 8 percent were obtained after aging for 1000 hours at 125°C. Niobium boride films of similar resistivities but unprotected increased in resistance from 4 to 9 percent after 1000 hours at 125°C; lower resistivity specimens of this series may show better aging characteristics. Figures 22 and 23 show typical aging during 1000 hours at 125°C. Post-deposition baking in air did not stabilize the films of this series. One would expect to obtain adequate passivation of the films with an over-layer of SiO.

It was interesting to note that the films of the first 8 specimens in the niobium boride series exhibited transparency to great thickness ranges. For example, NbB_2-1 and 2 had a thickness of 2,325 and 3,480 Angstroms, respectively, and to the naked eye showed a transparency similar to that normally observed for pure metal films of a thickness of about 1000 Angstroms. Pure metal films become opaque at a thickness of about 1500 Angstroms.

It is probable these films will have high thermoelectric coefficients; however, no tests were made to establish their thermoelectric properties or their sensitivity to light.

6.5 Nickel Boride Films: Evaporations of Nickel Boride, Ni_2B, were made from tungsten baskets in high vacuum. The evaporant was in the form of

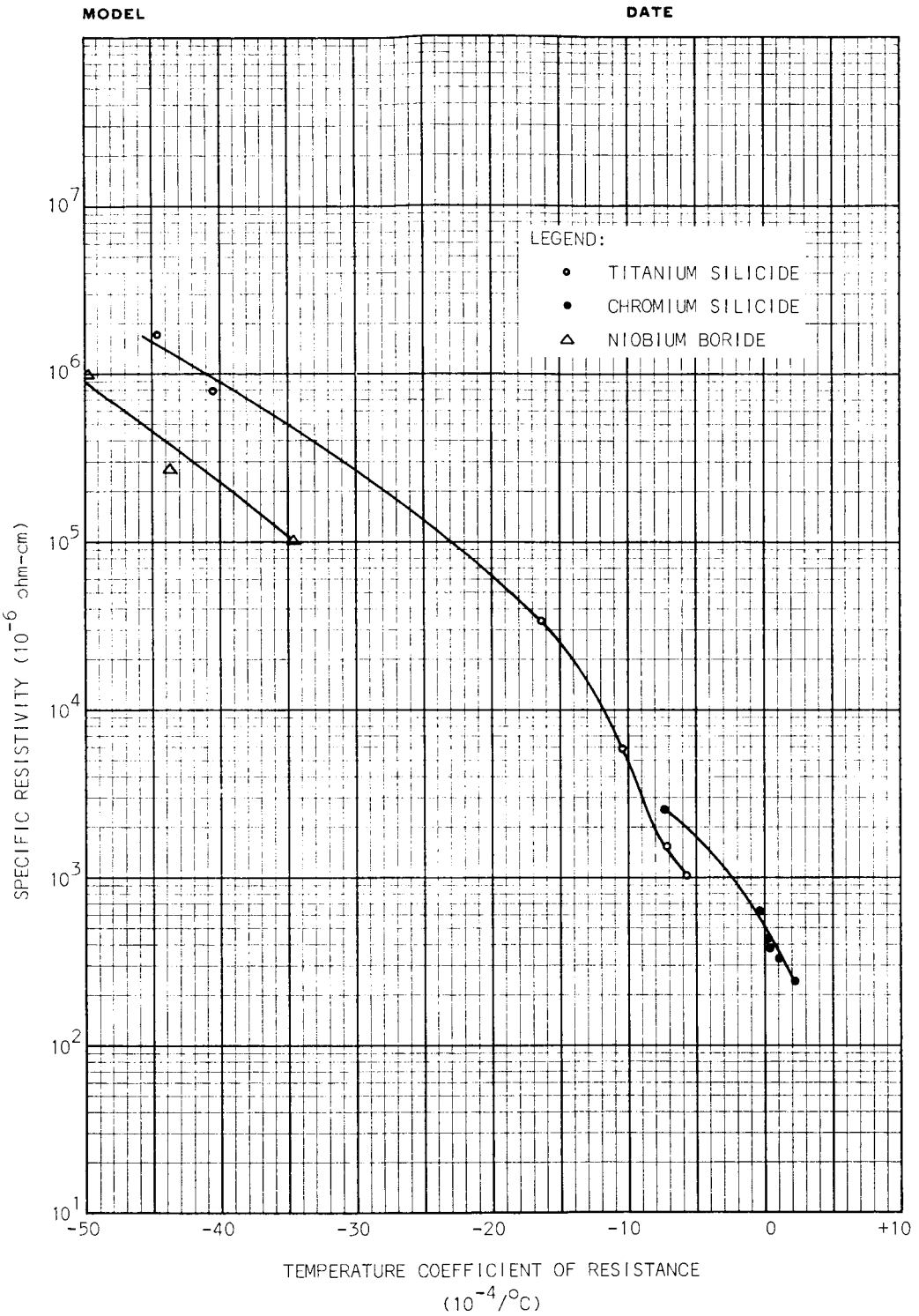

Figure 21. Specific Resistivity vs TCR of Boride and Silicide Films.

SPECIMEN: NbB_2 -5

R-FILM FABRICATION DATE: 11/10/66

PROTECTIVE MECHANISM: None

DATE:

PARAMETERS:

INITIAL RESISTANCE: 84,500 ohms

RESISTIVITY: R/sq = 8,450 ohms

$\rho = \approx 2.4 \times 10^5$ microhm - cm

INITIAL TCR: $-40.3 \times 10^{-4}/^{\circ}C$

AGING:

TEST OR TREATMENT	DATE (FROM) (TO)	ΔR DURING TEST (%)	TCR AT END OF TEST ($10^{-4}/^{\circ}C$)
TCR cycle #1	≈30' to 125°C in AIR	-0.32	
125 °C Air Storage	For 1000 hours	+4	

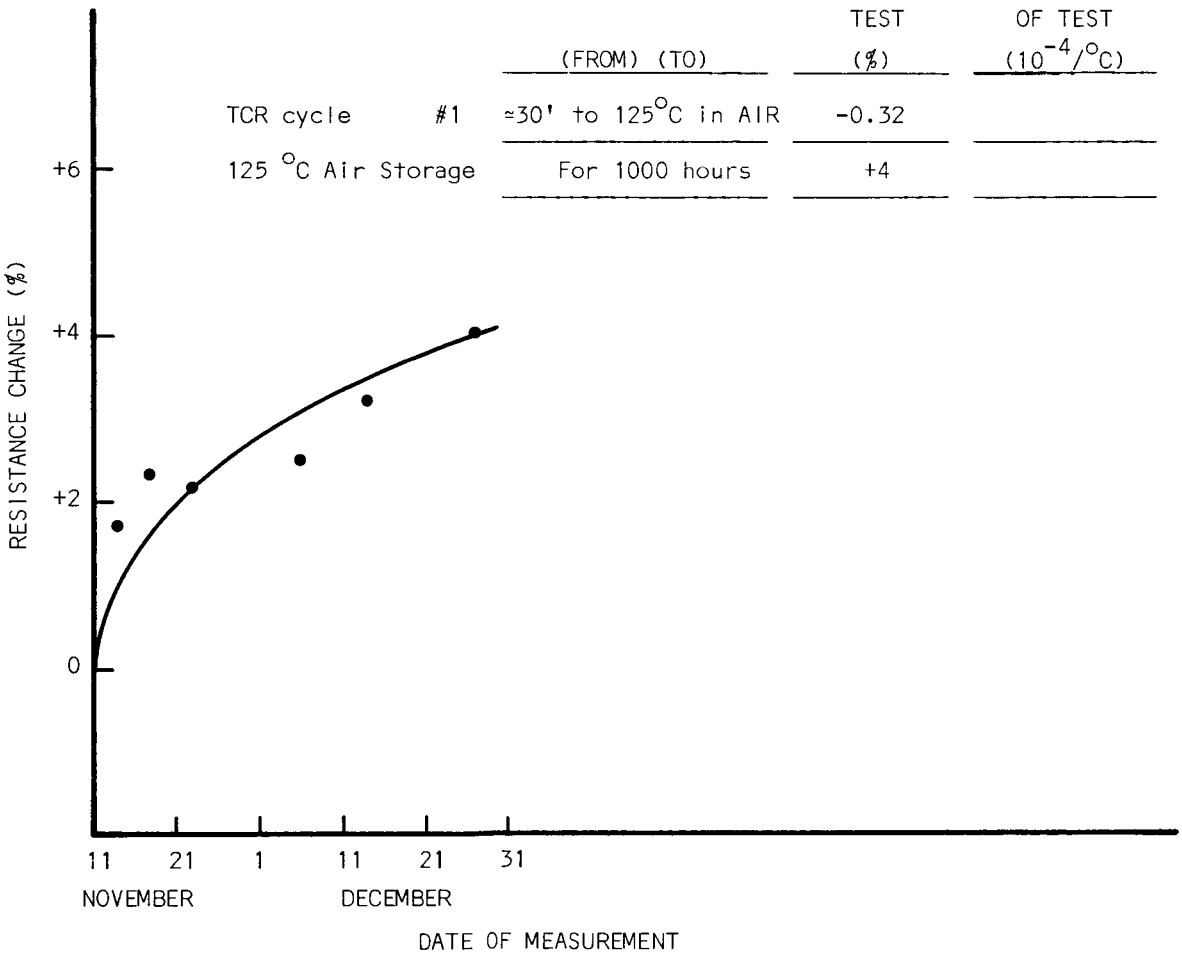

Figure 22. Resistance Aging at 125°C in Air of a Typical Unprotected NbB_2 Film.

SPECIMEN: NbB_2-8

R-FILM FABRICATION DATE: 11/10/66

PROTECTIVE MECHANISM: Air Bake

DATE:

PARAMETERS:

INITIAL RESISTANCE: 54,010 ohms

RESISTIVITY: R/sq = 5,400 ohms

$\rho = \approx 8 \times 10^4$ microhm - cm

INITIAL TCR: $-32.6 \times 10^{-4}/^{\circ}C$

THICKNESS:

COMPOSITION:

AGING:

TEST OR TREATMENT	DATE (FROM)	DATE (TO)	ΔR DURING TEST (%)	TCR AT END OF TEST ($10^{-4}/^{\circ}C$)
Air Bake: 300 °C 3 hrs	11/11/66		+170	
TCR cycle #1	≈30' to 125°C in AIR		-0.02	(Before Bake)
125 °C Air Storage	For 1000 hours		+8	

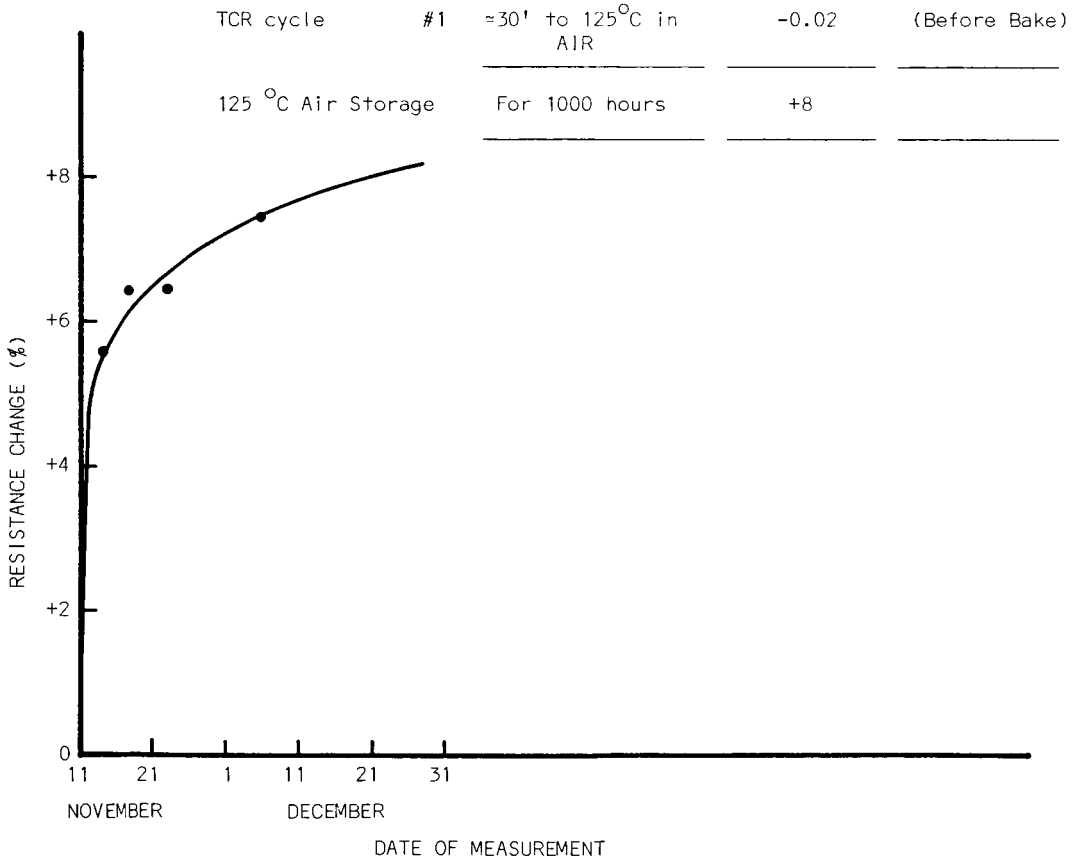

Figure 23. Resistance Aging at 125°C in Air of a Typical NbB_2 Film Post-Baked in Air.

SPECIMEN: $CrSi_2$ -9

R-FILM FABRICATION DATE: 10/19/66

PROTECTIVE MECHANISM: None

DATE:

PARAMETERS:

INITIAL RESISTANCE: 53.7 ohms

RESISTIVITY: R/sq = 53.7 ohms

ρ = ≃450 microhm - cm

INITIAL TCR: +0.59 X $10^{-4}/^{\circ}C$

AGING:

TEST OR TREATMENT	DATE (FROM) (TO)	ΔR DURING TEST (%)	TCR AT END OF TEST ($10^{-4}/^{\circ}C$)
TCR cycle #1	≃30' to 125°C in AIR	+0.2	+0.59
125 °C Air Storage	For 1000 hours	-0.6	

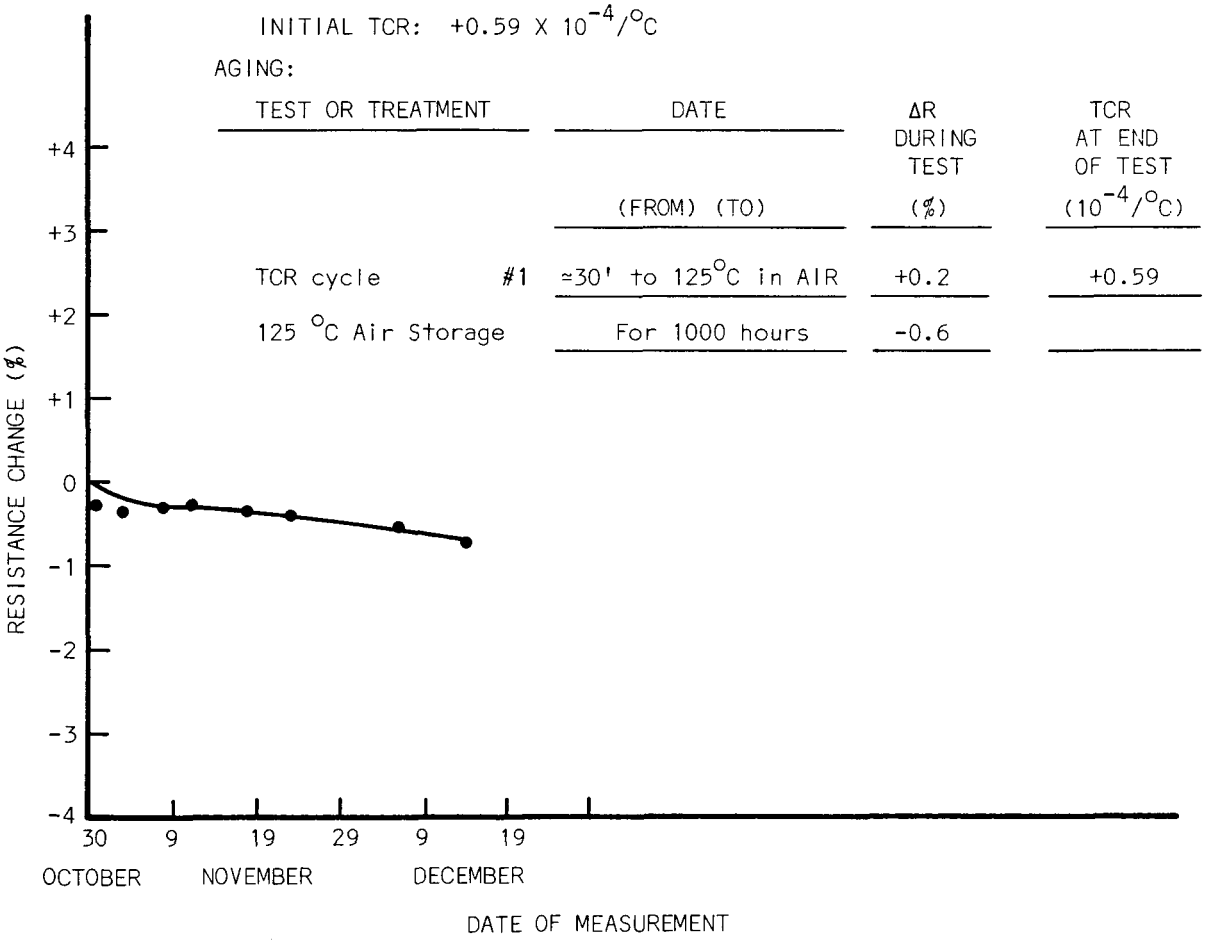

Figure 24. Resistance Aging at 125°C in Air of a Typical Unprotected $CrSi_2$ Film.

SPECIMEN: $CrSi_2$ -4

R-FILM FABRICATION DATE: 10/10/66

PROTECTIVE MECHANISM: Baked in Air

DATE:

PARAMETERS:

INITIAL RESISTANCE: 53.3 ohms

RESISTIVITY: R/sq = 53.3 ohms

ρ = ≈450 microhm - cm

INITIAL TCR: $+0.59 \times 10^{-4}/^{\circ}C$

THICKNESS:

COMPOSITION: Cr_3Si

AGING:

TEST OR TREATMENT	DATE (FROM) (TO)	ΔR DURING TEST (%)	TCR AT END OF TEST ($10^{-4}/^{\circ}C$)
Air Bake: 300 °C 5 hrs	10/25/66	+4.2	
TCR cycle #1	≈30' to 125°C	0.0	Before Air Brake
125 °C Air Storage	For 1000 hours	+0.2	

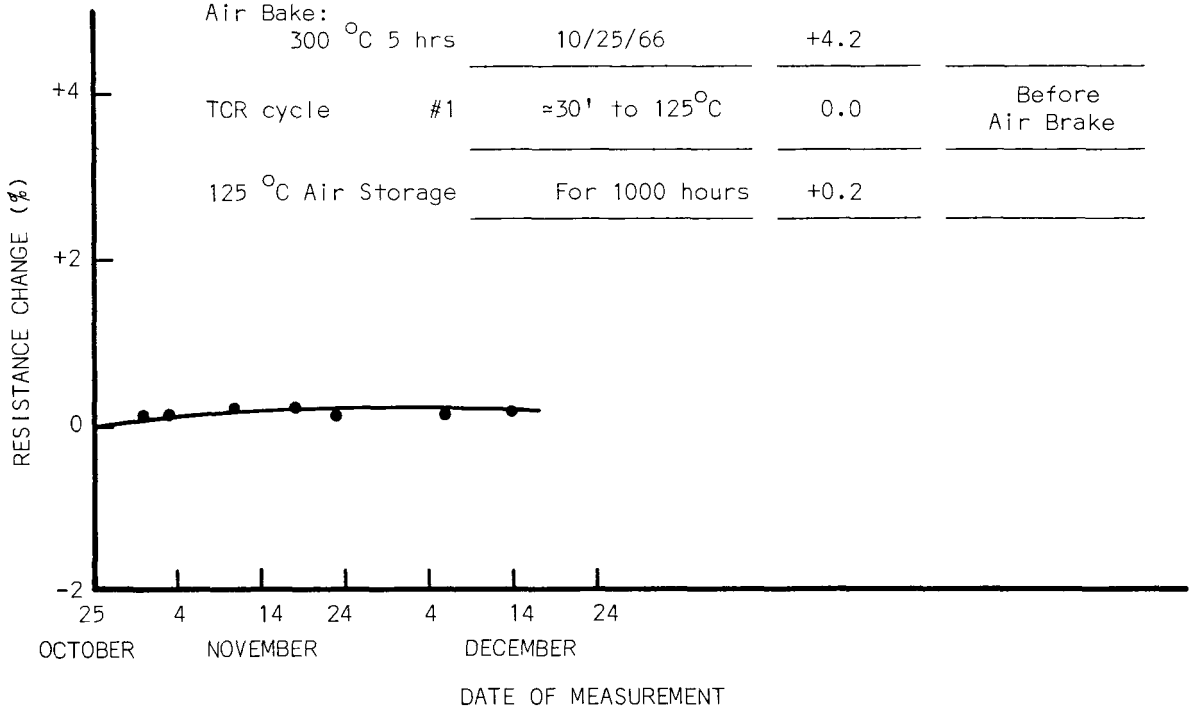

Figure 25. Resistance Aging at 125°C in Air of a Typical $CrSi_2$ Film Post-Baked in Air.

chunks ranging from small pellets to a nominal diameter of 3/8 inches. The evaporant melted at a basket temperature of about 1200°C. According to (9), the melting point of Ni_2B is 1050°C. Specimen Ni_2B -1 was evaporated at temperatures near the melting point, and the evaporation rate was slow which resulted in a very thin film as indicated in Table I. Specimens Ni_2B -2 were evaporated at filament temperatures exceeding 1300°C but less than 1600°C. Electron diffraction analysis of grids coated similtaneously with the resistors indicated a composition of nickel. As indicated in Tables I and V the resistivity values were relatively low, and the TCR values were relatively high. It is apparent that stoichiometric Ni_2B films can not be obtained readily by evaporating the material at the source temperatures employed. Possibly source temperatures higher than 1600°C will result in nickel boride films more nearly approaching stoichiometric properties.

Extended aging studies of these films were not conducted. During the initial TCR measurements, the films increased in resistance by small percentages.

6.6 Titanium Boride. Of the silicide and boride compounds studies, Titanium Boride, TiB_2, is one of the more refractory. Its melting point is about 2950°C. However, resistive films of the material were deposited on soft glass substrates by sublimation in high vacuum at considerably lower temperatures than the melting point. Five resistors were fabricated in groups of two and three in two electron beam evaporations from a powdered charge of TiB_2. The respective substrate temperatures were 260°C and 370°C. The specimens were cooled to 75°C before removing from the vacuum chamber. The films of both depositions were severely reticulated in areas of direct contact with the glass substrate; however, no reticulation occurred where the films were over the pre-deposited chromium-gold terminals.

The TCR values of the films in the second deposition ranged from -430 ppm/°C to -172 ppm/°C. Because of surface roughness of the reticulated films thickness measurements could not be made with the interferometer used for this purpose; however, by visual observation it was obvious that all three films were much greater than 1500 Angstroms thick. Thus, from the known R/sq values the specific resistivity of the films were estimated to be $> 10^4$ microhm-cm.

Electron diffraction patterns were made of films deposited on grids during the two depositions. A strong Ti line was observed for the first deposition at (2 to 5.6)KW beam power. A pattern could not be obtained for the second deposition, and no identification of film composition was made. The beam power during this deposition was in the range (2 to 3.5)KW.

During the TCR measurements, the films were cycled to 125°C in air over an interval of 20 to 30 minutes, and the films increased in resistance by an average value of 11 percent. The poor aging probably resulted from the large area subject to oxidation due to high porosity and as a result of reticulation. The films were not placed on extended aging tests.

Films deposited at 370°C were somewhat less reticulated than those deposited on 250°C substrates. This indicated that the reticulation could probably be eliminated by using considerably higher substrate temperatures. The highly refractory nature of this material, its potentially inherent protection offered by the formation of a tenacious surface layer of oxide composed of oxides of titanium and boron, and its potentially attainable resistivity and TCR characteristics by evaporation or sputtering are very desirable features. The material is very promising for film resistor application provided a proper choice of substrate and substrate deposition temperature can eliminate the reticulation problem encountered.

6.7 Chromium Silicide Films. Chromium silicide film resistors were deposited by evaporating the compound $CrSi_2$ from tungsten boats at pressures of about 1×10^{-5} torr. The material sublimated at boat temperatures in the range 1300 to 1400°C which is slightly below its melting point of 1425°C. At the sublimation temperatures, some reaction of the evaporant with the tungsten boat occurred and a 5 mil thick boat was destroyed after 5 evaporations. At the melting point and above, the compound destroyed the tungsten boat rapidly; hence, evaporations from tungsten could not be made at temperatures above the melting point. The parameters of the chromium silicide films deposited are listed in Tables I and V. The substrate temperatures of specimens 1 through 3 were in the range of 375 to 450°C. Substrate temperatures during deposition of the remaining films were in the range of 275 to 350°C. Specimens $CrSi_2$ - 1, 2 and 3 were deposited in 1-1/2, 1, and 3 minute periods, respectively. A

10 minute deposition period was used for specimens $CrSi_2$ - 4, 5, 6, and 7. All of the substrates were Corning type 7059 glass. For analytical purposes, an electron microscope grid was coated simultaneously with deposition of each resistor slide.

A complete set of data was obtained for the first two specimens. As can be seen in Table I, the resistivity of the thinner film (320 Å) was 615 microhm-cm. The thicker film had a specific resistivity of 332 microhm-cm and was 1350 Å thick. The respective TCR values were $-36 \times 10^{-6}/°C$ and $+105 \times 10^{-6}/°C$. The magnitude of the TCR is small for the resistivity range of 332 to 615 microhm-cm. TCR values of the first seven film resistors having a film composition of Cr_3Si ranged from $(-744 \text{ to } +125)\ 10^{-6}/°C$. Two additional chromium silicide resistors, $CrSi_2$-8 and -9, were fabricated in this manner at the highest practicable evaporation rate for the tungsten boat used. The TCR values of these were $+229 \times 10^{-6}/°C$ and $+59 \times 10^{-6}/°C$, respectively. A resistivity of 246 microhm-cm was obtained for $CrSi_2$ -8; this was the lowest resistivity obtained for the chromium silicide series.

The electron beam apparatus was used to evaporate $CrSi_2$ at slightly above its melting point. Two resistors, $CrSi_2$ -12 and 13 were prepared by evaporating from a melt of $CrSi_2$. Average TCR and resistivity values were $+351 \pm 50$ ppm/°C and 408 ± 10 microhm-cm. In Figure 21, it may be seen that these points fit a curve of resistivity versus TCR of the specimens prepared previously with the tungsten boat evaporations.

An electron diffraction analysis of films deposited on grids with the $CrSi_2$ resistors indicated a film composition of Cr_3Si for the first five evaporations from a tungsten boat. On the other hand, a strong chromium composition was obtained for the electron beam evaporation from the melt.

According to reference (9) $CrSi_2$ is a semiconductor. The fact that films deposited from the compound show metallic conduction properties is further evidence that the films are of different composition than the evaporant and that partial distillation effects occurred at the source.

The lower resistivity and higher TCR values (more positive) were obtained for films where sublimation of the $CrSi_2$ was conducted at just below its melting point from tungsten boats and for evaporation from the melt with an electron beam. The higher resistivity and negative TCR values were obtained at slightly

lower evaporation temperatures of about 1300°C from tungsten boats. Figure 21 shows that for these specimens the resistivity increased from 250 microhm-cm at a TCR of +220 ppm/°C to 2,500 microhm-cm at a TCR of -700 ppm/°C. At zero TCR the resistivity was about 500 microhm-cm.

The chromium silicide films were hard and strongly adherent to glass substrates. Aging characteristics were superior, also. After 1000 hours at 125°C in air, the maximum change in resistance obtained was a decrease in resistance of 2 percent for unprotected films. A maximum increase in resistance of 0.55 percent was obtained after 1000 hours at 125°C for films baked in air at 300°C after deposition. During the initial TCR measurements, the chromium silicide films usually decreased slightly in resistance; this tendency to decrease in value during aging indicates that the films were not completely annealed during the deposition phase. A summary of the aging of the films appears in Table III. Figures 24 and 25 are typical aging curves.

In Tables II and II A, the changes in resistance during post-deposition baking are given. The maximum change in resistance during the bake was an increase in resistance of 15 percent for $CrSi_2$-6. In general, the changes in resistance were less. One film, $CrSi_2$-5, decreased in value by 0.47 percent. For most resistor application, post-deposition baking should not be required for properly annealed films. However, to meet stability requirements of 1 percent or less, post-deposition baking or other methods of passivation are recommended. Post-deposition baking has an advantage in that, in addition to annealing and passivating, it can be used to trim resistors in a positive direction by oxidation to a specified value. From a fabrication standpoint, it would be desirable to passivate and adjust the resistors to value at room temperature; one might achieve this by anodization techniques; both chromium and silicon form anodic films.[10]

From a standpoint of ease of fabrication, stability, and low magnitude of TCR, chromium silicide is recommended highly for film resistor application that can be met by films of medium specific resistivity. In general, the resistivity of these films in the ±500 ppm/°C range of TCR is about an order of magnitude higher than that usually reported for pure tantalum films deposited

by diode sputtering. Before serious consideration is given to using the material as precision resistors, the thermoelectric and noise properties should be established.

6.8 Titanium Silicide Films. Twelve titanium silicide resistors were deposited by heating a powder of the compound $TiSi_2$ in a tungsten boat at temperatures in the range 1400° to 1600°C. Sublimation of the compound occurred in this range of boat temperatures. The boat temperatures were measured with a pyrometer and appear to be in slight disagreement with the reported melting temperature of 1500°C for $TiSi_2$; however, the temperature of the powder was probably less than that of the boat because of losses in heat transfer between the two. At temperatures > 1600°C gas evolution blew portions of the powder from the boat. Parameters of the deposited films are listed in Table I. Electron diffraction analysis of the first 10 films indicated a film composition of $TiSi_2$ plus free Si. Analyses of $TiSi_2$ -11 and -12 indicated that these films were composed primarily of $TiSi_2$. The highest boat temperature and resultant evaporation rate were used for these two films. It is apparent that fractional distillation of the compound occurred at the source when heated to the lower range of temperatures employed; hence, silicon enrichment of the deposited film occurred. As the boat temperature was increased, the film properties approached the bulk properties of the evaporant. Due to excessive spitting of the $TiSi_2$ powder, attempts to melt and evaporate the material with an electron beam gun were unsuccessful.

By varying the boat temperature, a wide range of TCR values were obtained. TCR values of $-10.3 \times 10^{-4}/°C$ to $-3.61 \times 10^{-4}/°C$ were characteristic for boat temperatures in the range of 1500 to 1600°C. Correspondingly, the specific resistivity varied from 6,000 to 1,000 microhm-cm. Values of TCR from $-45 \times 10^{-4}/°C$ to $-10.3 \times 10^{-4}/°C$ were obtained by varying the boat temperature in the range 1,400 to 1,500°C. A plot of the resistivity versus TCR of this species is included in Figure 21. It appears that the resistivity of this species will be lower near zero TCR than that obtained for $CrSi_2$. To reproduce resistors of the titanium silicide species at a given TCR or resistivity value, precision control of boat and substrate temperatures will be required.

The films exhibited excellent adherence to glass substrates and were quite hard. Typical specimens were placed on aging at 125°C in air for a minimum period of 1000 hours. Both unprotected and post-deposition baked films were included in the aging studies. Two unprotected resistors with resistivities in the range $(0.5 < 1 \leq 5)10^3$ microhm-cm increased in resistance by 17 percent after 1000 hours of aging; whereas, similar films baked in air at 300°C for 5 hours after deposition increased in resistance an average of 0.35 percent. In the unprotected state the resistors increased in value 1 to 20 percent during the initial TCR measurements where they were cycled to 125°C in air over a period of about 30 minutes. During the post-deposition baking at 300°C, the resistance values increased by approximately 28 percent. Figures 26 and 27 show the typical aging of the films.

It can be concluded from the aging data that post-deposition baking or other methods of passivating, such as anodization, will be required for the titanium silicide films, and that the films can be stabilized by baking in air. The low aging of the post-baked films was about equal to that obtained for similarly treated chromium silicide films. However, the films were not as resistant to oxidation in the unprotected state as were the latter.

6.9 Chromium Silicide-Titanium Silicide Films. Seven Chromium Silicide-Titanium Silicide resistors were fabricated by evaporating a mixture of $CrSi_2$ and $TiSi_2$ powders. The powders were mixed in a 1:1 mass ratio. This was placed in a massive copper crucible and melted with an electron beam. Evaporations were then made from the molten pool of the material. The seven resistors were deposited during three successive evaporations with a beam power of (2-3)KW, (3-3.5)KW, and 4KW, respectively. The same melt was used for all three depositions and only a very small portion was evaporated. Other fabrication details are listed in Table I.

A carbon coated copper electron microscope grid was placed adjacent to resistors $CrSi_2$ + $TiSi_2$ -3 and 4 during the first deposition at (2-3)KW of beam power. Electron diffraction analysis of the grid indicated a film composition of $CrSi_2$, only. There was no evidence of titanium or titanium silicide.

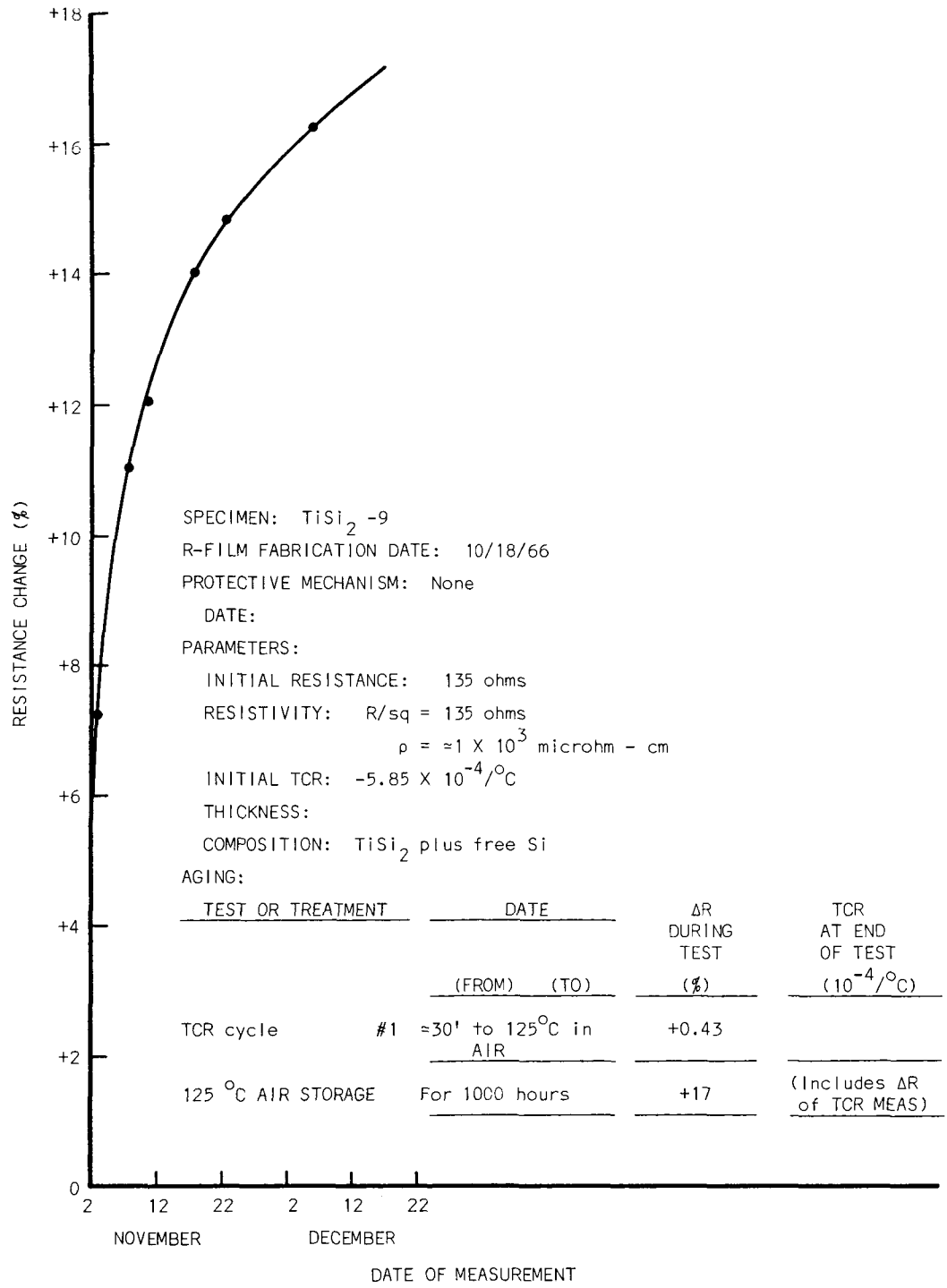

Figure 26. Resistance Aging at 125°C in Air of a Typical Unprotected $TiSi_2$ Film.

SPECIMEN: $TiSi_2$ -12

R-FILM FABRICATION DATE: 10/31/66

PROTECTIVE MECHANISM: Air Bake

DATE: 11/1/66

PARAMETERS:

INITIAL RESISTANCE: 110 ohms

RESISTIVITY: R/sq = 110 ohms

$\rho \simeq 1 \times 10^{3}$ microhm - cm

INITIAL TCR: $-5.13 \times 10^{-4}/^{\circ}C$

THICKNESS:

COMPOSITION: $TiSi_2$ plus free Si

AGING:

TEST OR TREATMENT	DATE (FROM)	DATE (TO)	ΔR DURING TEST (%)	TCR AT END OF TEST ($10^{-4}/^{\circ}C$)
Air Bake: 300 °C 5 hrs	11/1/66		+29	
TCR cycle #1	≈30' to 125°C in Air		+0.09	(Before Bake)
125 °C Air Storage	For 1000 Hours		+0.35	

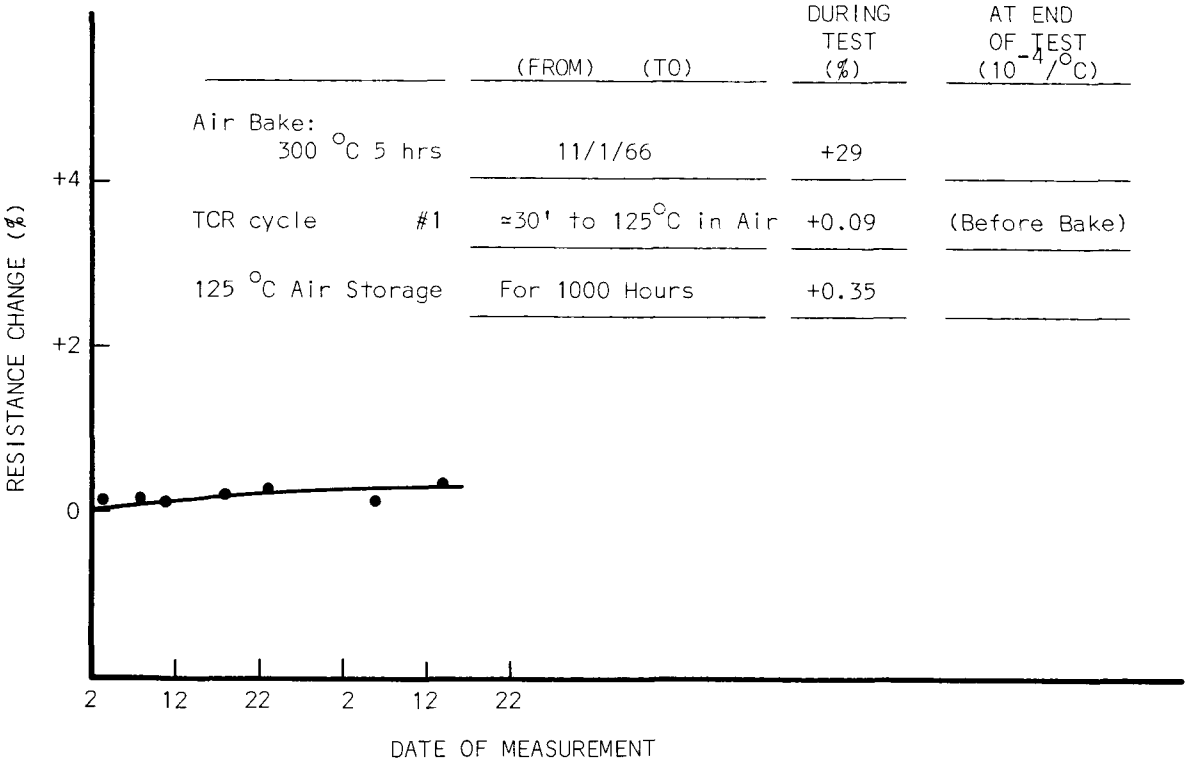

Figure 27. Resistance Aging at 125°C in Air of a Typical $TiSi_2$ Film Post-Baked in Air.

The resistive parameters of the films were definitely related to the beam power during evaporation. The dependence was as follows:

Electron Beam Power (KW)	Average Specific Resistivity (microhm-cm)	Average TCR (10^{-4}/°C)
2 to 3	3,560	-4.4
3 to 3.5	1,150	-1.4
4	800	-3

Considering the possible distillation effects and the film analysis by electron diffraction, it is believed that the $CrSi_2$ + $TiSi_2$ films deposited at the highest beam power had the highest content of chromium and titanium with respect to the silicon; on the other hand, in the first two depositions at lower evaporant temperatures, titanium was probably evaporated in considerably less proportions with respect to the other components of the evaporant.

After deposition and initial measurements, two specimens, $CrSi_2$ + $TiSi_2$ -6 and 8, were baked in air at 300°C for 4 1/2 hours; subsequent to this protective measure, they were stored in the 125°C aging ovens for stability studies. One specimen, $CrSi_2$ + $TiSi_2$ -9, was placed on aging without taking any protective measures. As indicated in Figures 28 and 29, aging of both the unprotected and post-baked films was small indeed.

6.10 Chromium Silicide-Silicon Boride Films. Three resistors were fabricated by evaporating a mixture of $CrSi_2$ and B_4Si powders. The mixture was 2 parts by mass of $CrSi_2$ and one part B_4Si. The charge was heated to sublimation temperatures with an electron beam at a beam power of 1/4 to 1 KW. Due to excessive spitting of the B_4Si component the temperature could not be increased to form a melt of the powders. Other fabrication details are listed in Table I. The three resistors ($CrSi_2$ + B_4Si - 1, 2, and 3) deposited during this evaporation had an average TCR of -2500 ppm/°C with an average resistivity of 93,600 microhm-cm.

Because of the spitting of the B_4Si component in the above charge, a different approach was tried for melting the two compounds together. A quantity of $CrSi_2$ powder was pre-melted and the slug was placed on a bed of B_4Si powder. The $CrSi_2$ was then melted by directing the beam to the slug; however, the melted $CrSi_2$ remained as a ball of liquid on top of the B_4Si powder, and wetting of

the B_4Si powder could not be obtained in this manner. Stray portions of the electron beam caused some spitting of the B_4Si. $CrSi_2$ + B_4Si - 4, 5, and 6, were deposited in this manner. It appeared that very little if any, of the B_4Si was evaporated, and it can be seen in Table I that the resistive parameters of the films were essentially equal to those obtained for the $CrSi_2$ series.

No further attempts were made to evaporate $CrSi_2$ + B_4Si mixtures because of the unsuccessful efforts to obtain a common melt of the compounds and the excessive spitting of the B_4Si powders. It may be possible to obtain a common melt by reducing considerably the proportion of B_4Si in a powder mixture of the materials.

Two films of the first series were selected for aging studies at 125°C in air. One was placed on aging without any additional protective measures and the other one was baked at 300°C in air prior to aging.

During 1000 hours of aging at 125°C, the unprotected film and post-deposition baked film aged about equally well. Two unprotected films were studied during the extended aging. One increased in resistance by 1 percent and the other decreased in resistance by 2 percent. The film baked in air at 300°C for 4 1/2 hours prior to aging studies increased in resistance by 1 percent. Thus, for similar treatment the higher resistivity films of this series aged slightly more than did the lower resistivity films of the previously discussed $CrSi_2$, $TiSi_2$, and $CrSi_2$ + $TiSi_2$ series. The extended aging at 125°C of the $CrSi_2$ + B_4Si species is represented in Figures 30 and 31.

6.11 Comments on the Silicide Series. It is interesting to compare films of the $CrSi_2$ + $TiSi_2$ series with the chromium silicide series and titanium silicide series. A film composition of Cr_3Si was obtained for $CrSi_2$ evaporated from tungsten boats at temperatures of about 1350°C, and a strong chromium composition was obtained for $CrSi_2$ evaporated from the melt by an electron beam at 2.6 KW. On the other hand, a film composition of $CrSi_2$ was obtained for the first deposition of $CrSi_2$ + $TiSi_2$ at an average beam power of 2.5 KW. Hence, it may be seen that the addition of $TiSi_2$ to the $CrSi_2$ resulted in a product which was composed largely of $CrSi_2$ in spite of the high source temperature.

SPECIMEN: $CrSi_2 + TiSi_2$ -9

R-FILM FABRICATION DATE: 11/28/66

PROTECTIVE MECHANISM: None

DATE:

PARAMETERS:

INITIAL RESISTANCE: 563 ohms

RESISTIVITY: R/sq = 56.3 ohms

ρ = ≈800 microhm - cm

INITIAL TCR: $-2.86 \times 10^{-4}/^{\circ}C$

THICKNESS:

COMPOSITION:

AGING:

TEST OR TREATMENT	DATE (FROM) (TO)	ΔR DURING TEST (%)	TCR AT END OF TEST ($10^{-4}/^{\circ}C$)
TCR cycle #1	≈30' to 125°C in AIR	-0.18	
125 °C Air Storage	For 1000 hours	-0.1	

(Reference point is Val. before TCR cycle)

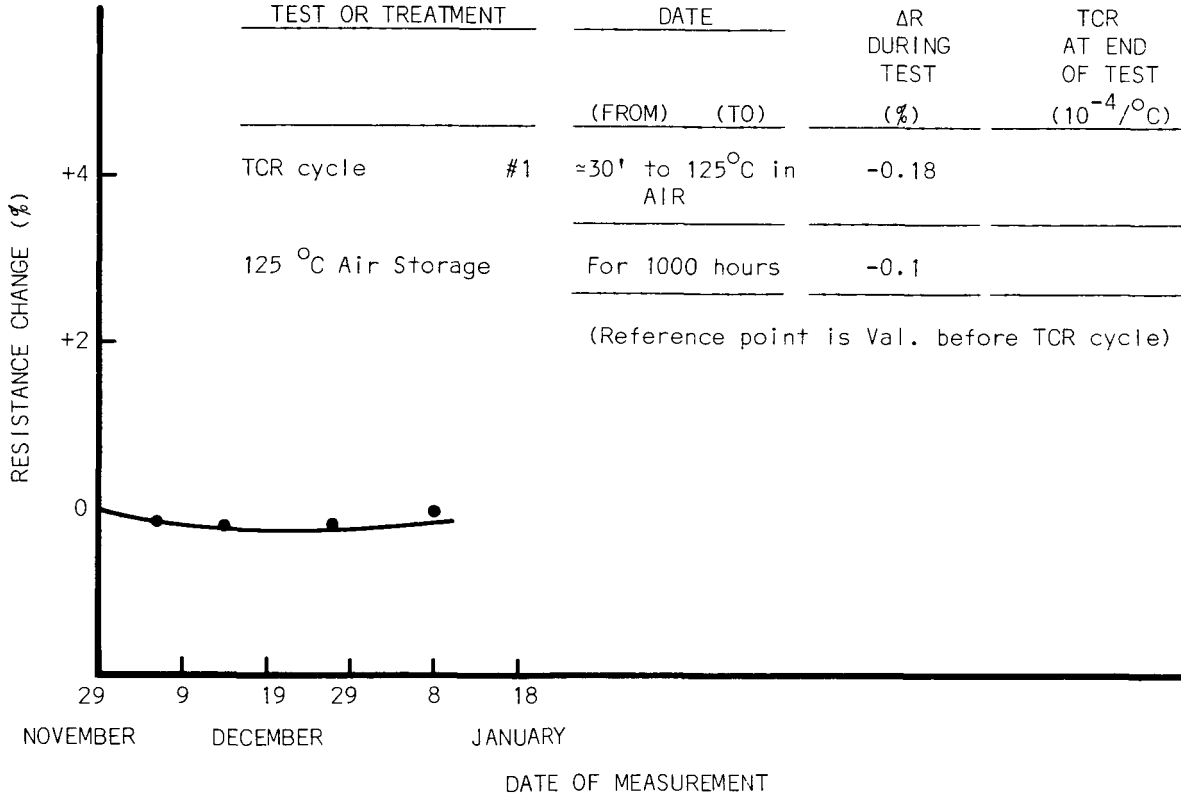

Figure 28. Resistance Aging at 125°C in Air of a Typical Unprotected $CrSi_2 + TiSi_2$ Film.

SPECIMEN: $CrSi_2 + TiSi_2$ -8

R-FILM FABRICATION DATE: 11/28/66

PROTECTIVE MECHANISM: Air Bake

DATE:

PARAMETERS:

INITIAL RESISTANCE: 598 ohms

RESISTIVITY: R/sq = 59.8 ohms

ρ =≈800 microhm - cm

INITIAL TCR: $-3.1 \times 10^{-4}/^{\circ}C$

THICKNESS:

COMPOSITION:

AGING:

TEST OR TREATMENT	DATE (FROM) (TO)	ΔR DURING TEST (%)	TCR AT END OF TEST ($10^{-4}/^{\circ}C$)
Air Bake: 300 °C 4½ hrs	11/29/66	-2.29	
TCR cycle #1	≈30' to 125°C in AIR	-0.17	(Before Bake)
125 °C Air Storage	For 1000 hours	+0.3	

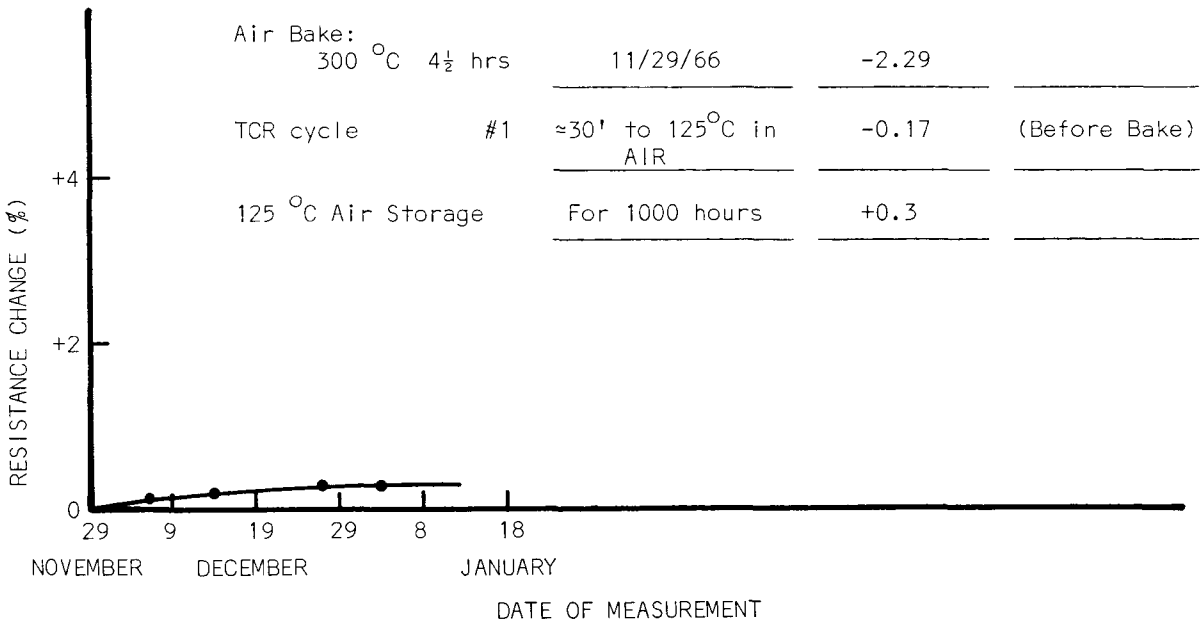

Figure 29. Resistance Aging at 125°C in Air of a Typical $CrSi_2 + TiSi_2$ Film Post-Baked in Air.

In addition, the generally higher film resistivity of the $CrSi_2$ + $TiSi_2$ mixture may be observed in the data. For instance, from Figure 21 and Table V, the resistivity of the $CrSi_2$ series was 1,600 microhm-cm at a TCR of -4.4×10^{-4}/°C; hence, the latter resistivity is slightly less than half that of the films of the $CrSi_2$ + $TiSi_2$ series for the same value of TCR. The resistivity of the $TiSi_2$ series at this TCR is about 800 microhm-cm (a projected value of Figure 21) compared to about 3600 microhm-cm for the $CrSi_2$ + $TiSi_2$.

The evaporation methods and relative ease of evaporating $CrSi_2$, $CrSi_2$ + $TiSi_2$, and $TiSi_2$ can be profitably compared. $CrSi_2$ and $TiSi_2$ were readily sublimated from tungsten boats at temperatures slightly below their respective melting points of 1425°C and $\approx$ 1500°C. From these evaporations it was apparent that the TCR and resistivity values were dependent on boat temperature. Attempts to evaporate $CrSi_2$ and $TiSi_2$ at or above their respective melting points from tungsten boats were not successful. Upon melting, the $CrSi_2$ quickly reacted with the boat and destroyed it. As the melting point of the $TiSi_2$ was approached, excessive spitting of the powder occurred. Both $CrSi_2$ and $CrSi_2$ + $TiSi_2$ were evaporated from melts of the respective charges with the electron beam gun, and again it was evident that composition, TCR, and resistivity were dependent on the evaporant temperature. Since $CrSi_2$ destroyed tungsten boats at or above their melting points, it was assumed that the same thing would occur with $CrSi_2$ + $TiSi_2$. Because of excessive spitting of powdered charges of $TiSi_2$, it could not be evaporated readily with the electron beam gun.

Though only a few depositions were made for each of the materials, it was evident that reproducibility of resistive parameters can be maintained by controlling the evaporant and substrate temperatures during deposition.

A minimum substrate temperature of 400°C is recommended for all three materials. To evaporate $CrSi_2$, either a tungsten boat or electron beam can be used to produce films with TCR values ranging from -800 ppm/°C to +200 ppm/°C. To obtain $CrSi_2$ + $TiSi_2$ films with TCR values in the range of -500 ppm/°C to -100 ppm/°C, electron beam evaporations are recommended. A tungsten boat is satisfactory for sublimating $TiSi_2$ to fabricate film resistors with TCR values in the range of -5,000 ppm/°C to -500 ppm/°C. The resistivity of films prepared from either of the materials was much higher than that which

can be obtained from elemental metal films. Another variable in the evaporation of $CrSi_2$ + $TiSi_2$ that will affect the resistive parameters of the films is the mass ratio of the constituent compounds in the powdered mixture. This ratio was not intentionally varied during this research.

The aging of the $CrSi_2$ + $TiSi_2$ was very low, being quite similar to the $CrSi_2$ series. The summary of aging during post-deposition baking appears in Table II. Aging at 125°C is summarized in Table III. The higher resistivity of the chromium silicide-titanium silicide mixture leads to a preference of this material over $CrSi_2$ or $TiSi_2$ for resistor application, see Table V.

7. Films of Niobium and Titanium Nitride

A few films of niobium nitride and of titanium nitride were prepared. The preparation details and parameters of the films are given in Table I (Appendix). The films of niobium nitride gave resistivities in the range 2900 to 6600 microhm-cm and TCR values of -360 to -570 x 10^{-6}/°C. The molten material destroyed the tantalum boat in only a few evaporations.

Nine films of titanium nitride were prepared. The maximum resistivity obtained was about 2070 microhm-cm with a negative TCR of -740 x 10^{-6}/°C. The data obtained are plotted in Figure 32. It is evident that neither of these materials compare well as resistive materials with some of the previously discussed ones such as Cr + SiO.

8. Film Aging Studies

As noted in Section II A 3, films were subjected to certain annealing, passivating, or overcoating technique in order to improve their aging properties. The effects of post-deposition baking on the resistive parameters are shown in Table II A of the Appendix and are summarized in Table II. As discussed in Section II A 4, the resistance parameters of selected resistors were monitored during extended periods of storage in air at 125°C, and the resultant data were recorded, tabulated and analyzed. A change in resistance of less than 1 percent after 1000 hours was considered excellent. A few films prepared early in the program were aged at 125°C for only a few hours, and during TCR measurements all specimens were cycled to 125°C in air. The aging at 125°C in air is summarized in Table III.

In general, aging increased with increasing resistivity for a given species of films. For this reason, the variously treated materials can be best compared in Table III by considering common resistivity ranges.

SPECIMEN: $CrSi_2$ +B_4Si -2

R-FILM FABRICATION DATE: 11/23/66

PROTECTIVE MECHANISM: None

DATE:

PARAMETERS:

INITIAL RESISTANCE: 11,448 ohms

RESISTIVITY: R/sq = 1,145 ohms

ρ = ≈93,600 microhm - cm

INITIAL TCR: $-25.2 \times 10^{-4}/^{\circ}C$

THICKNESS:

COMPOSITION:

AGING:

TEST OR TREATMENT	DATE (FROM) (TO)	ΔR DURING TEST (%)	TCR AT END OF TEST ($10^{-4}/^{\circ}C$)
TCR cycle #1	≈30' to 125°C in AIR	+0.61	
125 °C Air Storage	For 1000 hours	+0.9	

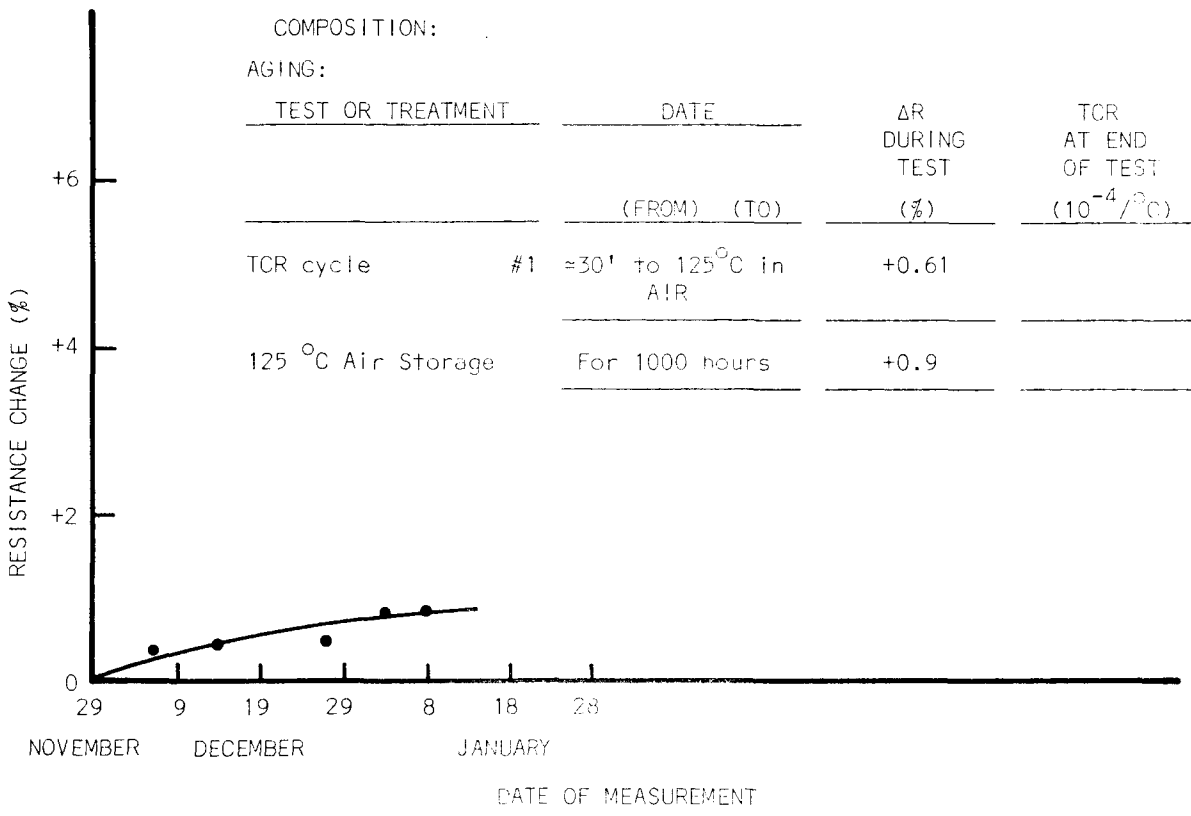

Figure 30. Resistance Aging at 125°C in Air of a Typical Unprotected $CrSi_2$ + B_4Si Film.

SPECIMEN: $CrSi_2 + B_4Si$ -1

R-FILM FABRICATION DATE: 11/23/66

PROTECTIVE MECHANISM: Air Bake

DATE:

PARAMETERS:

INITIAL RESISTANCE: 15,471 ohms

RESISTIVITY: R/sq = 1,547 ohms

ρ = ≃93,600 microhm - cm

INITIAL TCR: $-25 \times 10^{-4}/^{\circ}C$

THICKNESS:

COMPOSITION:

AGING:

TEST OR TREATMENT	DATE (FROM)	DATE (TO)	ΔR DURING TEST (%)	TCR AT END OF TEST ($10^{-4}/^{\circ}C$)
Air Bake: 300 °C 4½ hrs	11/29/66		+0.71	
TCR cycle #1	≃30' to 125°C in AIR		+0.5	(Before Bake)
125 °C Air Storage	For 1000 hours		+0.9	

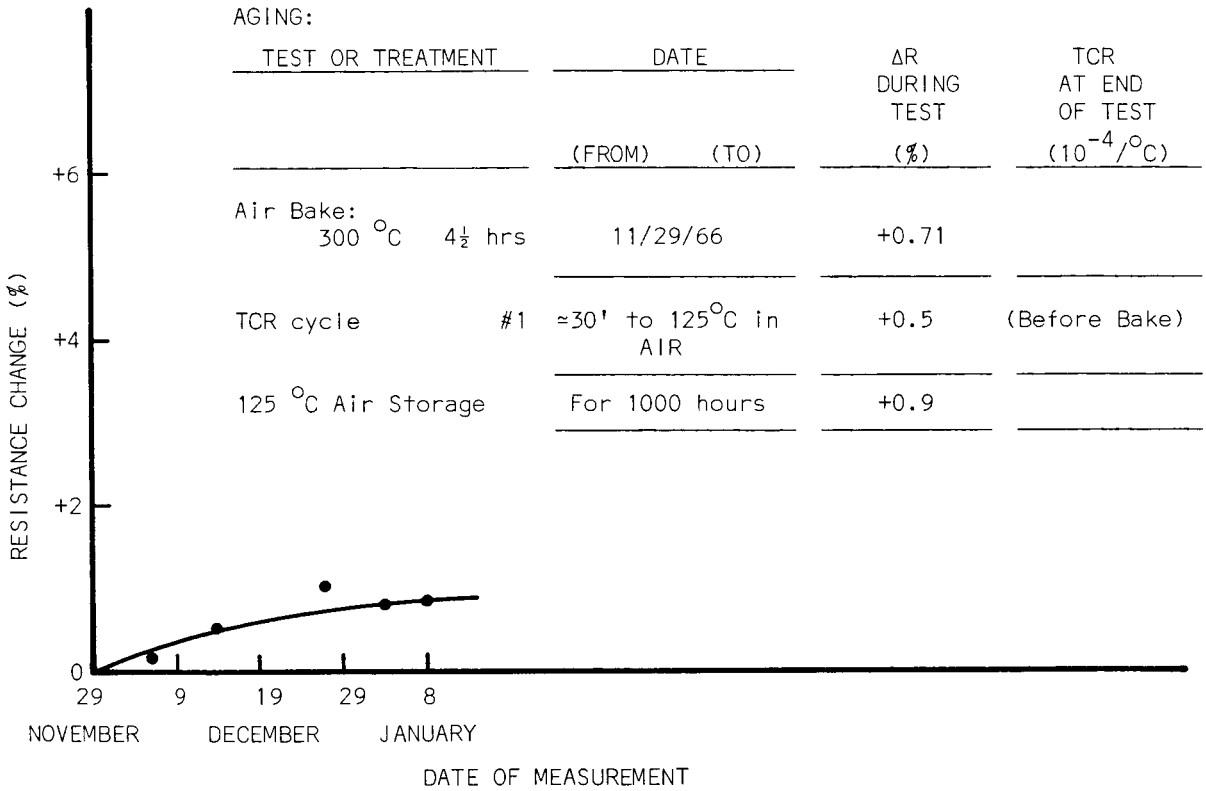

Figure 31. Resistance Aging at 125°C in Air of a Typical $CrSi_2 + B_4Si$ Film Post-Baked in Air.

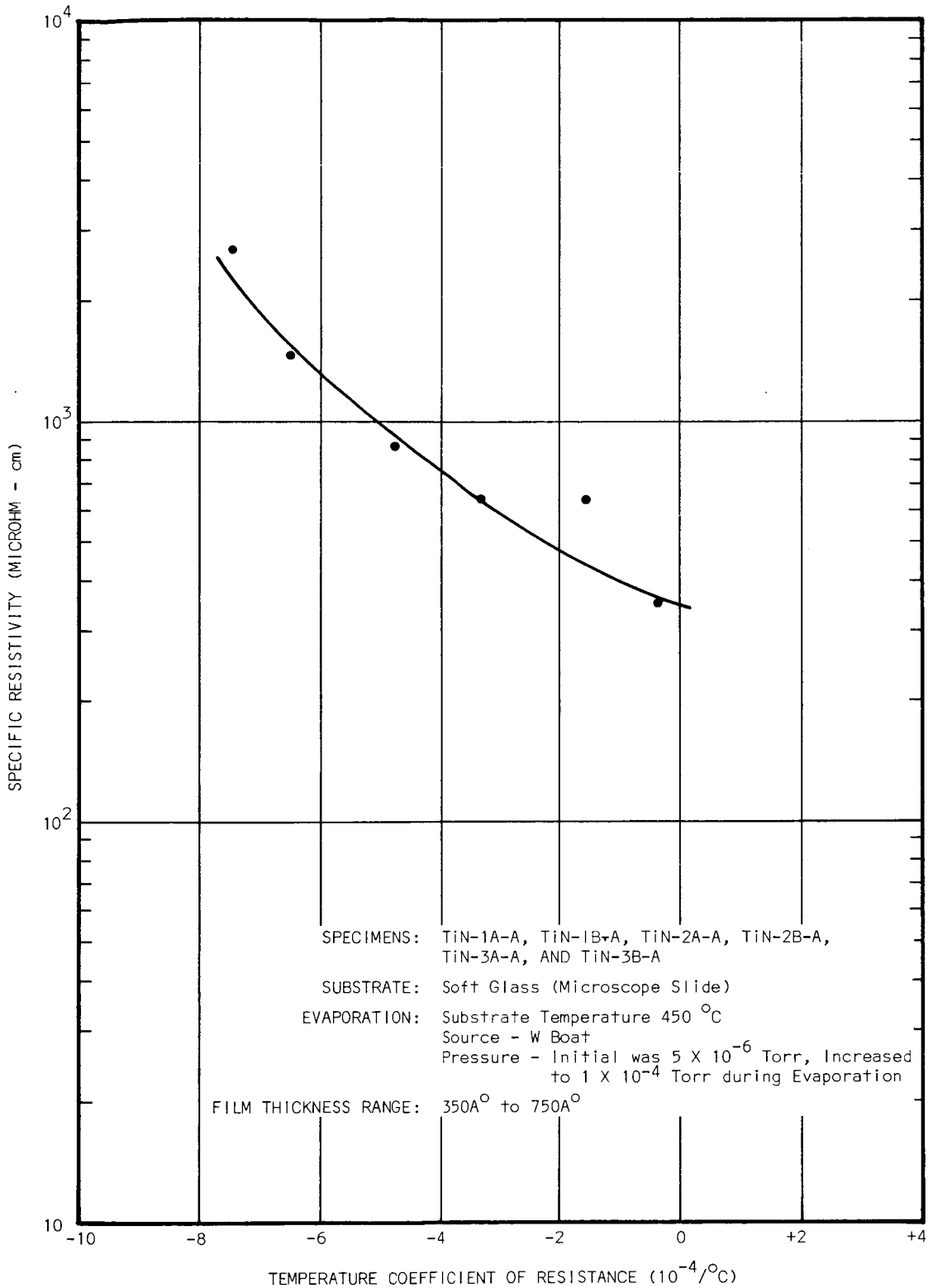

Figure 32. Specific Resistivity vs TCR of Evaporated Titanium Nitride Films.

The relation between aging rate and resistivity for a given material is best illustrated by Figures 33 and 34 for chromium-silicon monoxide films in unpassivated and passivated states and in Figure 35 for films of manganese-silicon monoxide in similar states. The superiority of the passivated Cr + SiO films above the other varieties is remarkable and changes of only a few tenths of a percent were noted for films of 10^4 microhm-cm after 1000 hours at 125°C. Comparatively, the Mn + SiO film changes were large even after the films were protected by an overlayer of silicon monoxide.

Aging of the Boride and Silicide films were discussed in section II B, 6 in the respective discussion for each material studied. Typical changes in resistance with time are shown in Figures 22 through 31. Of particular interest, was the similarity of behavior of the $CrSi_2$ films during extended aging to that of Cr + SiO films. With respect to aging, the silicide films were, essentially, as good as the Cr + SiO films; that is, except for $TiSi_2$, where this was true only after post-baking. With respect to the silicides and Cr + SiO, niobium boride films aged poorly.

9. Structures of the Films

Selected specimens of the various films were examined by electron diffraction and microscopy and by x-ray diffraction. Entries have been made in Table I (Appendix) in the column headed "composition" for the films examined.

For some materials it will be observed that where a single compound was evaporated from the source, it was partially reduced and the diffraction rings of the free metal usually appear in the electron diffraction pattern. An extreme example of this occurred in the case of nickel boride resulting in a specimen with low resistivity and a high positive TCR. Here the film specimen must have been essentially the metal, nickel. On the other hand, for niobium boride no clearly defined diffraction rings were obtained, indicating the amorphous nature of the compound which is also reflected in the high resistivities and large negative TCR values measured. Most materials fell within these extremes and the near amorphous structures of films with desirable electrical properties made diffraction pattern interpretation difficult for many of the specimens prepared.

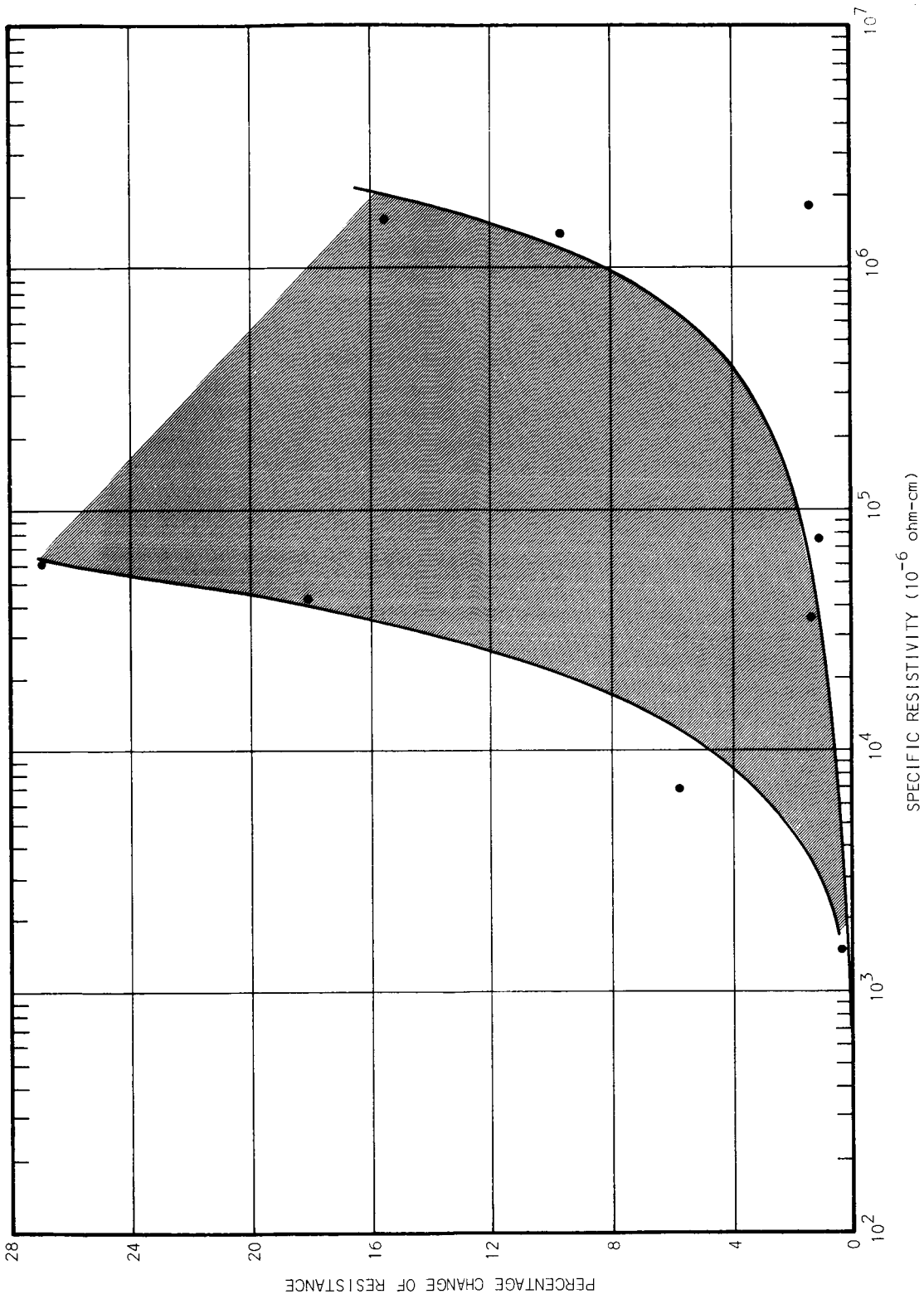

Figure 33. Aging of Unprotected Cr + SiO Film Resistors After 1000 Hours at 125°C in Air.

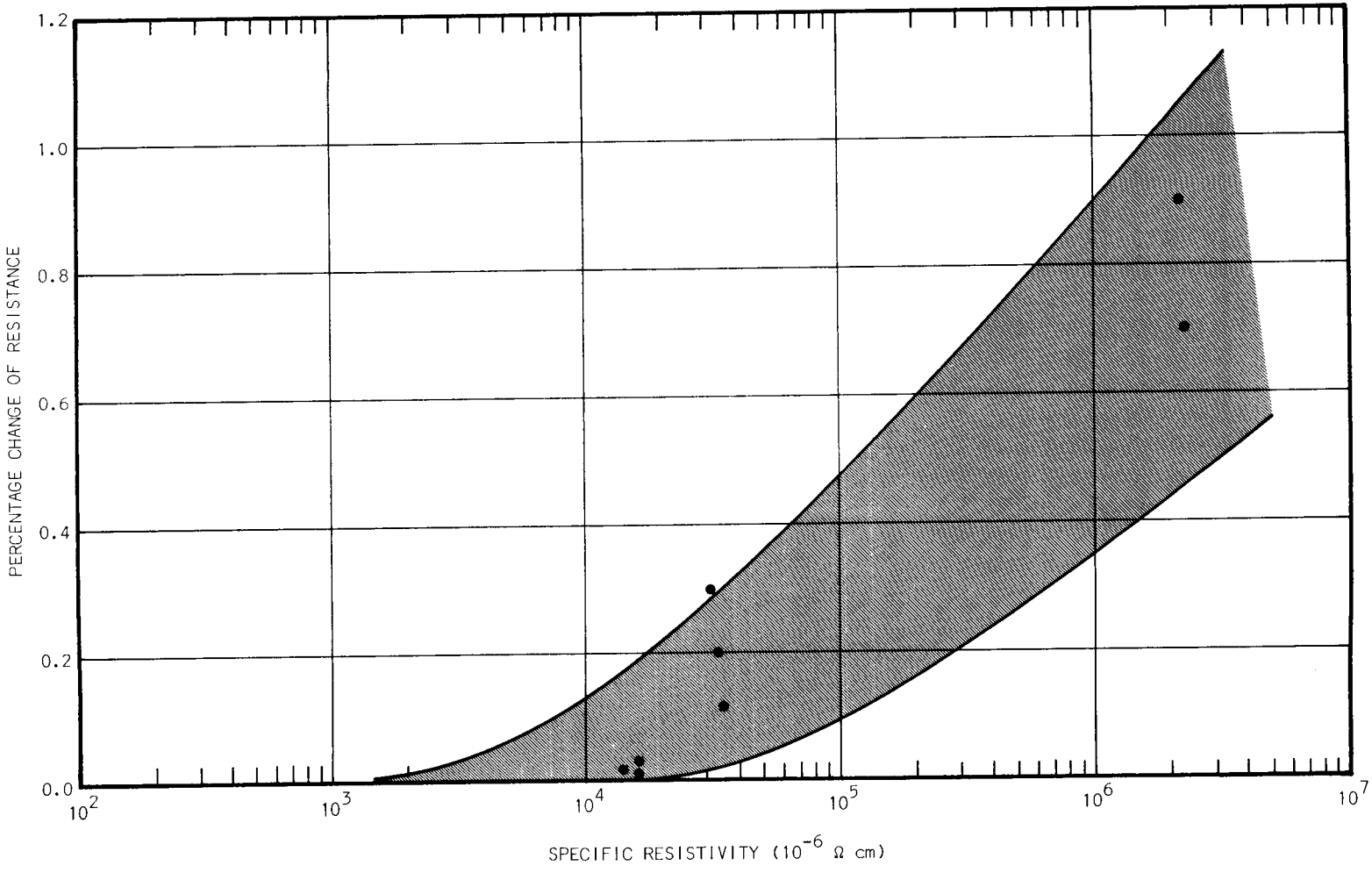

Figure 34. Aging of Cr + SiO Films Post-Baked in Air at 250°C to 325°C After 1000 Hours at 125°C in Air.

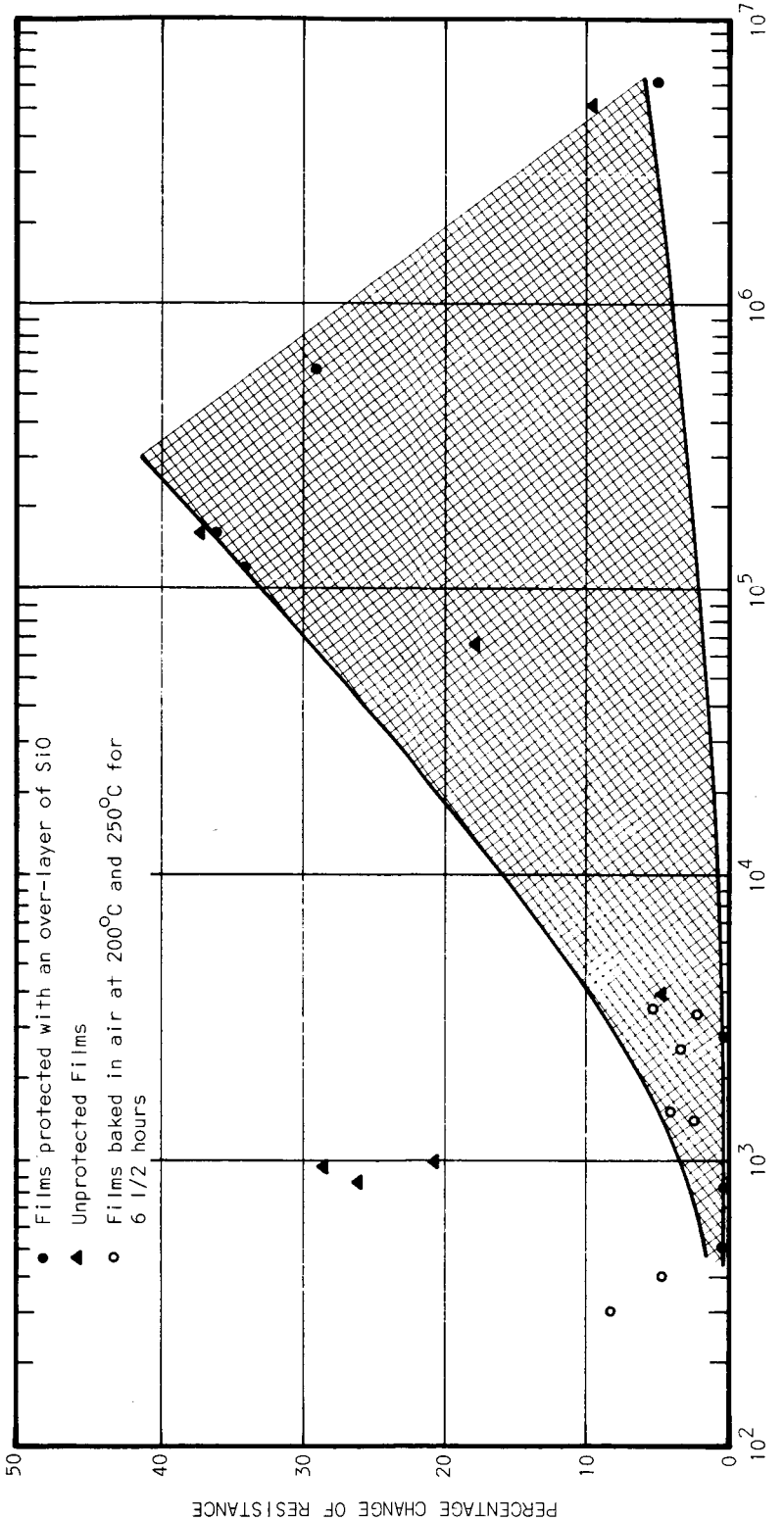

Figure 35. Aging of Mn + SiO Film Resistors After 1000 Hours at 125°C in Air.

Where two components were evaporated simultaneously such as in the cases of the various metals co-deposited with silicon monoxide, a behavior generally similar to that for the case of single compounds was obtained with the additional complexities added by the elements of the second compound.

Investigations of films of Al + SiO, Cu + SiO, Cr + SiO and Mn + SiO exhibited behavior generally similar to those described for the single compound evaporation. An example of the electron diffraction pattern of a film, Mn + SiO -12C, of low resistivity (1000 microhm-cm) and slightly positive TCR ($+72 \times 10^{-6}/°C$), is shown in Figure 36 with a portion of its micrograph (19,480x) shown beside it. The diffraction pattern exhibits the lines of α manganese and the micrograph displays particles randomly scattered through a more uniform interparticle matrix. The data for Mn + SiO -20C, a film of high resistivity (150,000 microhm-cm) and a TCR of $-1220 \times 10^{-6}/°C$ displays a much more nearly amorphous pattern and a film of little texture as shown in Figure 37. The diffraction pattern, however, did have discernible lines of α manganese.

Because of their relative importance a more detailed study of Cr + SiO films was made by both electron and x-ray diffraction methods. These films may have within them Si, SiO, SiO_2, Cr, or Cr_2O_3 leading to very complex structures. Details of an investigation of these films by members of our Diffraction Laboratories are reported below.

All the specimens were investigated by reflection electron diffraction and by x-ray diffraction techniques.

The obtained diffraction patterns consist - except for the chromium film - either of very weak or very weak and broad peaks. The error in the determination of the d-spacings is therefore probably high. It also seems that the experimental results can only be explained with the assumption of several chemical reactions during the evaporation process of the films. The reaction

$$2\ SiO \rightleftarrows Si + SiO_2$$

is possible as well as the reactions

$$2\ Cr + 3\ SiO \rightleftarrows Cr_2O_3 + 3\ Si$$

and

$$4\ Cr + 3\ SiO_3 \rightleftarrows 2\ Cr_2O_3 + 3\ Si$$

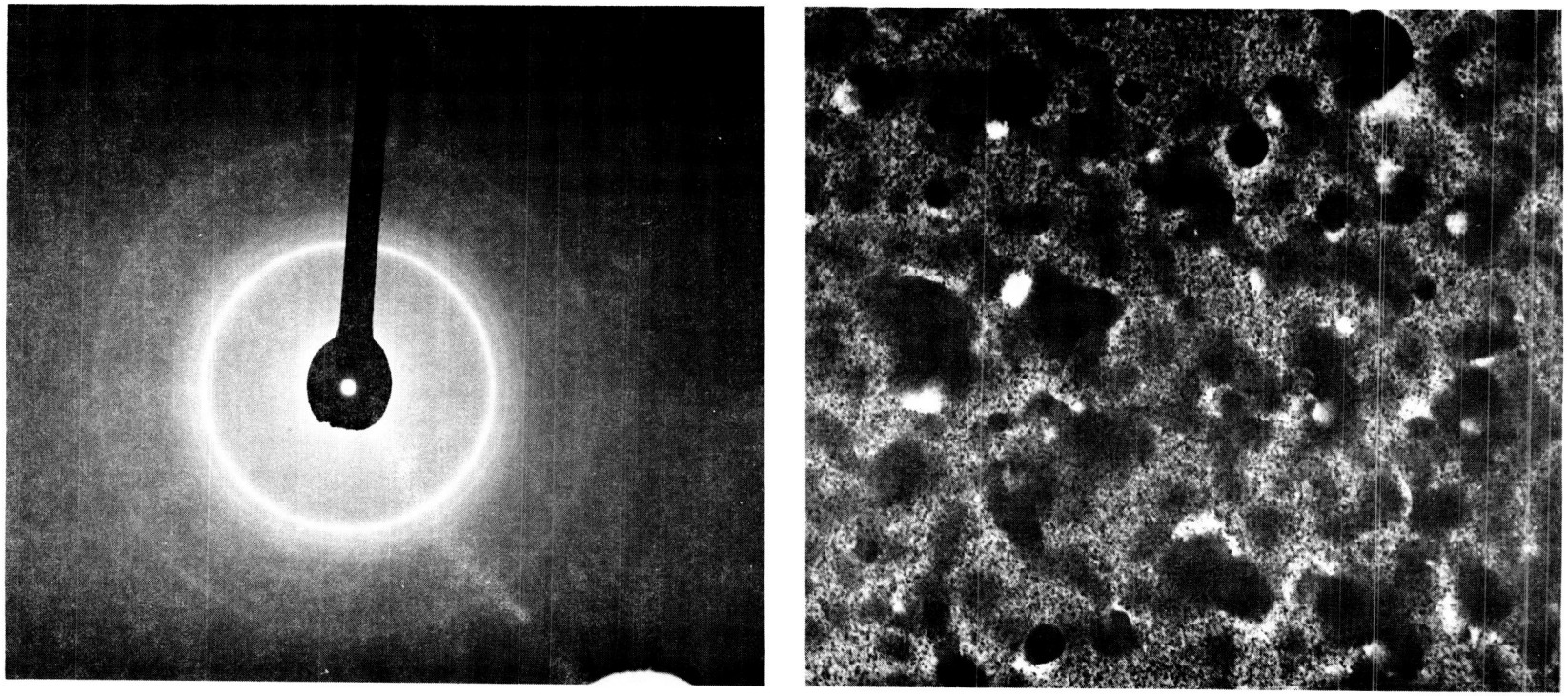

DIFFRACTION PATTERN
(α - Manganese)

MICROGRAPH
(10,700x)

Figure 36. Electron Diffraction Pattern and Micrograph of a Mn + SiO Film of Relatively Low Resistivity.

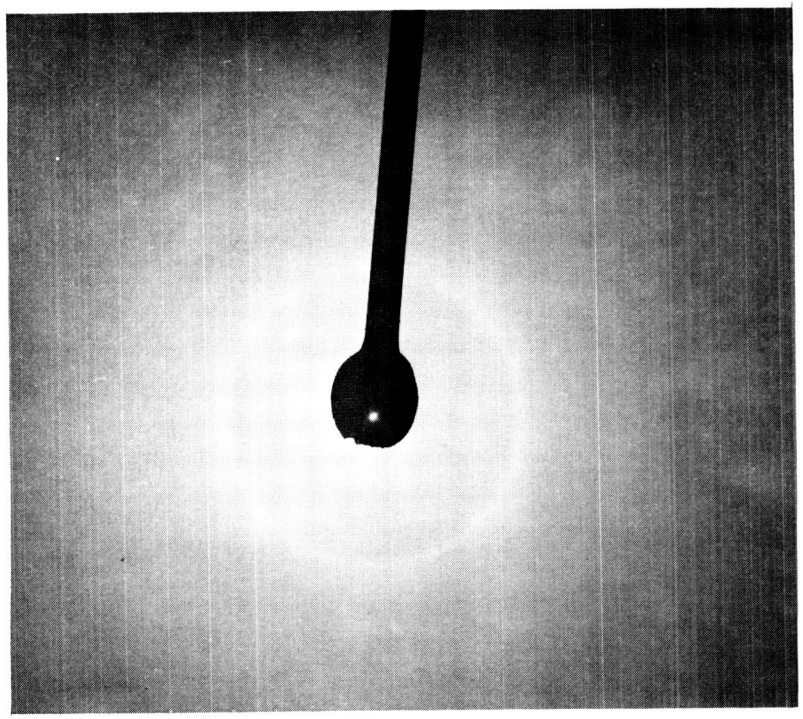

DIFFRACTION PATTERN
(α - Manganese)

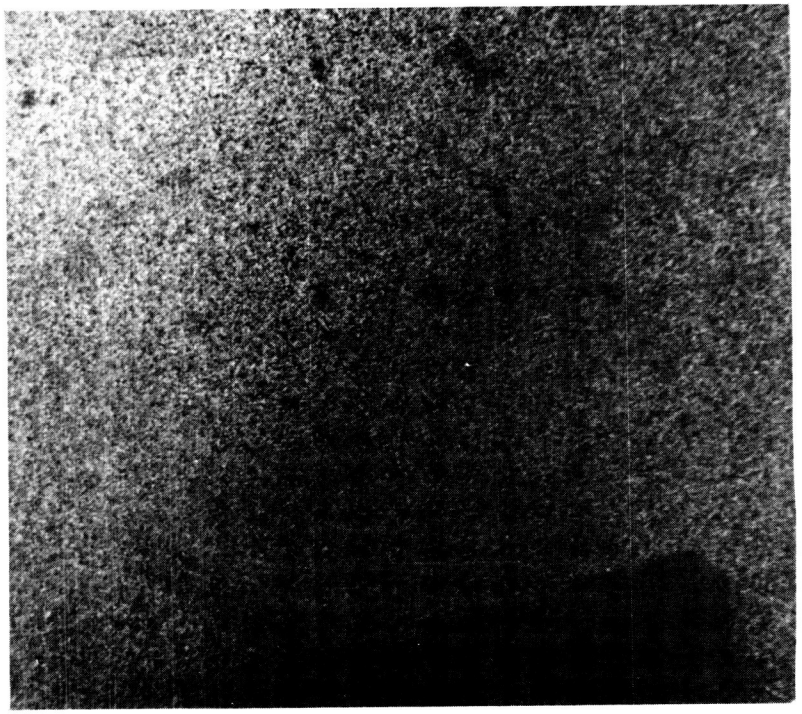

MICROGRAPH
(25,850x)

Figure 37. Electron Diffraction Pattern and Micrograph of a Mn + SiO Film of Relatively High Resistivity.

The formation of Cr_2O_3 is suggested by its relatively high heat of formation of about 266 kcal/mol (SiO: 103 kcal/mol, SiO_2(α-quartz): 201 kcal/mol). The formation of Cr_3Si and higher or lower oxides of the chromium cannot be excluded. For the interpretation of the experimental data, however, only the relatively stable compounds Cr_2O_3 and SiO_2(α-quartz) and necessarily also Cr, Si and SiO were considered. The results are presented in Table IV.

More reliable measurements of d-spacings would probably be obtained by transmission electron diffraction. For precise determinations by x-ray diffraction techniques thicker deposits would be desirable.

Of the films examined, films Cr + SiO 15C and 16C exhibited the more desirable electrical properties of about 10^4 microhm-cm and a TCR not greater than ± 200 ppm/°C for a film at least 1000 angstroms thick. For these films the presence of Cr, Si, Cr_2O_3, and SiO_2 appeared possible in both cases.

It is evident that in the resistivity and TCR ranges of interest the near amorphous nature of the film interferes with structure determination and the discrimination of the diffraction methods is insufficient to predict resistivity except in the general zone to be expected, i.e., low, intermediary or high. Similarly for TCR values predictions of strongly positive, near zero or highly negative could be expected. Although the methods lack precision for this purpose compared to the electrical method, the structures observed varied in accordance with the electrical properties of the materials exhibited in a manner that one would expect. Much more extensive and precise diffraction measurements undoubtedly would present an even better correlation of these two methods of measure. However, these further investigations appeared of little benefit to the objectives of the current research.

10. Analysis and Summary of Film Property Measurements

The extensive number of films examined and the large variety of film materials studied presents an extensive variety of data to be assembled, organized, and evaluated. In Tables I, II A, and III, detailed data concerning all films fabricated, measured, and aged have been reported. In Table V of the Appendix, film fabrication methods and parameters have been summarized. Along with the data reported in the various preceding figures certain conclusions have been formulated and these are recorded hereinafter.

TABLE IV

ELECTRON AND X-RAY DIFFRACTION ANALYSIS OF Cr + SiO FILMS AND A COMPARISON OF THEIR ELECTRICAL PARAMETERS

A. X-ray and Electron Diffraction Information

Sample	Material as indicated by reflection electron diffraction	Material as indicated by x-ray diffraction
Cr	Cr*)	Cr
SiO - 29	SiO**)	SiO
SiO - 32	-	Si or SiO_2***)
Cr + SiO - 8 - C	SiO, Si or Cr_2O_3	SiO_2, Cr or Cr_2O_3
Cr + SiO - 11 - C	SiO_2, Si or Cr_2O_3	SiO_2, Si or Cr_2O_3
Cr + SiO - 13 - C	SiO_2, Cr or Cr_2O_3	SiO, SiO_2
Cr + SiO - 15 - C	Cr, Si or Cr_2O_3, SiO_2	Cr, Cr_2O_3, Si or SiO_2
Cr + SiO - 16 - C	Cr, possibly Cr_2O_3	-
Cr + SiO - 17 - C	Cr, Cr_2O_3, Si or SiO_2	Cr, possibly Cr_2O_3

*) Strong preferred orientation with (111) as fiber axis. No other orientation present.

**) See also: Grube, G. and Speidel, H.: Z. Elektrochemie 53.399 (1949).

***) Modification assumed to be a α-quartz.

B. Electrical Parameters

Specimen No.	Thickness (Angstroms)	Resistivity (micro-ohm cm)	TCR (10^{-4}/°C
13 C	814	7.42×10^6	-37.9
8 C	3552	3.42×10^6	-30.9
11 C	2204	2.77×10^5	-16.9
17 C	2280	9.87×10^4	- 8.04
16 C	1580	1.7×10^4	- 1.87
15 C	1630	9.95×10^3	- 1.01

The following species are considered to be the most outstanding for film resistor application demanding low magnitude of TCR and high stability. Films for these species, baked in air, aged less than 1 percent in resistance value on the 1000 hours aging tests.

Cr + SiO - high resistivity--better method of deposition desirable in order to obtain uniform coatings of predictable resistivity.

$CrSi_2$ - Of those investigated - the silicides were the easiest

$CrSi_2 + TiSi_2$ compounds to evaporate from a single source. Though a

$TiSi_2$ specific process for producing films with known characteristics was not developed, initial experience indicates that controlled depositions are possible with less difficulty than with Cr + SiO.

The films discussed subsequently show some promise as resistors. Long term aging and preferred methods of stabilization were not determined. It was obvious from instability during TCR measurements that some form of passivation would be required.

Zr-zirconium oxide - Very slow deposition (< 100 Å/sec) in the 10^{-5} torr range at substrate temperatures of about 450°C or by more rapid evaporations of Zr in oxygen at low pressures produced high resistivity films. Oxidation by the latter method was difficult to control. It appeared that significant oxidation occurs in the lower 10^{-4} range for all species evaporated in O_2 and that the range of pressures for controllability is rather small. Around 5×10^{-4} torr there appeared to be an avalanche reaction rate and films were nearly completely oxidized. To obtain high resistivity films in the 10^4 microhm-cm range, the avalanche conditions had to be approached too closely for reliable results. Unprotected films aged rather poorly during TCR

measurements and after 4 to 7 hours at 125°C. Some of this poor performance can be attributed to the films being very thin, well below a desirable thickness of 500 Å.

ZrO_2 - Highest resistivity obtained for any species at small negative TCR values of about - 500 ppm/°C. Aged poorly during TCR measurements even though films were thick.

Poor aging during TCR measurements indicates that films of Zr and ZrO_2 do not form an oxide layer that is as protective to the material as do films with Si or SiO_2 components. Thus, possible improved protection may be realized by overcoating the Zr-ZrO_2 specimens with SiO.

Properties not investigated but which need to be to determined in order to define the full utility of the films investigated as resistors are:

Noise characteristics,

Thermoelectric properties,

Light sensitivity,

Voltage coefficients or sensitivity,

Pressure sensitivity, and

Aging characteristics under load.

11. Experiments to Increase Film Uniformity and Control

11.1 Introduction: One of the principal problems in production of resistive elements in a circuit is uniform thickness deposition and a uniform composition of a compound film over a desired substrate area such as 2" x 2". Since one of the most desirable compounds studied was one requiring the dual evaporation of chromium and silicon monoxide at controlled rates and to a desired resistivity, sources for the deposition of this compound were studied in some detail and are described fully in the subsequent paragraphs.

11.2 Dual Source for Evaporating Cr and SiO: The chromium-silicon monoxide cermet films were excellent from the standpoints of stability and high resistivity at low magnitude of TCR. However, the ability to fabricate films at pre-selected resistivity or TCR values in successive batch quantities was exceedingly difficult. This difficulty was encountered particularly in the evaporation of the materials from a common grain box source, R. D. Mathis

type ME-1. From past experience, the technique of flash evaporating mixed powders was also considered unsatisfactory as a production process. Hence, attention was directed toward designing an evaporation source for reliably producing resistors of this species. It was desirable that such a source provide the following:

(1) Uniform mixing of the vapors of the two materials before or upon arrival at the substrate surface,

(2) Controlled proportional mixing of the Cr and SiO vapors,

(3) Uniform deposits over a relatively large substrate area of at least 2" x 2",

(4) Large capacity or relatively constant emission characteristics for long term application in successive batch depositions, and

(5) Simple operation and economical.

Although desirable, a common source design meeting the general requirements was not conceived at this time; the primary limitation was the large difference between the vapor pressures of Cr and SiO. Any improvement on the initial method was considered worthwhile, so a dual design was considered.

A source other than the usual tantalum grain box source for evaporating SiO was desired. Graphite cloth* was tested and found satisfactory for SiO but not for chromium. In these tests, separate evaporations in high vacuum of chromium and SiO from and through densely woven graphite cloth were made. The respective materials were wrapped within the cloth in such a manner that they were completely enclosed. The cloth was electrically terminated and was heated to the desired temperature by the passage of current. Due to reaction with chromium the cloth was unsatisfactory as a source material. On the other hand, it proved to be quite satisfactory for the evaporation of SiO. No adverse reaction between the SiO and carbon was detected from a visual inspection of unevaporated SiO and the cloth; however, silicon atoms resulting from any disassociation of the evaporant at the source may react with the graphite cloth and remain on the source as the less volatile compound silicon carbide.[11]

* The use of graphite cloth as a heater for evaporants, particularly SiO, originated at Georgia Tech on another project, Contract No. NAS8-20577.

The SiO films deposited in this manner exhibited the usual brownish color and possessed good dielectric qualities. Wrapping the SiO within a double layer of the cloth prevented the spitting usually associated with the evaporation of SiO. The graphite cloth has a resistivity of about 1/2 ohms per square and requires a relatively low current compared to commonly used metal filament sources for a given source temperature. The material thus has several advantages over the commonly used tantalum chimney and box sources for the evaporation of SiO.

Chromium can be evaporated quite satisfactorily from tungsten boats, so a design employing two parallel tungsten boats along side a planar graphite source was selected. The graphite cloth source was 1.5" x 1.5" area and centered between but slightly below the boats with respect to the substrate. The arrangement and geometry of the sources are illustrated in Figure 38. The SiO source was loaded with 20 grams of SiO particles ranging from 10 mesh to pea size. Approximately 4.5 grams of chromium pellets were placed in each of the chromium sources for a total load of 9 grams. Evaporations were made with the source "A" to substrate geometry of Figure 39. During evaporations the two chromium sources were operated in parallel at a total current of 220 amperes and the SiO source at 55 amperes in order to obtain film resistivities of about 10,000 microhm-cm. Intense heat radiation from the sources caused considerable degassing in the vacuum chamber. As a result of this and the low pumping capacity of vacuum system "C", evaporations were made in the 1×10^{-4} torr range. Considerable oxidation of both the chromium and silicon monoxide can occur in the 1×10^{-4} torr range. This is particularly true for pressures exceeding 5×10^{-4} torr. (Essentially complete oxidation of SiO and Cr occurred in pressures of oxygen greater than 7×10^{-4} torr in other phases of the program.) To maintain the pressure in the lower half of this range for the total deposition period of 10 minutes it was necessary to interrupt the evaporation for pumping intervals and two to three successive deposition cycles were required. Before deposition of the resistive films, the source was operated with the substrate shutter closed to aid in degassing the vacuum chamber. During these periods the pressure increased to the upper limit of the 1×10^{-4} torr range. At the higher pressures some oxidation of the graphite cloth occurred, and its electrical resistance gradually increased

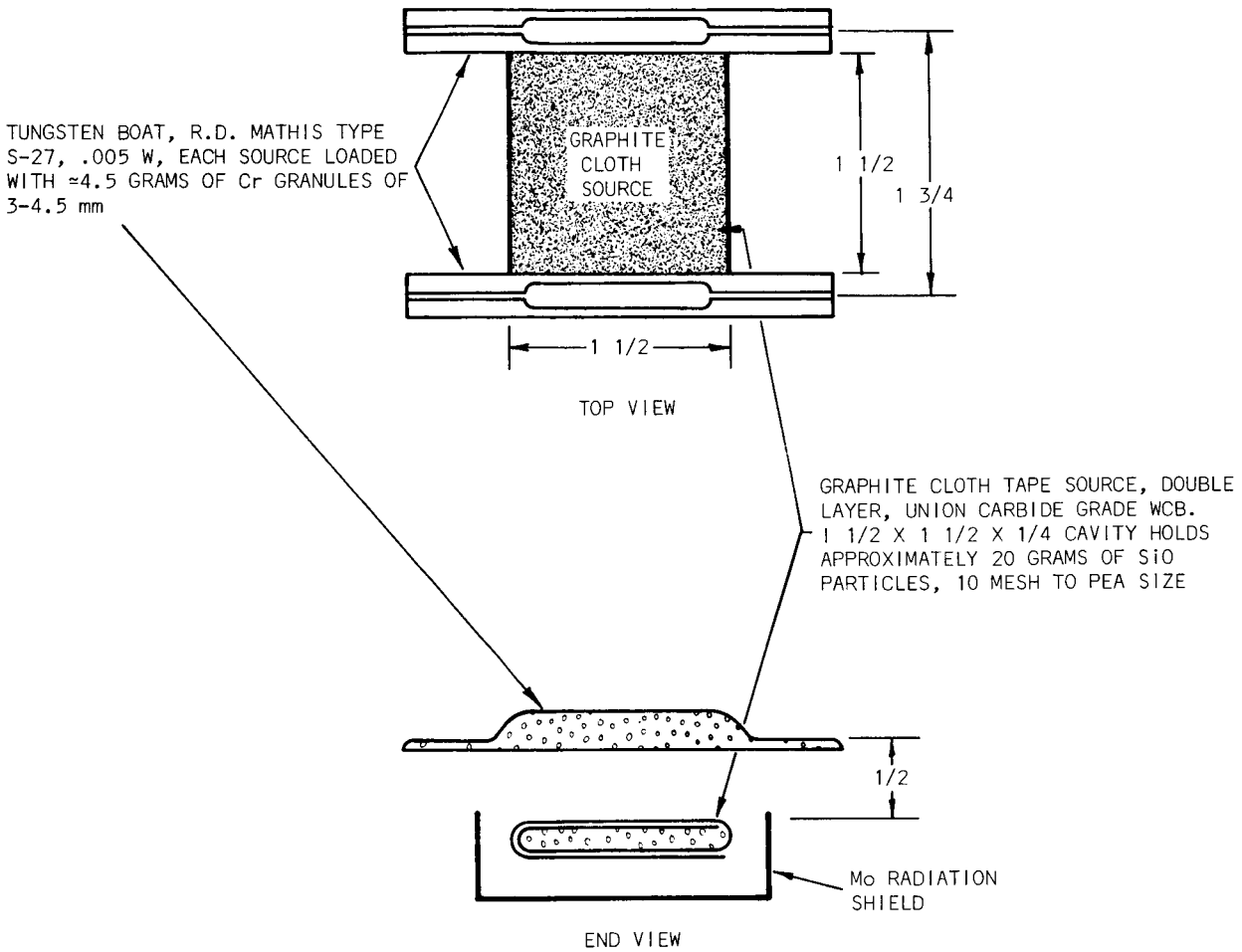

Figure 38. Experimental Dual Source for Co-Evaporation of Cr and SiO.

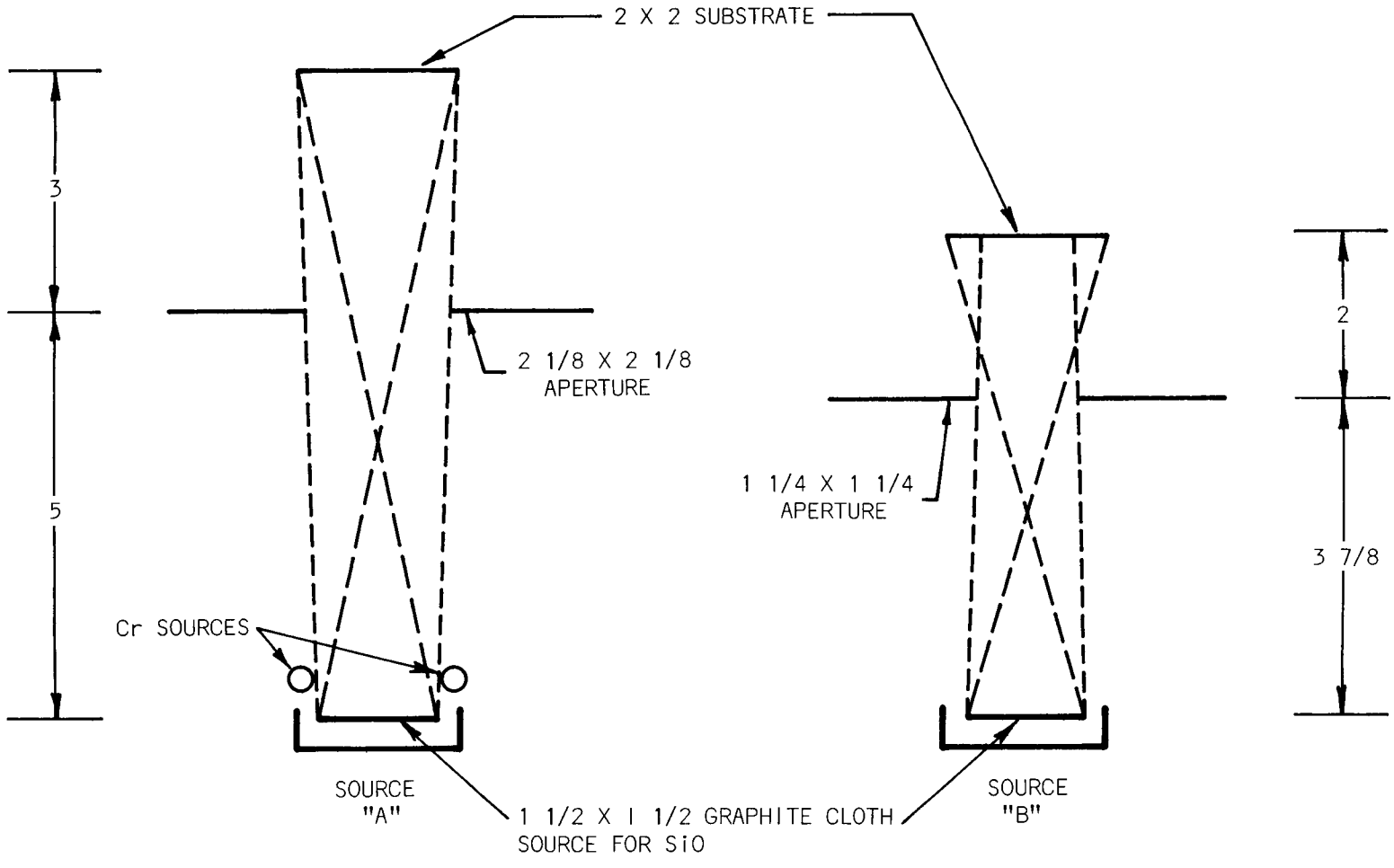

Figure 39. Source to Substrate Geometry of Experimental Source.

with time. Silicon monoxide vapor reaction with the graphite source probably contributed to an increase in resistance, as well. The reaction with chromium vapor from the chromium sources is less likely. A contact metal transmission mask was placed in front of the substrate to form 6 resistors on each substrate simultaneously. The substrate dimensions were 2" x 2" x 1/32". Locations of the resistors on the substrate are shown in Figure 40. Measurements of resistance, TCR, and thickness were made to determine uniformity of characteristics over an area corresponding to an average maximum radius of 3/4" with respect to the center of the substrate.

The resistivity of the specimens ranged from 6×10^3 to 1.7×10^8 microhm-cm. TCR values for a given resistivity were in general agreement with those of Figure 16 obtained with the grain box source. The resistivities were calculated from the R/sq and thickness values of each film. The thickness for each resistor was determined by taking the average value of measurements made at two positions on the film; these were made on opposite edges near the mid-point of each resistor. The mid-points of resistors 2 and 3, M and 5, and 1 and 4 are located at a substrate radius of 0.25", 0.56", and 0.75", respectively. Average thickness and resistivity values were obtained for each radius by calculating the mean values of respective resistor pairs. The thickness variation of Cr + SiO films on two substrates are shown in Figure 41-b. Values were normalized for a value of 1 at a radius of 0.25". The thickness of specimen No. 6 increased 61 percent at a radius of 3/4" with respect to the projected value of a film at the y intercept, or zero radius. This specimen showed the greatest variation in both thickness and resistivity. Specimen No. 8 had the least variation in thickness and resistivity. Corresponding values of other specimens lay between the limits of specimens No. 6 and No. 8. Since resistivity values increased in a similar manner across the substrate, it was suspected that SiO enrichment of the composite film occurred with increasing radius. To determine if this were true, separate evaporations were made with the chromium and SiO sources. For the chromium deposition, each resistor element lay in the thickness range 2030 ± 30 Å. Hence within the accuracy of measurements the chromium film was uniform. Two SiO specimens were deposited. One was deposited with the chromium sources energized but empty to simulate

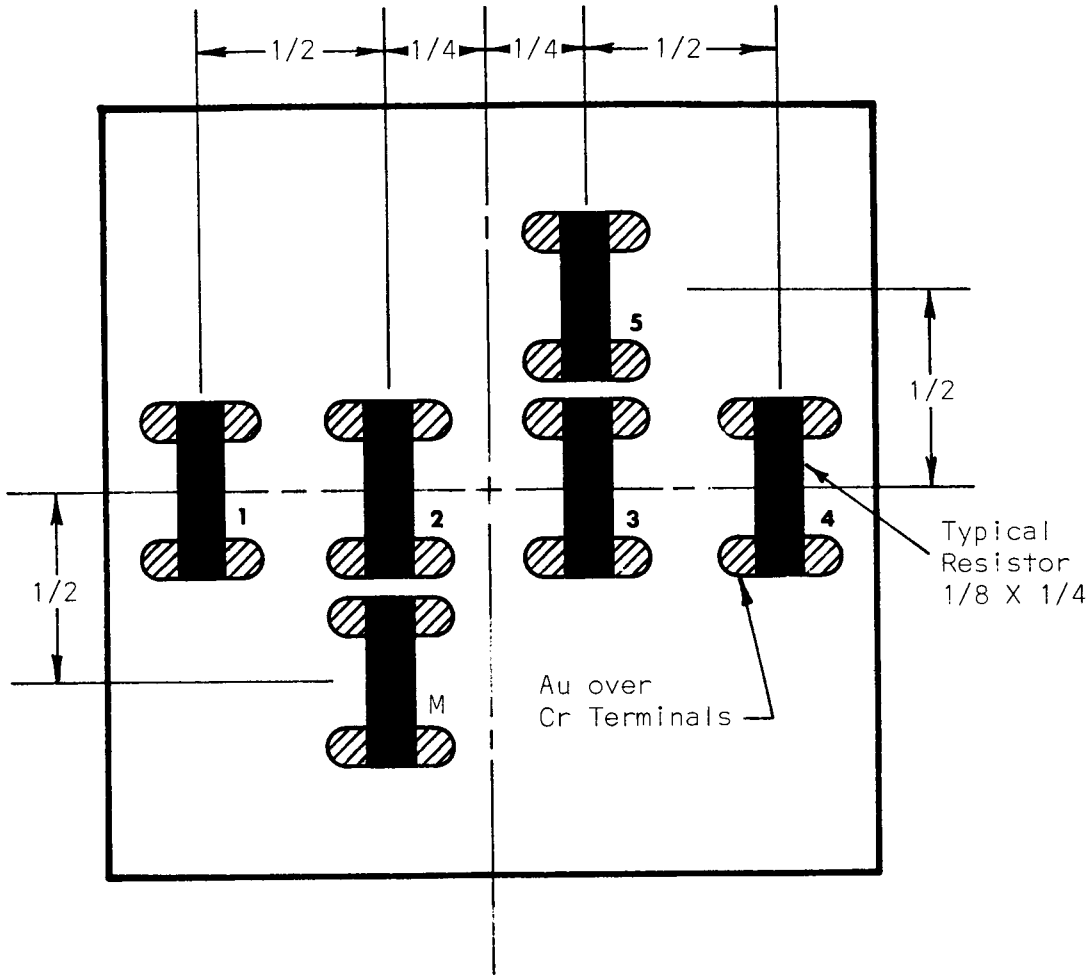

(DIMENSIONS ARE IN INCHES)

Figure 40. Resistor Layout on 2" x 2" Substrate.

the conditions for depositing the composite films; the other specimen was deposited with the chromium source off. The thickness variation of these films are shown in Figure 41-a. The thickness of both films increases positively with respect to the radius; however, that of the film deposited with the chromium source on increased to a greater extent and more rapidly with incrasing radius.

SiO depositions were made with a SiO source similar to that of source "A" of Figure 39 but with a source to substrate geometry as indicated in source "B" of Figure 39. In the source "B" arrangement, every point of the substrate is not in line of sight with every point of the source due to stopping effect of the aperture; also, the substrate to source distance was less. With source "B", a film thickness distribution was obtained that decreased in thickness with increasing substrate radius per Figure 42. Thus effects of the aperture as a stop between the source and substrate and the source to substrate distance are quite evident by comparing the results in Figures 41-a and 42.

A stop with a square aperture measuring 1" x 1" was installed between the graphite source and the chromium source of source "A" of Figure 39 to study its effects of film uniformity. The source to substrate geometry and stop location are sketched in Figure 43. Effects of the stop on uniformity of film thickness and resistivity were determined as previously discussed.

Average thickness variation obtained for SiO films deposited with the stopped source is shown in Figure 44-a. The increase in thickness of about 10 percent for a zero to 0.75 inches radius is much smaller than the increase of 17 to 60 percent obtained for the source operated without a stop. Hence, definite improvement in SiO thickness uniformity control was obtained with the stop.

Co-deposition of Cr and SiO were made with the stopped source. The lower curve of Figure 44-b shows the averaged variation in thickness obtained for these films. Comparing this curve with that of specimen No. 8 of Figure 41-b, it can be seen that the decreasing thickness with increasing radius above 0.56 inches was in opposite sense to that obtained for the source operated without a stop. This resulted in a lower overall thickness variation for the stopped source. The upper curve of Figure 44-b was the corresponding average variation in resistance with radius of resistance values of the six resistors

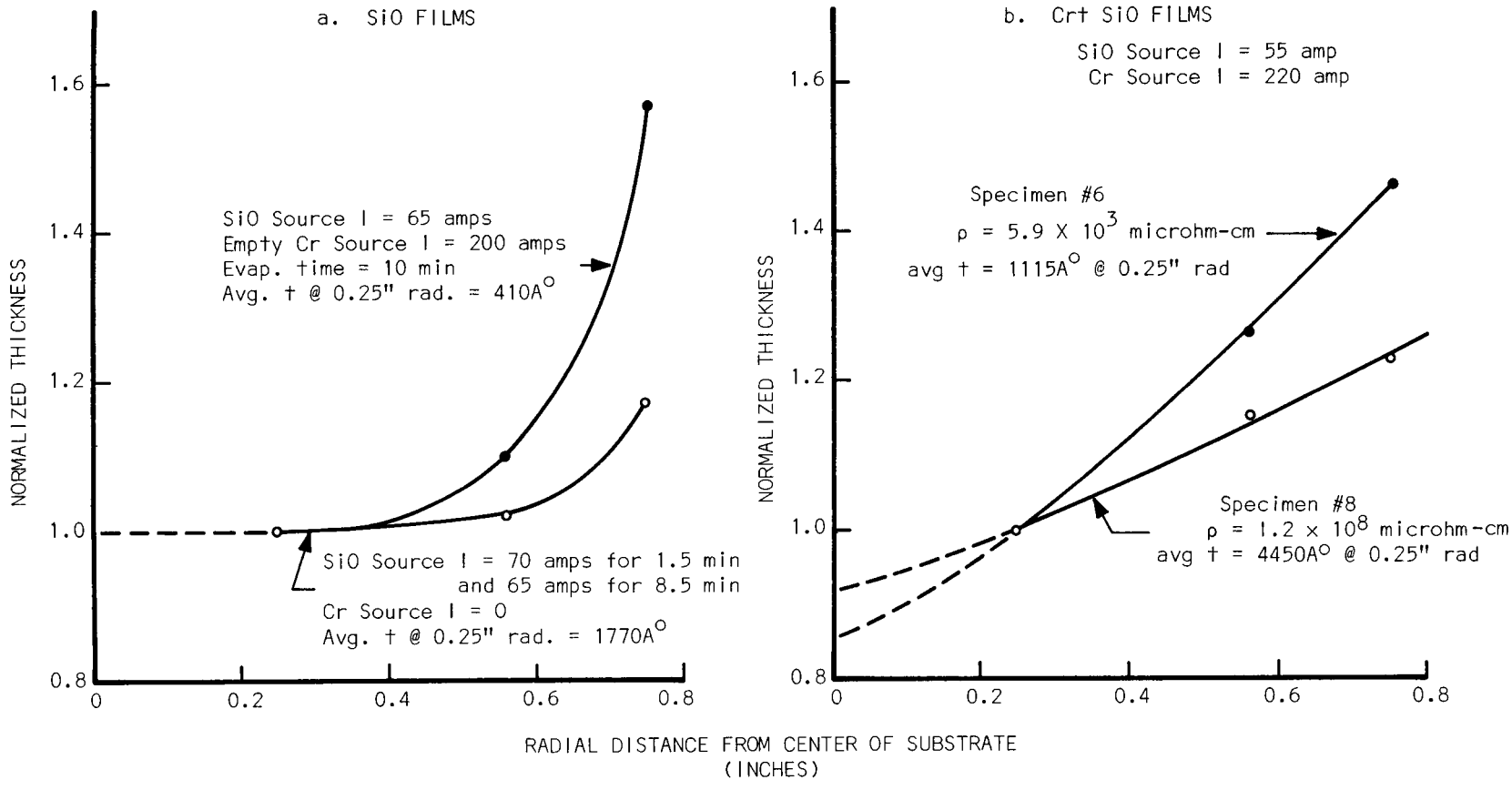

Figure 41. Uniformity of Films Deposited with Experimental Source for the Co-Evaporation of Cr and SiO.

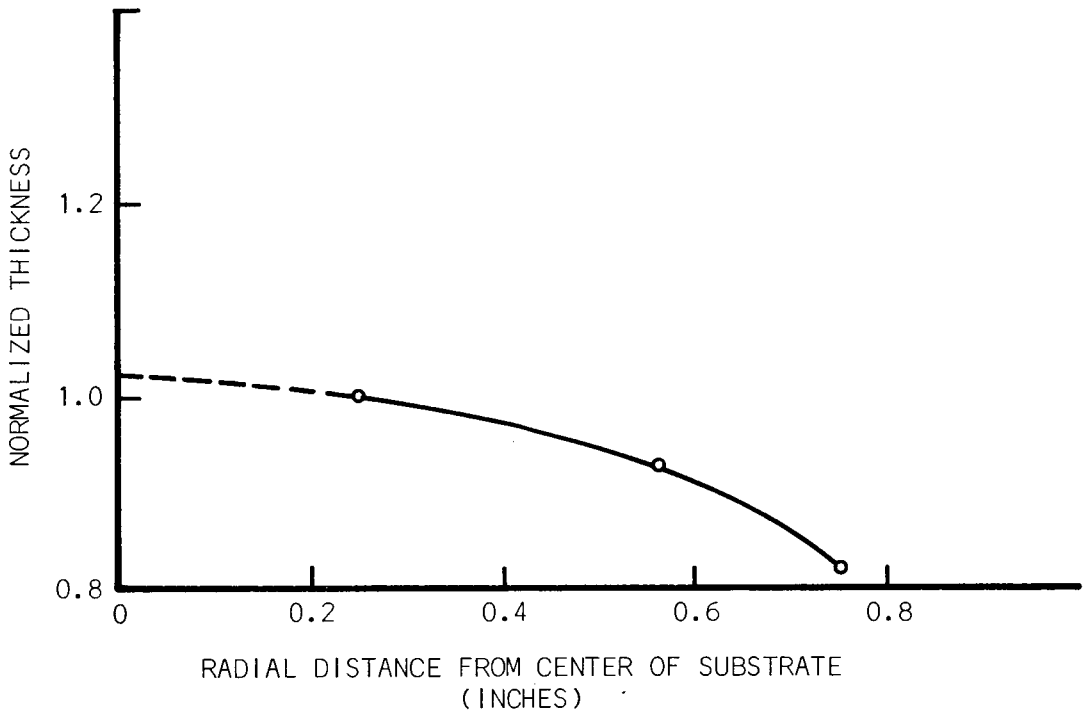

Figure 42. Uniformity of SiO Films with a Stop Between the Substrate and Source.

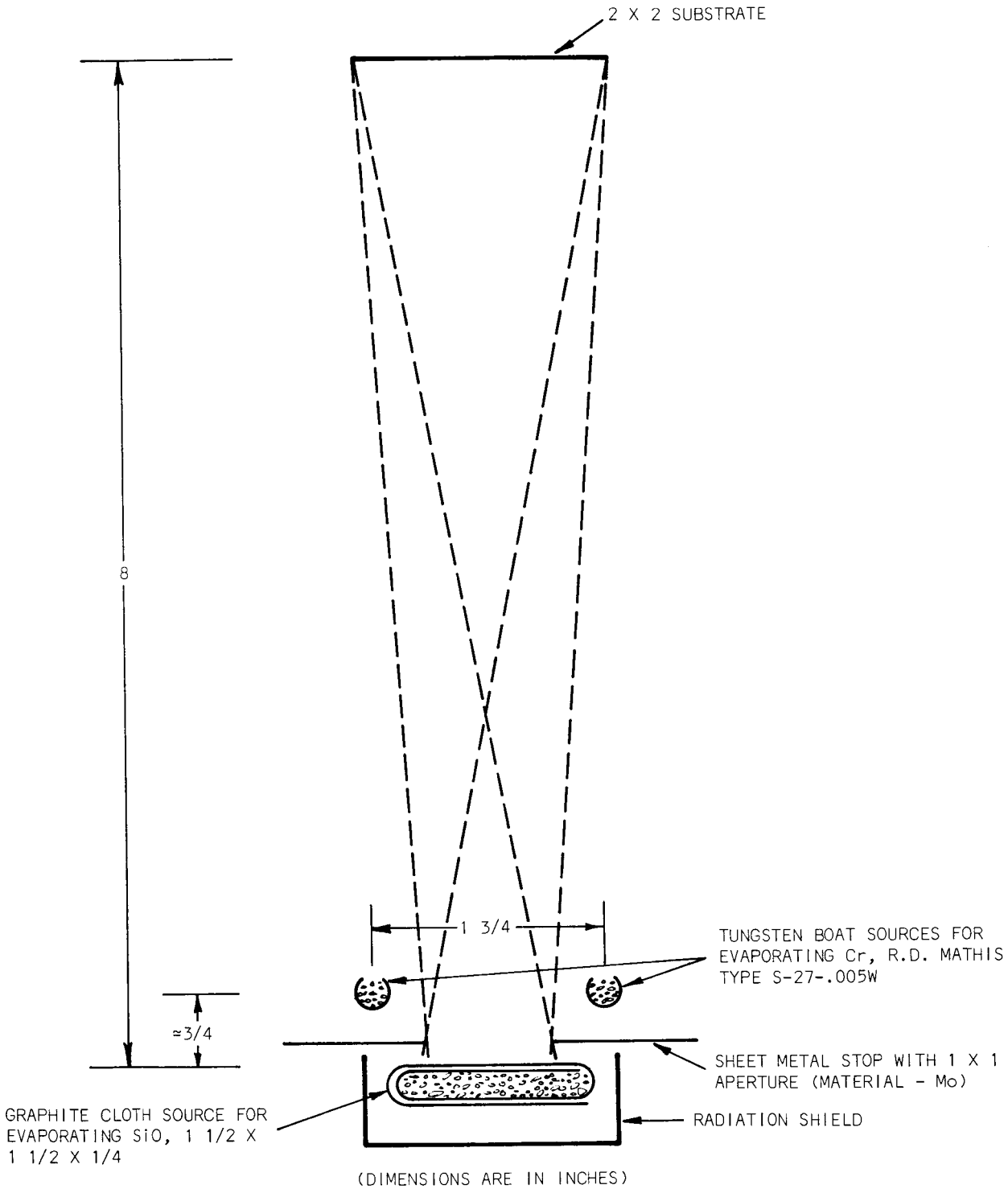

Figure 43. Source "A" to Substrate Geometry with Stop.

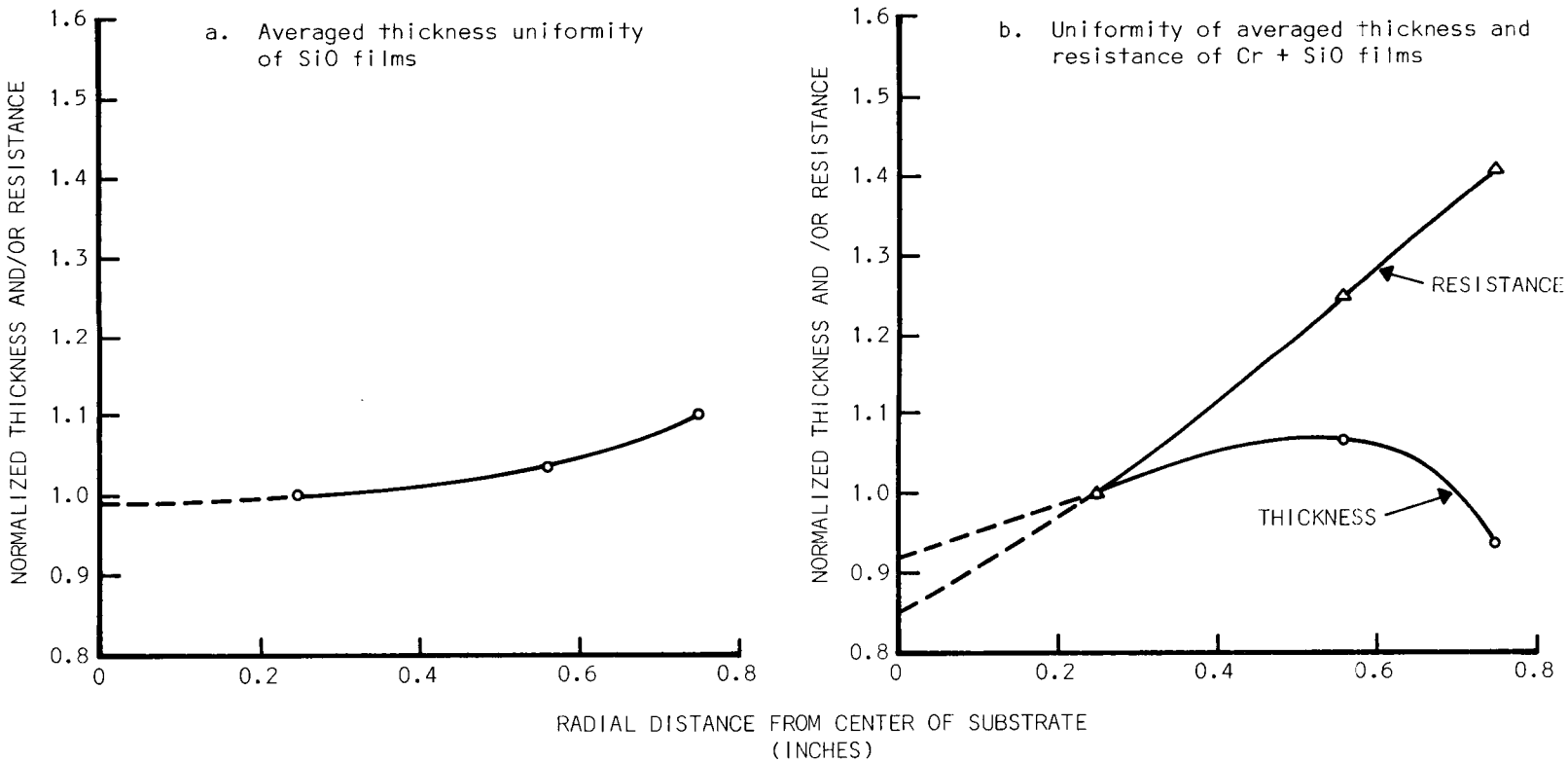

Figure 44. Uniformity of Cr, SiO, and Cr + SiO Films Deposited with the Stopped Experimental Source of Figure 43.

on four different substrates. TCR values of these films were quite low in magnitude; both small positive and small negative values occurred on each substrate within the range of ± 100 ppm/degree Centigrade; furthermore, the TCR values shifted in the negative sense with increasing radius. Thickness measurements indicated that the resistivity variation was not due solely to variation in SiO concentration. Hence, it appreared that major factors in addition to variations in SiO concentration were contributing to variations in resistivity over the substrate surface.

Thickness of Cr deposits were uniform within the accuracy of thickness measurements, yet, the resistivity of Cr films increased with radius similarly t to the Cr + SiO films. As a result, non-uniform heating of the substrate during deposition was suspected as having a primary influence on uniformity of resistivity and TCR values. To determine the significance of non-uniform heating on uniformity of electrical characteristics over the substrate surface, measurements of resistance values were made of chromium film resistors deposited on room temperature substrates; substrates heated with a graphite cloth source,* see Figure 4, to a reference temperature of 400°C; and substrates heated to a temperature corresponding to a temperature of 300 to 350°C of an aluminum plate in direct contact with the substrate. In the latter case, the aluminum plate was heated with the graphite cloth source and the temperature of the aluminum plate was determined from a thermocouple clamped to the aluminum plate with a screw. The aluminum plate was equal in length and width to the substrate and was 1/8 inches thick.

With the Cr sources spaced 1-3/4 inches apart, Cr deposits were made at each of the three substrate heating conditions; these results are shown in Figure 45. For Specimen No. 12 the substrate was heated with the regular graphite cloth source to the reference temperature of 400°C; this corresponds to the substrate heating used on the specimens of Figures 41 & 44. The resistance variation shown in Figure 45 is similar to that obtained for the Cr + SiO films in Figure 44-b. The corresponding average thickness variation

---

* The graphite cloth substrate heater was used as the substrate heater for the Cr + SiO and Mn + SiO film resistors fabricated early in the program to determine the resistivity versus TCR characteristics of Figures 16 and 19.

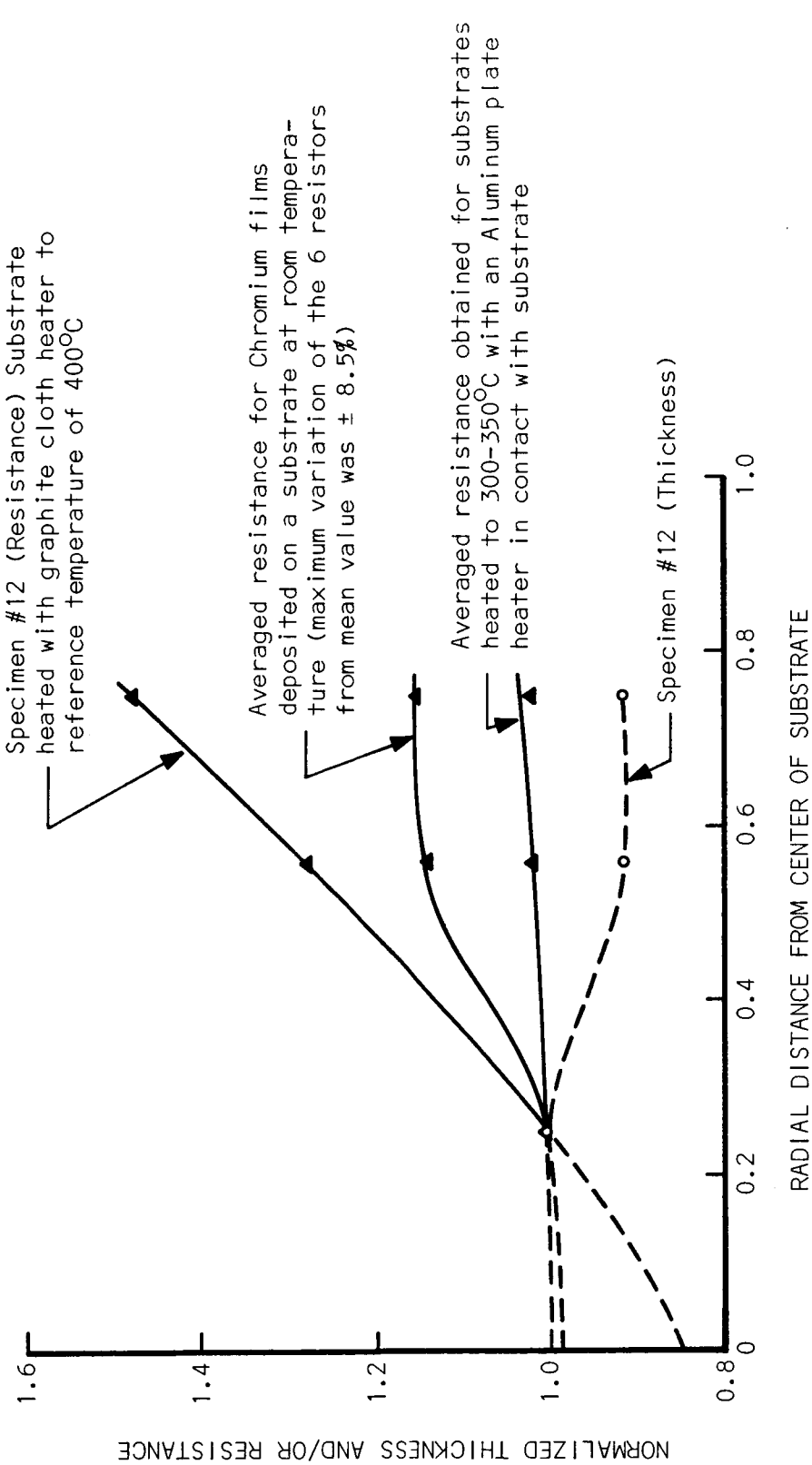

Figure 45. Effects of Substrate Heating on Resistance of Chromium Films.

obtained for specimen No. 12 is also shown in Figure 45; the 10 percent variation is within the error of measurements, and it cannot be said definitely that the point at a radius of 0.25 inch is actually thicker than the other measured values. It is quite evident, however, that a large part of the variation in resistivity is independent of variation in film thickness. The remaining plots of Figure 45 clearly show that non-uniform heating of the substrate is a primary factor contributing to the variation in resistivity of chromium resistors over a given substrate surface. The lowest variation in the averaged resistance of ± 2 percent was obtained for the substrates heated with the aluminum plate; whereas, the maximum variation from the mean value of resistance of the six resistors on each of these two substrates were ± 6.6 percent and ± 3.8 percent, respectively. For those substrates heated with aluminum plate it appears that the temperature was still somewhat higher in the center of the substrates compared to the outer sections.

With the source and source to substrate geometry of Figure 43 chromium depositions were made with the chromium sources spaced 1", 1-3/4", and 2-1/3" apart. No significant difference in variation of film resistivity over a substrate radius of 3/4 inch was obtained for the respective spacings. A maximum variation in resistivity of ± 7 percent over a substrate radius of 3/4 inch was obtained for each condition. In each case the substrate was heated with the aluminum plate substrate heater equal in length and width to the substrate.

A copper plate was substituted for the aluminum plate to heat the substrates, and the aperture of the stop in Figure 43 was increased to 1-1/8" x 1-1/8". Maintaining the source to the substrate geometry of Figure 43 and with the slightly larger aperture, co-depositions of Cr and SiO were made with the copper plate substrate heater at 350°C. For six separate depositions where the TCR values ranged from -2×10^{-4}/°C to -0.3×10^{-4}/°C, the average variation obtained for the six resistors of the substrates was ± 4.4 percent of the average resistance. The lowest variation obtained between the six resistors for any one substrate was ± 1.7 percent from the average value, and the maximum variation from the average on any one substrate was ± 9.8 percent. The resistance values were normalized for a radius of 0.25 inch, as was done in Figure 45, for each of the substrates; and averaged normalized variations

of 1.00, 1.01, and 1.02 at the respective radii of 0.25", 0.56", and 0.75" were obtained. From the measured resistivity versus TCR characteristics of Cr + SiO films, the resistivity values represented in these calculations ranged from (1 to 2)10^{+4} microhm-cm. At higher resistivities, greater variation of resistance between the resistors on a given substrate was experienced. The variation between the six resistors from the average value was ± 44 percent for a typical substrate with resistors having a TCR of approximately -30×10^{-4}/°C.

These data demonstrated that with a metal plate substrate heater and with the preceding sources and source to substrate geometry, the average variation in resistance of Cr + SiO films of resistivities near $1 \times 10^{+4}$ microhm-cm over a 3/4 inch substrate radius was ± 5 percent. Two-thirds of the six substrates had less variation, and one-third had variations between ± 5 and ± 10 percent. TCR values could be reproduced fairly well during successive evaporations by manually maintaining constant source currents with a variac. However, precision instrumental control of the source temperatures will be necessary to gain desired control on the resistive parameters. Evidence from about 50 evaporations indicated that the vapor output characteristics of the sources remained fairly constant for at least 2 hours of operation. Thus, a dual source arrangement similar to that of Figures 38 and 43 with appropriate stopping and temperature control promises to be useful for evaporating chromium-silicon monixide resistors with average tolerance requirements of 5 to 10 percent. It is suspected that temperature variations over the substrate surface and the relatively high vacuum pressures of (1 to 4)10^{-4} torr during the evaporations contributed considerably to the magnitude of the non-uniformity of the film parameters.

Further improvements in uniformity of the resistive parameters over large area substrates can possibly be realized by maintaining vacuum pressures within the 10^{-6} torr range or better during evaporation processes. In addition, attention must be devoted in the future to maintaining uniform substrate temperatures. The latter can be achieved by improved methods of substrate heating; an easier way, may be to select substrate materials with greater heat conductivity than that afforded by glass. The importance of maintaining uniform substrate temperatures cannot be over emphasized.

III. CONCLUSIONS AND RECOMMENDATIONS

Of the series of selected materials examined (metal-metal oxide, metal-silicon monoxide, borides, nitrides, silicides, and some combinations of the borides and silicides) the chromium-silicon monoxide films gave most consistently the required resistivity range of 10^4 microhm-cm, ± 200 x 10^{-6}/°C TRC, and displayed the least aging. Experiments on a dual source system for evaporating chromium and silicon monoxide, employing a diaphragm arrangement to control vapor deposition rate and distribution, proved capable of giving uniform deposits over a circular area of 1.5" diameter. An additional variable controlling resistivity was the temperature and the uniformity of the substrate heating at the time of deposition. Heated aluminum or copper supporting plates in contact with the substrates were found to be better than radiant heating with graphite cloth in distributing the heat uniformly over glass substrates. With the controls utilized, resistance variation of individual resistors of ± 2 to 10 percent were realized at resistivities of 1 to 2 x 10^4 microhm-cm over the substrate area. Some improvement may be expected with instrumental control of source temperatures or rates, better heat distribution at the substrate, and lower vacuum background pressures.

Resistive films of $CrSi_2$, $TiSi_2$, and $CrSi_2$ + $TiSi_2$ gave some promise as materials evaporable from a single source. However, resistivities, in general, were in the range 500 to 2000 microhm-cm, well under the target value of 10^4 microhm-cm.

Films deposited by evaporation of oxides or of metals in oxygen at low pressure were found to give films ranging from very high resistivity and high negative TCR values to films with essentially metallic type behavior, and the process was difficult to control. Of the metals or metal oxides examined zirconium evaporated in oxygen at low pressure produced films with the best properties, a resistivity of 2400 microhm-cm at a TCR of -88 x 10^{-6}/°C was obtained for one film. Examination of films of Zr-SiO appears to be a profitable future course.

With respect to aging the Cr + SiO films displayed excellent performance, exhibiting changes of < 1 percent in 1000 hour test periods. To attain this performance passification of the films by baking several hours at about 300°C

was employed. During this time resistors underwent positive changes of approximately 30%. The silicides also gave promise with respect to good aging properties. With the exception of $TiSi_2$, the silicides approached the performance of the Cr + SiO films, and the $TiSi_2$ was much improved after post deposition baking.

Films meeting the requirements of resistivity and TCR were obtained, and some progress in deposition of uniform and reproducible films was made. However, the answers obtained pointed to a considerable amount of further engineering development in order to produce reliably and reproducibly the films deposited in the laboratory. The intrinsic difficulties of dual source control point to a single source deposition method as the preferred technique. New developments in sputtering suggest this method as a possible alternative to evaporation as a choice for film resistor deposition. Its capabilities of deposition of uniform films over large areas and of depositing an alloy electrode essentially as the stoichiometric composition indicate that sputtering possesses intrinsically the capabilities which are so difficult to obtain for evaporation of multicomponent materials by any method. It is recommended that sputtering of Cr-SiO resistive elements be investigated.*

*A brief list of recent references concerning sputtering and related processes is included in the Bibliography.

REFERENCES

1. S. Tolansky, Multiple Beam Interferometry of Surfaces and Films, Clarendon Press, Oxford (1948).
2. G. D. Scott, T. A. McLauchlan, and R. S. Sennett, J. Appl. Phys. 21, 843 (1950).
3. M. Beckerman and R. E. Thun, Vacuum Technology Transactions, Pergamon Press, New York (1961).
4. M. Beckerman and R. E. Thun, Transactions 8th Vacuum Symposium 2, 905, (1962).
5. E. Keonjian et al, Microelectronics, McGraw Hill Book Company, New York (1963), pp. 181-191, 255-261.
6. Clifford A. Hampel, Rare Metals Handbook, Reinhold Publishing Corp., Second Edition (1961).
7. C. F. Powell, I. E. Campbell, and B. W. Gonser, Vapor-Plating, John Wiley & Sons, Inc., New York (1962).
8. R. M. Adams, Boron, Metallo-Boron Compounds, Interscience Publishers, John Wiley & Sons, Inc., New York (1964).
9. B. Aronsson, T. Lundstrom, and S. Rundqvist, Borides, Silicides, and Phosphides, John Wiley & Sons, Inc., New York, Methuen & Co., Ltd., London (1965).
10. L. Young, Anodic Oxide Films, Academic Press, London and New York (1961).
11. L. Holland, Vacuum Deposition of Thin Films, John Wiley & Sons, Inc., Fourth Printing, pp. 130-131 (1961).

BIBLIOGRAPHY

Anderson, D., "A Summary of Thin Film Deposition Techniques," SCP and Solid State Technology (December 1966).

Anderson, G. S., Mayer, W. N., and Wehner, G. K., J. Appl. Phys. 33, 2991 (1962).

Beckerman, M. and Bullard, R. L., Proceedings Electronic Components Conference, Washington, D. C., p. 53 (May 1962).

Belser, R. B., "Alloying Behavior of Thin Bimetal Films, Simultaneously or Successively Deposited," J. Appl. Phys. 31, 562 (1960).

Belser, R. B. and Hicklin, W. H., "Simple, Rapid Sputtering Apparatus," Rev. of Scient. Instr. 27, 293-296 (1956).

Belser, R. B. and Woolf, W. E., "Research on Vacuum Evaporated and Cathode Sputtered Thin Films," ASD TR 60-381, Part II, Contract No. AF 33(616)-6379, April 1962, pp. 64-68, 72.

Belser, R. B. and Woolf, W. E., "Research on Vacuum Evaporated and Cathode Sputtered Thin Films," ASD TR 60-381, Part III, Contract No. AF 33(616)-6379, May 1962, pp. 34-43.

Berry, R. W., Jackson, W. H., Parisi, G. I., and Schafer, A. H., "A Critical Evaluation of Tantalum Nitride Film Resistors," Proceedings of the Electronics Components Conference, pp. 86-96 (1964).

Bickley, W. P. and Campbell, D. S., Le Vide 17, 214 (1962).

Blevis, E. H., Glow Discharge Sputtering--Theory and Practice, Distributed by R. D. Mathis Co., Long Beach, California (February 1964).

Blevis, E. H., Hot Cathode and Radio Frequency Sputtering, Distributed by R. D. Mathis Co., Long Beach, California (February 1965).

Davidse, P. D., "Theory and Practice of R. F. Sputtering," Semiconductor Products and Solid State Technology 9 (December 1966).

Fehsenfeld, F. C., Evenson, K. M., and Broida, H. P., "Microwave Discharge Cavities Operated at 2450 MHz," Rev. of Scient. Instr. 36, 294-298 (1965).

Francombe, M. H., Transactions 10th National Vacuum Symposium, Macmillan, 316 (1963).

Frerich, R., J. Appl. Phys. 33, 1898 (1962).

Gerstenberg, D. and Mayer, E. H., Proceedings Electronic Components Conference, Washington, D. C., p. 57 (May 1962).

Holland, L., "The Cleaning of Glass in a Glow Discharge," Brit. J. Appl. Phys. 9 (October 1958).

Holland, L., Vacuum Deposition of Thin Films, Chapters 9-10, John Wiley & Sons, Inc., 4th printing (1961).

Holland, L. and Siddall, G., Vacuum 111, 245 (1953).

Holland, L. and Siddall, G., Vacuum 111, 375 (1953).

Huss, W. N., "Advances in Sputtering Equipment Technology," SCP and Solid State Technology (December 1966).

Kay, E., "Prevention of Oxidation in a Glow Discharge Environment with Sputtered Permalloy Films as an Example," J. Electrochem. Soc. 112, 6 (June 1965).

Lakshmanan, T. K. and Mitchell, J. M., Transactions 10th National Vacuum Symposium, Macmillan, 335 (1963).

Layer, E. H., 1959 Vacuum Technology Transactions, Pergamon Press, New York, p. 210 (1959), published 1960.

Layer, E. H., Chapman, C. M., and Olson, E. R., Proceedings 2d National Conference on Military Electronics, p. 96 (1958).

Maissel, L. I. and Schaiblr, P. S., J. Appl. Phys. 36, 237 (1965).

Pratt, I. H., 10th Conference on Military Electronics (1964).

Wehner, G. K., Phys. Rev. 114, 1270 (1959).

Wolsky, S. P., "Sputtering Processes and Film Deposition," SCP and Solid State Technology (December 1966).

APPENDIX

TABLE I

DETAILED FABRICATION DATA AND RESISTOR PARAMETERS

RESISTOR (SERIAL NO.)	SUB-STRATE (TYPE)	EVAPORATION PARAMETERS: SOURCE (TYPE)	EVAP-ORANT	SUB. T (°C)	DEP. PER. (MIN.)	P (TORR)	PROTECTION: NONE	SiO	BAKED PER. (HRS)	BAKED T (°C)	FILM PARAMETERS[1]: COMPOSITION[2]	THICKNESS (Å)	RESISTANCE (OHMS)	RESISTIVITY R/SQ. (OHMS)	RESISTIVITY SPECIFIC (μΩ Cm.)	TCR (10^{-4}/°C)	REMARKS
ALUMINUN – SILICON MONOXIDE																	
Al+SiO-1-B	CORNING	DUAL	Al WIRE	370	2	$(1-10)10^{-5}$	X				Al, Si	1980	585.4	585	1.16×10^{4}	- 11.2	
Al+SiO-2-B	# 7059	BN	AND	"	2	"	X					1300	3,746.	3,750	4.87×10^{4}	- 20.1	
Al+SiO-3-B	GLASS	CRUCI-	SiO	"	2	"	X				Al, Si	1270	507.9	508	6.46×10^{3}	- 8.57	
Al+SiO-4-B	"	BLES	POWDER	"	2	"	X				Al, Si	1780	870,000	870,000	1.55×10^{7}	- 64.7	
Al+SiO-5-B	"	INDE-	"	"	< 2	"		X				--	6.7	6.7	—	+ 5.85	
Al+SiO-6-B	"	PENTLY	"	"	3	$(2-10)10^{-5}$	X				Al	3550	2.72	2.72	96.5	+ 6.96	
Al+SiO-7-B	"	HEATED	"	"	2	$\approx 2\times10^{-5}$	X				Amorphous	513	$>10^{7}$	$>10^{7}$	—	—	
Al+SiO-8-B	"	TO-CO-	"	"	2	$(4-10)10^{-6}$	X					950	$\approx 1\times10^{7}$	$\approx 1\times10^{7}$	0.95×10^{8}	- 79	
Al+SiO-9-B	"	EVAPO-	"	"	2	2.5×10^{-4}	X				Al	5990	1.75	1.75	105	+ 5.82	
Al+SiO-10-B	"	RATE	"	"	2	$\approx 8\times10^{-5}$	X				Al	4530	2.06	2.06	95	+ 6.54	
Al+SiO-11-B	"	Al & SiO	"	"	2	$(1-10)10^{-6}$	X				Al, Si	1200	3.8	3.8	45.6	+ 9.81	
Al+SiO-12-B	"	"	"	"	2	4×10^{-6}	X				Al	2010	2.04	2.04	41	+ 7.63	
Al+SiO-13-B	"	"	"	"	1	6×10^{-6}	X				Al, Si	1020	32.5	32.5	326	+ 1.58	
Al+SiO-14-B	"	"	"	"	2	1×10^{-5}	X				Al, Al_2O_3, Si	2390	1.6×10^{6}	1.6×10^{6}	3.82×10^{7}	- 62.8	
Al+SiO-15-B	"	"	"	"	2	$(1-10)10^{-6}$	X				Al, Al_2O_3	--	6.9	6.9	—	+ 5.43	
Al+SiO-16-B	"	"	"	"	2	"	X				Al, Al_2O_3	2790	3.56	3.56	99.4	+ 7	
CHROMIUM																	
Cr-1A-FA	GLASS	W-BOAT	Cr	500	FLASH-ED	$\approx 5\times10^{-5}$	X						1.316	1.32		+ 11.4	
Cr-1B-FA	MICRO-	"	POWDER	"	"	"	X						1.829	1.83		+ 13.8	
Cr-1C-FA	SCOPE	"	"	"	"	"	X						—	—		—	
Cr-2A-FA	SLIDE	"	"	350	"	6×10^{-5}	X						7.323	7.32		+ 5.4	
Cr-2B-FA	"	"	"	"	"	"	X						11.11	11.1		+ 4.7	
Cr-2C-FA	"	"	"	"	"	"	X						--	--		—	
Cr-3A-FA	"	"	"	"	"	$(1-10)10^{-5}$	X						21.75	21.7		+ 7.54	
Cr-3B-FA	"	"	"	"	"	"	X						BROKE			--	
Cr-3C-FA	"	"	"	"	"	"	X						31.52	31.5		+ 6.0	

(Continued)

Note 1. Specimens with serial numbers ending in A, B, and C were fabricated in vacuum systems B, A, and C, respectively; those with no letter at the end of their serial numbers were fabricated in vacuum system D.

Note 2. Measurements of film parameters were made before the special treatments for protection or extended aging at 125°C in air.

Note 3. Film composition is that identified in an electron diffraction pattern of a film deposited on a carbon coated copper grid simultaneously with the resistive film. No pattern indicates an absence of rings in the diffraction pattern and is an indication that the film was amorphous.

TABLE I
(CONTINUED)
DETAILED FABRICATION DATA AND RESISTOR PARAMETERS

RESISTOR (SERIAL NO.)	SUB-STRATE (TYPE)	EVAPORATION PARAMETERS: SOURCE (TYPE)	EVAP-ORANT	SUB. T (°C)	DEP. PER. (MIN.)	P (TORR)	PROTECTION: NONE	SiO	BAKED PER. (HRS)	BAKED T (°C)	FILM PARAMETERS (1): COMPOSITION (2)	THICKNESS (Å)	RESISTANCE (OHMS)	RESISTIVITY R/SQ. (OHMS)	RESISTIVITY SPECIFIC (μΩ Cm.)	TCR (10^{-4}/°C)	REMARKS
						CHROMIUM CONTINUED											
Cr-4A-FA	GLASS	W-BOAT	Cr	350	FLASH-ED	$(1-10)10^{-5}$	X						9.536	9.54		+ 3.36	
Cr-4B-FA	MICRO-SCOPE	"	POWDER	"	"	"	X						9.337	9.34		+ 3.31	
Cr-4C-FA	SLIDE	"	"	"	"	"	X						15.30	15.3		+ 2.8	
						CHROMIUM – SILICON MONOXIDE											
Cr+SiO-1A-FA	"	"	APPROX. 1:1 VOLUME MIXTURE OF Cr & SiO POWDERS	350	FLASH-ED	2×10^{-5}	X					—	47.87	47.9	--	- 0.5	
Cr+SiO-1B-FA	"	"		"	"	"	X					857	47.47	47.5	407	- 0.25	
Cr+SiO-1C-FA	"	"		"	"	"	X					BROKE	68.38	68.4	--	- 0.51	
Cr+SiO-2A-FA	"	"		"	"		X						76.37	76.4	--	- 1.46	
Cr+SiO-2B-FA	"	"		"	"	"	X					--	68.55	68.6	—	- 1.31	
Cr+SiO-2C-FA	"	"		"	"	"	X					--	95.46	95.5	—	- 1.41	
Cr+SiO-1-C	"	H.V. METHOD TYPE ME-1	T. (°C) 1250 ± 50	220 mg SiO TABLET AND 2g Cr pwdr.	400	5	$\approx 5 \times 10^{-6}$	X				—		> 2 X 10^6	—	—	New Evaporant load for Cr+SiO-192-C, Cr+SiO-384-C deposited after #192 Without replenishing source load.
Cr+SiO-2-C	"	"			"	"	"	X				—		> 2 X 10^6	—	—	
Cr+SiO-3-C	"	"	1290 ± 50		"	3	"	X				--		> 2 X 10^6	—	—	
Cr+SiO-4-C	"	"		"	"	"	"	X				—		> 2 X 10^6	—	—	
Cr+SiO-5-C	"	"	1330 ± 50	"	"	1 1/2	"	X				—		> 2 X 10^6	—	—	
Cr+SiO-6-C	"	"	1410 ± 50	"	"	1	"	X				1790		7 X 10^5	1.24 X 10^7	-36.4	
Cr+SiO-7-C	"	"	1480 ± 50	"	"	1/2	"	X				1750		562	9.84 X 10^3	+ 0.24	
Cr+SiO-8-C	"	"	1450 ± 50	"	"	1	"	X			$SiO_2 Cr_2O_3$	3550		9.63 X 10^4	3.42 X 10^6	-30.9	New evaporant load for #9,
Cr+SiO-9-C	"	"	1480 ± 50	"	"	1/2	"	X				1530		1.16 X 10^5	1.77 X 10^6	-30.5	#7 deposited after #8 without
Cr+SiO-10-C	"	"	1480 ± 50	"	"	1/2	"	X				1460		2.56 X 10^4	3.74 X 10^5	-16.3	replenishing source load.
Cr+SiO-11-C	"	"	1520 ± 50	"	"	1/2	"	X			$SiO_2 Cr_2O_3$	2200		1.26 X 10^4	2.77 X 10^5	-16.9	New evaporant load for #9,
Cr+SiO-12-C	"	"		"	"	1/2	"	X				2090		3.54 X 10^4	7.4 X 10^5	-19.	#10 deposited after #9
Cr+SiO-13-C	"	"		"	"		"	X			$SiO_2 Cr_2O_3$	814		9.12 X 10^5	7.42 X 10^6	-37.9	Without replenishing source
Cr+SiO-14-C	"	"	1550 ± 50	"	"	1/2	"	X				2290		70.2	1.61 X 10^3	+ 1.13	load.
Cr+SiO-15-C	"	"	1520 ± 50	"	"	1/2	"	X			$Cr_2 Cr_2O_{3.3} O_3$	1630		612	9.95 X 10^3	- 1.01	
Cr+SiO-16-C	"	"	1480 ± 50	"	"	1/2	"	X			$Cr_2 Cr_2 O_3$	1580		1,080.	1.7 X 10^4	- 1.87	
Cr+SiO-17-C	"	"	1445 ± 50	"	"	1	"	X			$Cr_2 Cr_2 O_3$	2280		4,330.	9.84 X 10^4	- 8.04	

TABLE I (CONTINUED)

DETAILED FABRICATION DATA AND RESISTOR PARAMETERS

RESISTOR (SERIAL NO.)	SUB-STRATE (TYPE)	EVAPORATION PARAMETERS: SOURCE (TYPE)	SOURCE T(°C)	EVAPORANT	SUB. T (°C)	DEP. PER. (MIN.)	P (TORR)	PROTECTION: NONE	SiO	BAKED PER. (HRS)	BAKED T (°C)	COMPOSITION (2)	FILM PARAMETERS (1): THICKNESS (Å)	RESISTANCE (OHMS)	RESISTIVITY R/SQ. (OHMS)	RESISTIVITY SPECIFIC (μΩ Cm.)	TCR (10⁻⁴/°C)	REMARKS
								CHROMIUM–SILICON MONOXIDE (CONTINUED)										
Cr+SiO-18-C	GLASS	R.D.	1475 ±50	220 mg SiO TABLET W/2 g of Cr Powder	400	1	(1-5)10⁻⁵			6½	250		WHEN	2,240	224	3.1×10⁴	-4.12	Deposited simultaneously with new or full evaporant load in source.
Cr+SiO-19-C	MICRO-	MATRIX	"		"	1	"	X					THICKNESS	5,817	582	3.6×10⁴	-4.71	
Cr+SiO-20-C	SCOPE	TYPE	1450 ±50		"	1	"			6½	250		NOT	3,940	394	3.5×10⁴	-4.6	2nd evaporation with evaporant load used
Cr+SiO-21-C	SLIDE	ME-1	"		"	1	"	X					GIVEN,	18,170	1,817	7.5×10⁴	-7.97	1st time for #18 & 19.
Cr+SiO-22-C	"	"	1410 ±50		"	1 3/4	"			6½	250		P WAS	2,172	217	1.4×10⁴	-1.42	3rd evaporation with above evaporant load
Cr+SiO-23-C	CORNING	"	1475 ±50		"	1	(1-5)10⁻⁵			16	275		ESTIMATED	341,500	170,750	2.2×10⁶	-27.6	Deposited simultaneously
Cr+SiO-24-C	#7059	"	"		"	"	"		X				FROM	246,600	123,300	2.2×10⁶	-27.4	on 2"×2" substrate.
Cr+SiO-25-C	GLASS	"	"		"	"	"	X					PLOT OF	591,600	295,800	1.8×10⁶	-26.3	a new 220 mg SiO table!
Cr+SiO-27-C	"	"	"		"	"	"			16	275		P vs TCR	324,100	162,050	2.3×10⁶	-27.8	placed in source
Cr+SiO-28-C	"	"	"		"	"	"		X				OF	515,100	257,550	2.3×10⁶	-27.8	
Cr+SiO-29-C	"	"	1410 ±50		"	2	(1-5)10⁻⁵		X				SIMILARLY	603,200	301,600	1.7×10⁶	-25.8	Deposited simultaneously
Cr+SiO-30-C	"	"	"		"	"	"			16	275		FABRICATED	435,000	217,500	1.8×10⁶	-26.4	on 2"×2" substrate.
Cr+SiO-31-C	"	"	"		"	"	"	X					SPECIMENS	1.02×10⁶	510,000	1.6×10⁶	-25.3	2nd evaporation with
Cr+SiO-32-C	"	"	"		"	"	"		X					1.018×10⁶	509,000	1.5×10⁶	-24.7	evaporant for previous
Cr+SiO-33-C	"	"	"		"	"	"			16	275			641,300	320,650	1.6×10⁶	-25.3	five specimens
Cr+SiO-34-C	"	"	"		"	"	"	X						832,600	416,300	1.4×10⁶	-24.5	
Cr+SiO-35-C	"	"	1510 ±50		"	3 1/6	(1-5)10⁻⁵			10½	250			3,358.3	1,679	3.1×10⁴	-4.08	
Cr+SiO-36-C	"	"	"		"	"	"	X						3,941	1975	4.3×10⁴	-5.34	Deposited simultaneously
Cr+SiO-37-C	"	"	"		"	"	"			7	325			2,588	1294	1.6×10⁴	-1.73	on 2"×2" substrate.
Cr+SiO-38-C	"	"	"		"	"	"			10½	250			2,755.5	1378	1.6×10⁴	-1.86	full evaporant load
Cr+SiO-39-C	"	"	"		"	"	"	X						6,982	3491	6.1×10⁴	-6.94	
Cr+SiO-40-C	"	"	"		"	"	"			7	325			5,016	2,508	3.3×10⁴	-4.36	
Cr+SiO-41-C	"	"	"		"	1/2	"			10½	250			117.3	58.6	≈1×10³	+2.64	
Cr+SiO-42-C	"	"	"		"	"	"	X						118.2	59	1.5×10³	+1.94	Deposited simultaneously
Cr+SiO-43-C	"	"	"		"	"	"			7	325			91.9	45.9	≈100	+2.83	on 2"×2" substrate.
Cr+SiO-44-C	"	"	"		"	"	"			10½	250			96.3	48	≈100	+2.81	2nd Evaporation with
Cr+SiO-45-C	"	"	"		"	"	"	X						134.5	67	≈900	+2.16	load for previous 6 specimens
Cr+SiO-46-C	"	"	"		"	"	"			7	325			110.35	55	≈900	+2.16	

TABLE I (CONTINUED)

DETAILED FABRICATION DATA AND RESISTOR PARAMETERS

RESISTOR (SERIAL NO.)	SUB-STRATE (TYPE)	EVAPORATION PARAMETERS: SOURCE (TYPE)	SOURCE T(°C)	EVAPORANT	SUB. T (°C)	DEP. PER. (MIN.)	P (TORR)	PROTECTION: NONE	SiO	BAKED PER. (HRS)	BAKED T (°C)	FILM PARAMETERS (1): COMPOSITION (2)	THICKNESS (Å)	RESISTANCE (OHMS)	RESISTIVITY R/SQ. (OHMS)	RESISTIVITY SPECIFIC (μΩ Cm)	TCR (10^{-4}/°C)	REMARKS
							CHROMIUM SILICIDE											
		(TYPE)	T(°C)															
$CrSi_2$ – 1	CORNING #7059 GLASS	W BOAT	1350 ±50	$CrSi_2$ (-200,+325 MESH)	400 ±50	1+1½	4×10^{-6}	X				Cr_3Si	320.	192.2	192	615	-0.362	THE EVAPORANT WAS
$CrSi_2$ – 2	GLASS	BOAT	≈1400		〃	1	1×10^{-6}	X				Cr_3Si	1,350.	24.65	24.6	332	+1.05	SUBLIMATED AT TEMPERA-
$CrSi_2$ – 3	〃	〃			〃	3	3×10^{-6}	X				Cr_3Si		352.	352		-5.77	TURES NEAR AND SLIGHTY
$CrSi_2$ – 4	〃	〃	1350 ±50	〃	300 ±50	10	$(1-10)10^{-6}$			5	300	Cr_3Si		53.32	53.3		+0.588	BELOW ITS MELTING
$CrSi_2$ – 5	〃	〃	〃	〃	〃	10	〃			5	300	Cr_3Si		32.02	32.		+1.25	POINT FOR $CrSi_2$ – 1
$CrSi_2$ – 6	〃	〃	〃	〃	〃	10	2.3×10^{-6}			5	300			315.1	315		-4.22	THRU 9.
$CrSi_2$ – 7	〃	〃	〃	〃	〃	10	$(1-5)10^{-6}$	X					700	384.1	384	2,690.	-7.44	
$CrSi_2$ – 8	〃	〃	≈1400	〃	〃	2	$(1-5)10^{-6}$	X					1,900	12.93	12.9	246	+2.29	
$CrSi_2$ – 9	〃	〃	〃	〃	〃	½	$(1-10)10^{-6}$	X						53.71	53.7		+0.594	
$CrSi_2$ – 12	GLASS MICRO-SCOPE SLIDE	e-beam @ 2.6 KW, Cu Crucible		〃	250	3	〃	X				STRONG Cr LINE	1360	293	29.3	398	+0.401	FOR $CrSi_2$ – 12 AND 13, THE
$CrSi_2$ – 13				〃	〃	3	〃	X					1290	324	32.4	418	+0.302	EVAPORATION WAS FROM
																		MOLTEN POOL OF
																		EVAPORANT IN A MASS-
							CHROMIUM SILICIDE–SILICON BORIDE											IVE Cu CRUCIBLE.
$CrSi_2 + B_4Si$ – 1	GLASS	e-Beam @ (½ Coil) KW		PWDR. MIX-TURE OF	300	9	$(1-5)10^{-6}$			4½	300			15,471	1,547		-25.2	CONSIDERABLE SPITTING
$CrSi_2 + B_4Si$ – 2	MICRO-SCOPE SLIDE	Cu Crucible		MASS RATIO 2:1,	〃	〃	〃	X						11,448	1,145		-24.7	OF B_4Si
$CrSi_2 + B_4Si$ – 3		〃		$CrSi_2 : B_4Si$	〃	〃	〃	X					6,640	14,095	1,410	93,600.	-25.	
$CrSi_2 + B_4Si$ – 4	SLIDE	e-Beam @ (2-4) KW		$CrSi_2$ MELT ON BED	250	3	$(1-20)10^{-6}$	X					2,730	461.9	46.2	1,250	+1.23	FOR $CrSi_2 + B_4Si$ – 4, 5, & 6,
$CrSi_2 + B_4Si$ – 5	〃	Cu Crucible		OF B_4Si POWDER	〃	〃	〃	X						461.7	46.2		+1.36	THE E-BEAM WAS CENTERED
$CrSi_2 + B_4Si$ – 6	〃	〃		〃	〃	〃	〃	X					2,830	235.06	23.5	650	-0.631	ON A SPHERICAL MELT OF
																		$CrSi_2$ ON TOP OF A BED
																		OF B_4Si POWDER. THE $CrSi_2$
																		MELT DID NOT WET THE
																		B_4Si. VERY LITTLE, IF ANY,
																		OF THE B_4Si WAS EVAPORATED.
																		FILM COMPOSITION WAS
																		PROBABLY Cr_3Si.

TABLE I (CONTINUED)

DETAILED FABRICATION DATA AND RESISTOR PARAMETERS

RESISTOR (SERIAL NO.)	SUB-STRATE (TYPE)	EVAPORATION PARAMETERS: SOURCE (TYPE)	EVAP-ORANT	SUB. T (°C)	DEP. PER. (MIN.)	P (TORR)	PROTECTION: NONE	SiO	BAKED: PER. (HRS)	BAKED: T (°C)	FILM PARAMETERS (1): COMPOSITION (2)	THICKNESS (Å)	RESISTANCE (OHMS)	RESISTIVITY: R/SQ. (OHMS)	RESISTIVITY: SPECIFIC (μΩ Cm.)	TCR (10^{-4}/°C)	REMARKS
						CHROMIUM SILICIDE—TITANIUM SILICIDE											
$CrSi_2 + TiSi_2$-3	GLASS	E-BEAM (2-3) KW	1:1	250	4	6.6×10^{-6}	X				$CrSi_2$ ONLY	650	5,310	531	3,480	-4.42	
$CrSi_2 + TiSi_2$-4	MICRO-	Cu CRUCIBLE	MASS	"	"	"	X					709	5,130	513	3,640	-4.38	
$CrSi_2 + TiSi_2$-5	SCOPE	E-BEAM (3-3.5) KW	MIXTURE	275	3	2×10^{-6}	X					552	2,024	202	1,120	-1.06	
$CrSi_2 + TiSi_2$-6	SLIDE	Cu CRUCIBLE	OF $CrSi_2$	"	"	"			4½	300			1,981	198	(est) 1,200	-1.68	
$CrSi_2 + TiSi_2$-7	"	E-BEAM 4 KW	AND	250	2	$(2-10)10^{-6}$	X					1,380	563.5	56.3	777	-2.88	
$CrSi_2 + TiSi_2$-8	"	Cu CRUCIBLE	$TiSi_2$	"	"	"			4½	300			598	59.8		-3.1	
$CrSi_2 + TiSi_2$-9	"	"	POWDERS	"	"	"	X						563.1	56.3	est. 800	-2.86	
						COPPER—SILICON MONOXIDE											
Cu + SiO-1A-A	"	W. BOAT FOR Cu	Cu WIRE	450	4	9×10^{-6}	X					-	353.6	354	—	+4.28	
Cu + SiO-1B-A	"	& Ta BOAT FOR	& SiO	"	"	"	X				Cu, Cu_2O	-	675.4	675	—	-4.09	
Cu + SiO-1C-A	"	SiO	TABLET	"	"	"	X					-	5.58×10^6	5.58×10^6	—	R increased beyond Bridge Range during TCR	
Cu + SiO-2A-A	"	"	"	"	"	1×10^{-5}	X					1,110	5.11	5.11	56.7	+9.27	
Cu + SiO-2B-A	"	"	"	"	"	"	X					1,250	6.17	6.17	77.2	+9.23	
Cu + SiO-2C-A	"	"	"	"	"	"	X					838	13.99	14	117	+7.43	
Cu + SiO-3A-A	"	"	"	"	"	7×10^{-6}	X					-	1,484	1,480	—	+5.8	
Cu + SiO-3B-A	"	"	"	"	"	"	X					-	1,656	1,660	—	+6.98	
Cu + SiO-3C-A	"	"	"	"	"	"	X					975	3,881	3,880	37,800	+6.6	
Cu + SiO-4A-A	"	"	"	"	"	"	X					2,300	195.6	196	4,500	+9.7	
Cu + SiO-4B-A	"	"	"	"	"	"	X				Cu	1,955	226.5	226	4,430	-15.4?	
Cu + SiO-4C-A	"	"	"	"	"	"	X					1,620	875.2	875	14,200	+11	
Cu + SiO-5A-A	"	"	"	"	"	2×10^{-5}	X					-	1,610.5	1,610	—	+8.86	
Cu + SiO-5B-A	"	"	"	"	"	"	X					1,360	3,690	3,690	50,200	+8.48	
Cu + SiO-6A-A	"	"	"	"	"	"	X					-	516.4	516	—	+7.87	
Cu + SiO-6B-A	"	"	"	"	"	"	X				Cu	2,350	1,275	1,270	29,900	+7.38	
Cu + SiO-6C-A	"	"	"	"	"	"	X					1,040	6,757.5	6,760	70,300	+5.86	
Cu + SiO-7A-A	"	"	"	"	"	"	X					-	1,976	1,980	—	+4.13	
Cu + SiO-7B-A	"	"	"	"	"	"	X				Cu	2,735	7,017	7,200	192,000.	+4.07	
Cu + SiO-7C-A	"	"	"	"	"	"	X					1,940	2.09×10^5	2.09×10^5	40,600	-26.7	
Cu + SiO-8B-A	"	"	"	"	8	1×10^{-5}	X					1,410	966.4	966	13,800	+10.9	
Cu + SiO-8C-A	"	"	"	"	"	"	X					1,323	704	704	9,310	+10.5	
Cu + SiO-9A-A	"	"	"	"	8.5	2×10^{-5}	X					471	60.9	60.9	286	-15	
Cu + SiO-9B-A	"	"	"	"	"	"	X				NON-XTAL	706	7,779	7,780	55,000	-98.7	
Cu + SiO-9C-A	"	"	"	"	"	"	X					-	26,400	26,400	—	-85.4	

TABLE I (CONTINUED)

DETAILED FABRICATION DATA AND RESISTOR PARAMETERS

RESISTOR (SERIAL NO.)	SUB-STRATE (TYPE)	EVAPORATION PARAMETERS: SOURCE (TYPE)	EVAP-ORANT	SUB. T (°C)	DEP. PER. (MIN.)	P (TORR)	PROTECTION: NONE	SiO	BAKED PER. (HRS)	BAKED T (°C)	FILM PARAMETERS[1]: COMPOSITION[2]	THICKNESS (Å)	RESISTANCE (OHMS)	RESISTIVITY R/SQ. (OHMS)	RESISTIVITY SPECIFIC (μΩ Cm.)	TCR (10^{-4}/°C)	REMARKS
						COPPER – SILICON MONOXIDE (CONTINUED)											
Cu+SiO-1-B	CORN-	INDEPENDENTLY HEATED BN CRU-	Cu WIRE AND SiO POWDER	370	2	7×10^{-6}	X					921	1.28×10^{6}	1.28×10^{6}	1.18×10^{7}	-35.7	
Cu+SiO-2-B	ING			"	2	5×10^{-6}	X				Cu	923	1.77×10^{5}	1.77×10^{5}	1.63×10^{6}	-24.8	
Cu+SiO-3-B	#7059	CIBLES FOR Cu & SiO		"	2	$(1-10)10^{-6}$	X					–	40.5	40.5	–	+ 1.8	
Cu+SiO-4-B	GLASS			"	2	1.3×10^{-5}	X					971	4.33	4.33	42	+ 2.76	
Cu+SiO-5-B	"	"	"	"	2	$(1-10)10^{-6}$	X					–	1.49	1.49	–	+ 4.75	
Cu+SiO-6-B	"	"	"	"	1	"	X					–	3.96	3.96	–	+ 5.58	
Cu+SiO-7-B	"	"	"	"	1	"	X				Cu	1,476	1.6	1.6	23.7	+ 5.48	
Cu+SiO-8-B	"	"	"	"	1	"	X					–	3.71	3.71	–	+ 4.11	
Cu+SiO-9-B	"	"	"	"	1	"	X					–	6.2	6.2	–	+ 6.07	
Cu+SiO-10-B	"	"	"	"	2	"	X				Cu	5,065	21.42	21.4	1.08×10^{3}	+ 4.08	
Cu+SiO-11-B	"	"	"	"	1	"	X					–	7.64	7.64	–	+ 4.0	
Cu+SiO-12-B	"	"	"	"	2	"	X					–	9.86	9.86	–	+ 4.9	
Cu+SiO-13-B	"	"	"	"	4	"	X				Cu, CuO	–	5.1×10^{6}	5.1×10^{6}	–	-30.1	
Cu+SiO-14-B	"	"	"	"	2	"	X				Cu, (? CuO OR Cu_2O)	765	2.44	2.44	18.6	+ 7.87	
						GADOLINIUM											
Gd-1A-B	GLASS MICRO-	Ta BOAT	Gd	450	≈5	3×10^{-5}	X					5,890	56.4	5.64	332	+ 5.96	OBSERVED RAPID CHANGE IN
Gd-1B-B	SCOPE SLIDE	"	TURN-	"	"	"	X						46.7	4.67		+ 7.6	APPEARANCE WITH TIME DUE
Gd-1C-B	"	"	INGS	"	"	"	X					2,490	52.7	5.27	132	+ 6.74	TO SURFACE OXIDATION WITH
Gd-1D-B	"	"	"	"	"	"	X						76.4	7.64		+ 5.03	EXPOSURE TO AIR UPON
																	REMOVAL FROM VACUUM.
						GADOLINIUM EVAPORATED IN OXYGEN											
$Gd+O_2$-1A-B	"	"	"	"	4	1×10^{-5}	X					1,369	157	15.7	214	+ 6.2	A+O_2 BLED INTO BELL JAR
$Gd+O_2$-1B-B	"	"	"	"	4	"	X						–	–		–	TO INCREASE PRESSURE
$Gd+O_2$-1C-B	"	"	"	"	4	"	X					1,213	272	27.2	330	+ 5.87	FROM ≈ 2×10^{-6} TORR TO
$Gd+O_2$-1D-B	"	"	"	"	4	"	X						445	44.5		+ 5.35	INDICATED VALUE. FILMS
$Gd+O_2$-2A-B	"	"	"	"		5×10^{-5}	X					1,186	518	51.8	616	+ 3.89	WERE SUPPOSEDLY DEPOSITED
$Gd+O_2$-2B-B	"	"	"	"		"	X						488	48.8		+ 4.6	IN A PARTIAL PRESSURE
$Gd+O_2$-2C-B	"	"	"	"		"	X						–	–		–	OF OXYGEN, BUT INCOM-
$Gd+O_2$-2D-B	"	"	"	"		"	X					577	910	91	525	+ 3.9	PLETE PURGING OF THE
																	BLEEDER LINE RESULTED
																	IN ADMISSION OF A+O_2
																	CONSISTING PRIMARILY OF A.

TABLE I (CONTINUED)

DETAILED FABRICATION DATA AND RESISTOR PARAMETERS

RESISTOR (SERIAL NO.)	SUB-STRATE (TYPE)	EVAPORATION PARAMETERS: SOURCE (TYPE)	EVAPORANT	SUB. T (°C)	DEP. PER. (MIN.)	P (TORR)	PROTECTION: NONE	SiO	BAKED PER. (HRS)	BAKED T (°C)	FILM PARAMETERS (1): COMPOSITION (2)	THICKNESS (Å)	RESISTANCE (OHMS)	RESISTIVITY R/SQ. (OHMS)	RESISTIVITY SPECIFIC (μΩ Cm)	TCR (10^{-4}/°C)	REMARKS
						MANGANESE											
Mn - 1 - C	GLASS	R.D.	Mn	400	5	$(5-8)10^{-5}$	x						91.32	11.4		-0.33	
Mn - 2 - C	MICRO-	MATHIS	(96%	"	"	"	x						61.28	6.13		+ 1.39	
Mn - 3 - C	SCOPE	TYPE	Carbon	"	10	2×10^{-5}	x				Mn (C?)	130	286.75	28.7	210	+ 1.46	
Mn - 4 - C	SLIDE	ME-1	free)	"	"	"	x						276.68	27.7			
						MANGANESE — SILICON MONOXIDE											
		(TYPE)	T (°C)														
Mn + SiO - 1 - C	"	ME-1	1050 ± 50	0.5g Mn, 1g SiO.	"	2	$\simeq 5 \times 10^{-6}$	x				500		134	670	+ 0.81	
Mn + SiO - 2 - C	"	"	"	0.05g Mn/1g SiO.	"	7	"	x				1,945		106	2,060	+ 0.52	
Mn + SiO - 3 - C	"	"	"	0.05g Mn/2g SiO.	"	2	"	x				670		103	690	+ 0.86	
Mn + SiO - 4 - C	"	"	"	0.05g Mn/2g SiO	"	20	"	x				1,880		690,000.	1.3×10^{7}	- 33.3	
Mn + SiO - 5 - C	"	"	"	0.1g Mn/2g SiO	"	15	"	x			Mn (3), Mn_3O_4	803		1,030	8,270.	- 2.32	
Mn + SiO - 6 - C	"	"	"	After #5	"	20	"	x				1,130		34,900.	3.95×10^{5}	- 20.8	
Mn + SiO - 7 - C	"	"	1075 ± 50	After #6	"	10	"	x				873		2,030	1.77×10^{4}	- 3.65	
Mn + SiO - 8 - C	"	"	"	MIXTURE OF Mn & SiO	"	10	$(1-5)10^{-5}$	X				1,500	43,514	4,356	6.7×10^{4}	- 8.8	
Mn + SiO - 9 - C	"	"	"	"	"	10	"		X			480	331,380	33,140	1.6×10^{5}	-11.5	THICKNESS AND SPECIFIC
Mn + SiO - 10 - C	"	"	"	"	"	15	"	X			α Mn	3,700	1,027	103	3,800.	- 0.466	RESISTIVITY VALUES
Mn + SiO - 11 - C	"	"	"	"	"	15	"		X			1,300	2,205.8	221	2,700.	- 0.02	OF Mn + SiO - 8 - C THRU
Mn + SiO - 12 - C	"	"	"	"	"	5	"	X			α Mn	1,200	845.9	84.6	1,000	+ 0.728	31 - C WERE ESTIMATED
Mn + SiO - 13 - C	"	"	"	"	"	"	"		X			640	778.5	77.8	500	+ 1.4	BY USING THE TCR VS
Mn + SiO - 14 - C	"	"	1050 ± 50	"	"	"	"	X			α Mn	1,200	708.5	70.8	850	+ 0.81	N CHARACTERTICS OF
Mn + SiO - 15 - C	"	"	"	"	"	"	"		X			430	1,177.2	117.7	500	+ 1.4	Mn + SiO - 1 - C THRU 7 - C.
Mn + SiO - 16 - C	"	"	"	"	"	"	"	X				910	1,101.4	111	1,006	+ 0.703	
Mn + SiO - 17 - C	"	"	"	"	"	"	"		X			330	2,101.7	210	700	+ 1.13	
Mn + SiO - 18 - C	"	"	"	"	"	7	"	X				660	1,443.4	144	950	+ 0.79	
Mn + SiO - 19 - C	"	"	"	"	"	"	"		X			450	1,769	177	800	+ 0.92	
Mn + SiO - 20 - C	"	"	1075 ± 50	"	"	15	"	X			α Mn	2,200	66,910	6,691	1.5×10^{5}	- 12.2	
Mn + SiO - 21 - C	"	"		"	"	"	"		X			1,400	432,080	43,210	6×10^{5}	-19.5	

TABLE I (CONTINUED)

DETAILED FABRICATION DATA AND RESISTOR PARAMETERS

RESISTOR (SERIAL NO.)	SUB-STRATE (TYPE)	EVAPORATION PARAMETERS: SOURCE (TYPE)	SOURCE T(°C)	EVAPORANT	SUB. T (°C)	DEP. PER. (MIN.)	P (TORR)	PROTECTION: NONE	SiO	BAKED PER. (HRS)	BAKED T (°C)	FILM PARAMETERS (1): COMPOSITION (2)	THICKNESS (Å)	RESISTANCE (OHMS)	RESISTIVITY R/SQ. (OHMS)	RESISTIVITY SPECIFIC (μΩ Cm.)	TCR (10^{-4}/°C)	REMARKS
							MANGANESE-SILICON MONOXIDE (CONTINUED)											
		(TYPE)	T(°C)															
Mn+SiO-22-C	GLASS	ME-1	1125 ±50	MIXTURE	400	8	$(1-5)10^{-5}$	x				NON-XTAL	1,800	2.824×10^{18}	282,000	5×10^{6}	-30.8	Mn in source possibly depleted
Mn+SiO-23-C	MICRO-	"	"	OF Mn	"	"	"		x				709	7.64×10^{6}	764,000	6×10^{6}	-32	before deposition period
Mn+SiO-24-C	SCOPE	"	≈1180	& SiO	"	7	2×10^{-5}			6 3/4	200			1,791	179	3,400	- 0.42	completed for #22 & 23.
Mn+SiO-25-C	SLIDE	"	"	"	"	"	"			6 3/4	200			638.3	63.8	2,500	+ 0.44	
Mn+SiO-26-C	"	"	"	"	"	3	"			6 3/4	200			732.1	73.2	400	+ 1.56	
Mn+SiO-28-C	"	"	"	"	"	"	"			6 1/2	250			513.8	51.4	300	+ 1.76	
Mn+SiO-29-C	"	"	"	"	"	"	"			6 1/2	250			688.5	68.8	1,400	+ 0.67	
Mn+SiO-30-C	"	"	"	"	"	10	$(5-10)10^{-5}$			6 3/4	200			647.8	64.8	1,500	+0.47	
Mn+SiO-31-C	"	"	"	"	"	10	"			6 1/2	250			709.1	70.9	3,300	-0.36	
							NIOBIUM BORIDE											
NbB_2-1	CORNING #7059	E-BEAM (1.5 to 2) KW		NbB_2;	250	4	$(1-10)10^{-6}$	x					2,325	33,200	33,200	7.73×10^{5}	-50.7	
NbB_2-2	GLASS	Cu CRUCIBLE		-150,	"	10	$(0.5-6)10^{-6}$	x				NO PATTERN	3,480	8,255	8,255	2.88×10^{5}	-43.6	
NbB_2-3	FUSED QUARTZ	"		+325	"	10	$(1-10)10^{-6}$			3	300	"		313,000	31,000	—	-49.9	
NbB_2-4	"	"		MESH	"	10	"	x				"	2,840	376,000	37,600	1.07×10^{6}	-50.4	
NbB_2-5	"	E-BEAM (2-2.5) KW			"	10	$(4-6)10^{-7}$	x						84,500	8,450		-40.3	
NbB_2-6	"	Cu CRU.		"	"	10	"	x						87,600	8,750		-39.6	
NbB_2-7	"	E-BEAM ≈2KW		"	240	10	$(1-7)10^{-6}$	x					1,580	65,000	6,500	1.03×10^{5}	-34.4	
NbB_2-8	"	Cu CRU.		"	"	10	"			3	300			54,010	5,401		-32.6	
NbB_2-9	"	E-BEAM ≈3.5 KW		"	235	3	$(2-3.5)10^{-6}$	x				NO PATTERN		2,790	279		- 4.76	E-BEAM MELTED SPOT ON STAINLESS STEEL SHUTTER;
NbB_2-10	"	Cu CRU.		"	"	"	"					BROKE		—	—		—	HENCE, #9 MAY HAVE S.S. COMPONENTS.
NbB_2-11	"	"		"	270	1	$(1-10)10^{-6}$	x						335,420	33,540		-53.7	
NbB_2-12	"	E-BEAM ≈4.2 KW		"	230	1	$(8-20)10^{-6}$	x				NO PATTERN		93,500	9,350		-46.8	
NbB_2-13	"	Cu CRU.		"	"	1	"	x				"		186,000	18,600		-46.3	
NbB_2-14	"	"		"	"	1	"	x						178,000	17,800		-48.8	
NbB_2-15	GLASS MICROSCOPE SLIDE	E-BEAM ≈3.6 KW	Cu CRU.	"	260	3	$(3-60)10^{-7}$	x						67,850	6,785		-39.1	

TABLE I (CONTINUED)

DETAILED FABRICATION DATA AND RESISTOR PARAMETERS

RESISTOR (SERIAL NO.)	SUB-STRATE (TYPE)	EVAPORATION PARAMETERS: SOURCE (TYPE)	EVAP-ORANT	SUB. T (°C)	DEP. PER. (MIN.)	P (TORR)	PROTECTION: NONE	SiO	BAKED PER. (HRS)	BAKED T (°C)	FILM PARAMETERS (1): COMPOSITION (2)	THICKNESS (Å)	RESISTANCE (OHMS)	RESISTIVITY R/SQ. (OHMS)	RESISTIVITY SPECIFIC (μΩ Cm)	TCR (10^{-4}/°C)	REMARKS
NIOBIUM NITRIDE																	
NbN-1A-A	GLASS MICRO	Ta-BOAT	NbN	450	½ /	$(4-10)10^{-5}$	X					518	1,275	1270	6,600	-4.1	Ta BOAT DESTROYED FROM
NbN-1B-A	SCOPE SLIDE	"	POWDER	"	≈ 1	"	X					400	725	725	2,900	-3.6	REACTION WITH EVAPORANT.
NbN-1C-A	"	"	"	"	≈ 1	"	X					309	1,510	1510	4,670	-5.7	
NICKEL BORIDE																	
Ni_2B-1-B	CORNING	W-BASKET	Ni_2B	300 ±50	≈ 1	$(1-10)10^{-6}$	X				PRIMARILY Ni	< 100	3,003	3003	$<3\times10^3$	-2.12	
Ni_2B-2-B	#7059	"	PELLET	"	1½	"	X				"	405	10.47	10.5	42.4	+15.4	
Ni_2B-3-B	GLASS	W-BOAT	"	"	1	"	X				Ni ONLY	350	16.76	16.8	58.7	+16.5	
TANTALUM OXIDE																	
Ta_2O_5-1A-A	GLASS	Ta-BOAT	Ta_2O_5	450	≈1	$\approx 1\times10^{-5}$	X						8.01×10^6	8.01×10^6		≈-80	
Ta_2O_5-1B-A	MICRO-	"	POWDER	"	"	"	X						9.5×10^6	9.5×10^6			
Ta_2O_5-2A-A	SCOPE	"	"	"	3	5×10^{-6}	X					658	9.51×10^6	9.51×10^6		-64	
Ta_2O_5-2C-A	SLIDE	"	"	"	3	"	X					614	5.72×10^6	5.72×10^6	3.5×10^7	-71	
Ta_2O_5-3-A	"	W-BOAT	"	"	≈1	2×10^{-5}	X						$>10^7$	$>10^7$	—	—	
Ta_2O_5-4A-A	"	"	"	"	≈2	2×10^{-6}	X						40,160	40,160		-54.6	
Ta_2O_5-4B-A	"	"	"	"	≈2	"	X						24,420	24,420		-49.3	
Ta_2O_5-4C-A	"	"	"	"	≈2	"	X					865	56,300	56,300	4.87×10^5	-54.4	
TITANIUM																	
Ti-1-B	"	STRAND-ED W	Ti WIRE	275	≈½	$(1-10)10^{-5}$	X						21.86	13		+21	

TABLE I (CONTINUED)

DETAILED FABRICATION DATA AND RESISTOR PARAMETERS

RESISTOR (SERIAL NO.)	SUB-STRATE (TYPE)	EVAPORATION PARAMETERS: SOURCE (TYPE)	EVAP-ORANT	SUB. T (°C)	DEP. PER. (MIN.)	P (TORR)	PROTECTION: NONE	SiO	BAKED PER. (HRS)	BAKED T (°C)	FILM PARAMETERS (1): COMPOSITION (2)	THICKNESS (Å)	RESISTANCE (OHMS)	RESISTIVITY R/SQ. (OHMS)	RESISTIVITY SPECIFIC (μΩ Cm.)	TCR (10^{-4}/°C)	REMARKS
						TITANIUM EVAPORATED IN OXYGEN											
$Ti+O_2-1-B$	GLASS	STRANDED W	Ti WIRE	≈400	≈ ½	5×10^{-5}	X						30.89	17.9		+8	FOR $Ti+O_2$ SPECIMENS,
$Ti+O_2-2-B$	MICRO-	"	"	"	"	5×10^{-4}	X						18.81	10.7		+21	A $+O_2$ WAS ADMITTED INTO
$Ti+O_2-4A-B$	SCOPE	"	"	"	≈5	1×10^{-3}	X					767	332.1	35.2	270	+1.95	BELL JAR TO INCREASE
$Ti+O_2-4B-B$	SLIDE	"	"	"	"	"	X					504	484.6	51.6	260	−0.18	THE PRESSURE FROM
$Ti+O_2-4C-B$	"	"	"	"	"	"	X					305	709.4	66.5	203	−0.88	≈ 2×10^{-6} TORR TO INDICATED
$Ti+O_2-4D-B$	"	"	"	"	"	"	X						1142	107		−0.25	VALUE. FOR Ti_2+O_2-1
$Ti+O_2-8A-B$	"	"	"	"	"	1×10^{-5}	X					456	5,009.	470	2,140	−13.4	THRU 4, THE GAS
$Ti+O_2-8B-B$	"	"	"	"	"	"	X					—	4,520.	424	—	−15.1	ADMITTED WAS PRIMARILY
$Ti+O_2-8C-B$	"	"	"	"	"	"	X					663	2,584	258	1,710	−16.8	ARGON WITH A TRACE OF O_2.
$Ti+O_2-8D-B$	"	"	"	"	"	"	X					238	9,991	1050	2,500	−21.8	
$Ti+O_2-9A-B$	"	"	"	"	10	5×10^{-5}	X					1230	17,890	1,790	22,000	−33.5	
$Ti+O_2-9B-B$	"	"	"	"	10	"	X					498	32,090	3,210	16,000	−36.2	
$Ti+O_2-9C-B$	"	"	"	"	10	"	X					586	82,800	7,770	45,000	−41.6	
$Ti+O_2-9D-B$	"	"	"	"	10	"	X						351,700	30,700		−44.1	
$Ti+O_2-10A-B$	"	"	"	"		1×10^{-4}	X					504	62,780	6,670	33,600	−49.8	
$Ti+O_2-10B-B$	"	"	"	"	"	"	X						148,400	15,800		−51.6	
$Ti+O_2-10C-B$	"	"	"	"	"	"	X					250	1,119,000	111,600	279,000	−54.4	
$Ti+O_2-11A-B$	"	"	"	"	12	7.5×10^{-5}	X					556	39,690	3,970	22,000	−48.4	
$Ti+O_2-11B-B$	"	"	"	"	"	"	X					530	201,800	20,200	107,000	−54.9	
$Ti+O_2-11C-B$	"	"	"	"	"	"	X						1,707,000	171,000		−57.8	
$Ti+O_2-12-B$	"	"	"	"	10	2.5×10^{-4}	X						$>10^7$				
						TITANIUM MONOXIDE											
$Ti_2O-1A-FA$	"	W-BOAT	Ti_2O	350	FLASH-ED	5×10^{-5}	X					1070	122.1	122	1,370	−3.99	
$Ti_2O-1B-FA$	"	"	POWDER	"	"	"	X						113.5	113	—	−3.53	
$Ti_2O-1C-FA$	"	"	"	"	"	"	X						173.7	174	—	−4.53	

TABLE I (CONTINUED)

DETAILED FABRICATION DATA AND RESISTOR PARAMETERS

RESISTOR (SERIAL NO.)	SUB-STRATE (TYPE)	EVAPORATION PARAMETERS: SOURCE (TYPE)	EVAP-ORANT	SUB. T (°C)	DEP. PER. (MIN.)	P (TORR)	PROTECTION: NONE	SiO	BAKED PER. (HRS)	BAKED T (°C)	FILM PARAMETERS (1): COMPOSITION (2)	THICKNESS (Å)	RESISTANCE (OHMS)	RESISTIVITY R/SQ. (OHMS)	RESISTIVITY SPECIFIC (μΩ Cm.)	TCR (10^{-4}/°C)	REMARKS
TITANIUM MONOXIDE (CONTINUED)																	
Ti O - 2A - FA	GLASS	W-BOAT	Ti O	350	FLASH-ED	4×10^{-5}	X					655	274	274	1,790	-4.05	
Ti O - 2C - FA	MICRO-	"	POWDER	"	"	"	X						392.02	392		-4.06	
Ti O - 3A - FA	SCOPE	"	"	"	"	"	X						7,483	7,483		-9.5	
Ti O - 3B - FA	SLIDE	"	"	"	"	"	X					EST. 100	4,036	4,036	4,000	-7.5	
Ti O - 3C - FA	"	"	"	"	"	"	X						10,680	10,680		-14.9	
Ti O - 4A - FA	"	Ta-BOAT	"	"	"	2×10^{-5}	X						105.1	105.1		-5.05	
Ti O - 4B - FA	"	"	"	"	"	"	X					700	97.0	97	679	-5.05	
Ti O - 4C - FA	"	"	"	"	"	"	X					600	157.2	157.2	943	-5.38	
Ti O - 5A - A	"	"	"	"	≈1	7×10^{-6}	X						74.24	74.2		-4.24	
Ti O - 5B - A	"	"	"	"	≈1	"	X					1280	53.72	53.7	687	-4.13	
Ti O - 5C - A	"	"	"	"	≈1	"	X						68.43	68.4		-4.63	
TITANIUM DIOXIDE																	
TiO_2 - 1A-FA	"	"	Ti_2O_3	350	FLASH-ED	2×10^{-5}	X						167.3	167		-8.55	
TiO_2 - 1B-FA	"	"	POWDER	"	"	"	X					923	102.6	103	947	-7.0	
TiO_2 - 1C - FA	"	"	"	"	"	"	X						138.8	139		-7.75	
TiO_2 - 2A - A	"	"	"	450	4	"	X						93.91	93.9		-9.57	
TiO_2 - 2B - A	"	"	"	"	4	"	X					1090	70.82	70.8	772	-7.96	
TiO_2 - 2C - A	"	"	"	"	4	"	X						112.17	112		-10.3	
TiO_2 - 3B - A	"	Mo BOAT	"	"	≈1	5×10^{-5}	X					< 100	10,460.	10,460	$< 1.05 \times 10^4$	-33.8	Mo BOAT ATTACKED SEVERELY
TiO_2 - 4A - A	"	W BOAT	"	"	≈1	2×10^{-5}	X					555	118,400	118,400	6.57×10^5	-50.7	
TiO_2 - 4C - A	"	"	"	"	≈1	"	X					484	92,710	92,710	4.48×10^5	-54.0	
TITANIUM BORIDE																	
$Ti B_2$ - 1	"	E-BEAM (2-5.6)KW	$Ti B_2$; -.20	260	2 1/5	$(3-30)10^{-6}$	X				STRONG Ti LINE	BOTH OF	FILMS ONE OF	RETICULATED; HOWEVER, THESE		WAS	THE RESISTANCE 2500 Ω.
$Ti B_2$ - 2	"	Cu CRU	+325 MESH	"	"	"	X										

TABLE I (CONTINUED)

DETAILED FABRICATION DATA AND RESISTOR PARAMETERS

RESISTOR (SERIAL NO.)	SUBSTRATE (TYPE)	EVAPORATION PARAMETERS: SOURCE (TYPE)	EVAPORANT	SUB. T (°C)	DEP. PER. (MIN.)	P (TORR)	PROTECTION: NONE	SiO	BAKED PER. (HRS)	BAKED T (°C)	FILM PARAMETERS (1): COMPOSITION (2)	THICKNESS (Å)	RESISTANCE (OHMS)	RESISTIVITY R/SQ. (OHMS)	RESISTIVITY SPECIFIC (μΩ Cm)	TCR (10^{-4}/°C)	REMARKS
TITANIUM BORIDE (CONTINUED)																	
TiB_2 – 3	GLASS MICRO-SCOPE SLIDE	E-BEAM (2-3.5)KW	TiB_2;	370	2	$(1-10)10^{-6}$	X				NO PATTERN	EST. > 1,500	3,507	350	ESTIMATED > 1×10^4	– 4.13	FILMS RETICULATED.
TiB_2 – 4	"	Cu CRU	– 150, + 325	"	"	"	X				"		13,219	1,320		– 4.29	COULD NOT MEASURE
TiB_2 – 5	"	"	MESH	"	"	"	X				"		8,947	895		– 1.72	THICKNESS BECAUSE OF SURFACE ROUGHNESS.
TITANIUM NITRIDE																	
TiN – 1A – A	"	W BOAT	TiN	450	5	1×10^{-4}	X					768	44.87	44.9	345	– 0.31	EVAPORANT SUBLIMED
TiN – 1B – A	"	"	POWDER	"	"	"	X					588	106.93	107	630	– 1.54	ON TiN SPECIMENS.
TiN – 1C – A	"	"	"	"	"	"	X						54.72	54.7		– 0.67	
TiN – 2A – A	"	"	"	"	5	1.6×10^{-4}	X					708	292.6	293	2,070	– 7.4	
TiN – 2B – A	"	"	"	"	"	"	X					583	147.54	148	863	– 4.67	
TiN – 2C – A	"	"	"	"	"	"	X						203.5	203		– 5.93	
TiN – 3A – A	"	"	"	"	"	1×10^{-4}	X					413	348.71	349	1,440	– 6.46	
TiN – 3B – A	"	"	"	"	"	"	X					357	180.59	181	646	– 3.26	
TiN – 3C – A	"	"	"	"	"	"	X						219.24	219		– 5.02	
TITANIUM SILICIDE																	
$TiSi_2$ – 1 – B	CORNING #7059	W BOAT	$TiSi_2$;	25	$\frac{5}{12}$	$(1-10)10^{-6}$	X				$Si + TiSi_2$	1,060	2,716	2,716	3.45×10^4	– 16.3	SOURCE TEMPERATURE
$TiSi_2$ – 2 – B	"	"	– 200, + 325	300	$\frac{1}{3}$	"	X				$Si + TiSi_2$	250	3.8×10^6	3.8×10^6	9.5×10^6	– 63.6	RANGE FOR $TiSi_2$ – 1 THRU 5
$TiSi_2$ – 3 – B	GLASS	"	MESH	"	$\frac{1}{2}$	"	X				$Si + TiSi_2$	542	6.56×10^6	6.56×10^6	3.06×10^7	– 65	WAS 1400°C to 1500°C.
$TiSi_2$ – 4 – B	"	"	"	"	$2\frac{1}{2}$	"	X				$Si + TiSi_2$	584	123,650	123,650	7.22×10^5	– 41	
$TiSi_2$ – 5 – B	"	"	"	"	4	$(0.3-2)10^{-6}$	X				$Si + TiSi_2$	773	243,810	243,810	1.89×10^6	– 44.2	
$TiSi_2$ – 6 – B	"	"	"	"	$\frac{1}{6}$	$(1-10)10^{-6}$	X				$Si + TiSi_2$	780	134.5	134.5	1,050	– 5.76	SOURCE TEMPERATURE
$TiSi_2$ – 7 – B	"	"	"	"	$\frac{1}{20}$	1×10^{-6}	X				$Si + Ti_5Si_2$	365	429.2	429.2	1,570	– 7.36	RANGE FOR $TiSi_2$ – 6 THRU 12
$TiSi_2$ – 8 – B	"	"	"	"	$\frac{1}{20}$	$(1-10)10^{-6}$	X				$Si + Ti_5Si_2$	374	1,605.9	1,606	6,120	– 10.3	WAS 1500°C TO 1600°C.
Ti_5Si_2 – 9 – B	"	"	"	"	$\frac{1}{12}$	"	X						135.1	135.1	est. 1×10^3	– 5.85	
Ti_5Si_2 – 10 – B	"	"	"	"	$\frac{1}{12}$	"	X				$Si + Ti_5Si_2$		148.8	148.8	est. 1.7×10^3	– 7.5	

TABLE I (CONTINUED)

DETAILED FABRICATION DATA AND RESISTOR PARAMETERS

RESISTOR (SERIAL NO.)	SUBSTRATE (TYPE)	EVAPORATION PARAMETERS: SOURCE (TYPE)	EVAPORANT	SUB. T (°C)	DEP. PER. (MIN.)	P (TORR)	PROTECTION: NONE	SiO	BAKED PER. (HRS)	BAKED T (°C)	FILM PARAMETERS (1): COMPOSITION (2)	THICKNESS (Å)	RESISTANCE (OHMS)	RESISTIVITY R/SQ. (OHMS)	RESISTIVITY SPECIFIC (μΩ Cm.)	TCR (10^{-4}/°C)	REMARKS
TITANIUM SILICIDE (CONTINUED)																	
$TiSi_2$ – 11 – B	CORNING #7059	W BOAT	$TiSi_2$ – 200 + 325 MESH	300	1/2	$(1-10)\times10^{-6}$			7	300	$TiSi_2$		41.32	41.32		-3.61	
$TiSi_2$ – 12 – B	GLASS	"		"	1/2	"			7	300	$TiSi_2$		109.7	109.7		-5.13	
THULIUM																	
Tm – 1A – B	GLASS	Ta BOAT	Tm	400	10	5×10^{-6}	X						45.74	4.57		+13.8	Tm reacted with the
Tm – 1B – B	MICRO-	"	"	"	10	"	X						44.4	4.44		+11.8	Ta boat severely.
Tm – 1C – B	SCOPE	"	"	"	10	"	X						51.57	5.16		+13.1	
Tm – 1D – B	SLIDE	"	"	"	10	"	X						31.86	8.19		+12.2	
THULIUM EVAPORATED IN OXYGEN																	
Tm + O_2 – 2A – B	"	W BASKET	Tm	400	10	3×10^{-5}	X						249.7	25		+10.5	For Tm + O_2 SPECIMENS
Tm + O_2 – 2B – B	"	"	"	"	"	"	X						296.1	29.6		+8.9	ARGON + O_2 WAS BLED
Tm + O_2 – 5A – B	"	"	"	"	1	1×10^{-4}	X						318.2	31.8		+10.0	INTO BELL JAR TO
Tm + O_2 – 5B – B	"	"	"	"	1	"	X					743	316.2	31.6	235	+9.5	INCREASE THE PRESSURE
Tm + O_2 – 6A – B	"	"	"	"	1	$8.\times10^{-4}$	X						449.5	45		+6.7	FROM ≈ 2×10^{-6} TORR
Tm + O_2 – 6B – B	"	"	"	"	1	"	X						195	19.5		+8.5	TO INDICATED VALUE.
Tm + O_2 – 7A – B	"	"	"	"	5	5×10^{-5}	X						162	16.2		+10.5	THERE WAS ONLY A TRACE
Tm + O_2 – 7B – B	"	"	"	"	"	"	X						184.7	18.5		+11.2	OF OXYGEN IN THE
Tm + O_2 – 8A – B	"	"	"	"	15	$\approx1\times10^{-5}$	X						172.3	17.2		+10.5	ARGON AND LITTLE, IF
Tm + O_2 – 8B – B	"	"	"	"	"	"	X						219.0	21.9		+9.0	ANY, OXIDATION OF THE
																	Tm OCCURRED.
VANADIUM																	
V – 1A – A	"	STRANDED W	V WIRE	450	≈1	$\approx1\times10^{-6}$	X					742	13.2	13.2	96.3	+8.54	
V – 1B – A	"	"	"	"	≈1	"	X					920	9.81	9.81	90.2	+9.25	
V – 1C – A	"	"	"	"	≈1	"	X					925	11.0	11.0	102	+8.37	

TABLE I (CONTINUED)

DETAILED FABRICATION DATA AND RESISTOR PARAMETERS

RESISTOR (SERIAL NO.)	SUB-STRATE (TYPE)	EVAPORATION PARAMETERS: SOURCE (TYPE)	EVAP-ORANT	SUB. T (°C)	DEP. PER. (MIN.)	P (TORR)	PROTECTION: NONE	SiO	BAKED PER. (HRS)	BAKED T (°C)	COMPOSITION (2)	FILM PARAMETERS (1): THICKNESS (Å)	RESISTANCE (OHMS)	RESISTIVITY R/SQ. (OHMS)	RESISTIVITY SPECIFIC ($\mu\Omega$ Cm)	TCR (10^{-4}/°C)	REMARKS
						VANADIUM EVAPORATED IN OXYGEN (CONTINUED)											
V + O_2 - 3C - A	GLASS	STRANDED W	V WIRE	450	~1	1×10^{-4}	X					1080?	27.5	27.5	? 297	+14.5	LINE RESULTED IN
V + O_2 - 4A - A	MICRO-	"	"	"	~2	1×10^{-4} W/TESLA	X					333	24.4	24.4	81.3	+15.5	ADMISSION OF A MIXTURE
V + O_2 - 4C - A	SCOPE	"	"	"	~2	"	X					590	16.5	16.5	97.4	+13.7	OF ARGON AND O_2
V + O_2 - 1A - B	SLIDE	STRANDED Mo	"	400	3	$\sim 8 \times 10^{-6}$	X						31,090.	3,310		-19.2	IN SOME INSTANCES,
V + O_2 - 1B - B	"	"	"	"	"	"	X					156					
V + O_2 - 1C - B	"	"	"	"	"	"	X						445,400	44,540		-84	
V + O_2 - 1D - B	"	"	"	"	"	"	X						3.38×10^6	340,000		-236	
V + O_2 - 2A - B	"	"	"	"	1/15	"	X						30,600	3,060		- 9.9	
V + O_2 - 2B - B	"	"	"	"	"	"	X						73,600	6,940		-22.8	
V + O_2 - 2C - B	"	"	"	"	"	"	X						536,000	50,500		-39.8	
V + O_2 - 3A - B	"	"	"	"	5	3×10^{-5}	X					603	563.1	56.3	352	-1.2	
V + O_2 - 3B - B	"	"	"	"	"	"	X					509	504.5	53.6	273	+0.07	
V + O_2 - 3C - B	"	"	"	"	"	"	X					287	605.5	60.5	174	+0.44	
V + O_2 - 3D - B	"	"	"	"	"	"	X					237	1325	132.5	314	-1.66	
						VANADIUM EVAPORATED IN AIR											
V + AIR - 1A - A	"	STRANDED W	"	450	~2	5×10^{-5}	X					654	16.7	16.7	109	+5.85	SUPPOSEDLY AIR WAS
V + AIR - 1B - A	"	"	"	"	~2	"	X					718	16.95	16.9	122	+6.47	ADMITTED TO BELL JAR TO
V + AIR - 1C - A	"	"	"	"	~2	"	X					694	21.4	21.4	148	+6.95	INCREASE PRESSURE FROM
V + AIR - 2A - A	"	"	"	"	~2	1×10^{-4}	X					330		56.7	184	+3.8	APPROXIMATELY 2×10^{-6} TORR
V + AIR - 2B - A	"	"	"	"	~2	"	X					339		61.8	210	+3.02	TO INDICATED VALUE.
V + AIR - 2C - A	"	"	"	"	~2	"	X							76.4		+3.17	APPARENTLY, INCOMPLETE
V + AIR - 3A - A	"	"	"	150	5	5×10^{-4}	X							43.3	-	+6.84	FLUSHING OF THE BLEEDER
V + AIR - 3B - A	"	"	"	"	"	"	X					567		28.7	163	+9.23	LINE OF ARGON RESULTED
V + AIR - 3C - A	"	"	"	"	"	"	X					669		26.5	177	+10.4	IN ADMISSION OF AN ARGON - AIR MIXTURE

TABLE I (CONTINUED)

DETAILED FABRICATION DATA AND RESISTOR PARAMETERS

RESISTOR (SERIAL NO.)	SUB-STRATE (TYPE)	EVAPORATION PARAMETERS: SOURCE (TYPE)	EVAP-ORANT	SUB. T (°C)	DEP. PER. (MIN.)	P (TORR)	PROTECTION: NONE	SiO	BAKED PER. (HRS)	BAKED T (°C)	FILM PARAMETERS (1): COMPOSITION (2)	THICKNESS (Å)	RESISTANCE (OHMS)	RESISTIVITY: R/SQ. (OHMS)	RESISTIVITY: SPECIFIC (μΩ Cm.)	TCR (10⁻⁴/°C)	REMARKS
VANADIUM OXIDE																	
V_2O_5-1A-A	GLASS MICRO-SCOPE SLIDE	W-BOAT	V_2O_5	450	~2	(1-20)10⁻⁵	X						1572.	1572.		-47.2	
V_2O_5-2A-A	"	"	POWDER	"	"	"	X						687,000.	687,000.		-87.9	
V_2O_5-2B-A	"	"	"	"	"	"	X					4,290	500,000.	500,000.	2.15×10^{7}	-86.3	
V_2O_5-2C-A	"	"	"	"	"	"	X					3,705	766,000.	766,000.	2.84×10^{7}	-87.9	
ZIRCONIUM																	
Zr-1A-B	"	T1.015 W	Zr WIRE	450	8	2.5×10^{-6}	X					VERY THIN		266	--	-1.47	
Zr-1B-B	"	"	"	"	"	"	X					" "		336		-1.9	
Zr-1C-B	"	"	"	"	"	"	X					" "		564		-2.4	
Zr-1D-B	"	"	"	"	"	"	X					" "		905		-2.1	
Zr-2-B	"	"	"	"	"	5×10^{-6}	X					" "		$>10^{6}$	....	--	
Zr-3A-B	"	"	"	"	"	"	X					330		422	1,390	-2.69	
Zr-3B-B	"	"	"	"	"	"	X					VERY THIN		655	--	-2.99	
Zr-3C-B	"	"	"	"	"	"	X					" "		944	--	-2.32	
Zr-3D-B	"	"	"	"	"	"	X					" "		1,480		-2.73	
Zr-4A-B	"	"	"	360	5 min 5 periods	3×10^{-6}	X					975		827	8,060	-4.22	
Zr-4B-B	"	"	"	"	"	"	X					817		1,199	9,800	-3.11	
Zr-4C-B	"	"	"	"	"	"	X					588		1,629	9,580	-4.11	
Zr-4D-B	"	"	"	"	"	"	X					869		2,106	18,300	-4.32	
Zr-5A-B	"	"	"	450	5	4.2×10^{-6}	X					1,182		53.4	631	-1.12	
Zr-5B-B	"	"	"	"	"	"	X					1,050		61.9	655	-1.59	
Zr-5C-B	"	"	"	"	"	"	X					738		106	783	-2.42	
Zr-5D-B	"	"	"	"	"	"	X					Est 500		233	1165	-3.3	
Zr-6A-B	"	"	"	"	"	4.8×10^{-6}	X					1,125		15.6	174	+5.01	
Zr-6B-B	"	"	"	"	"	"	X					Est 1,050		22.9	240	+3.02	
Zr-6C-B	"	"	"	"	"	"	X					735		34.1	250	+1.45	
Zr-6D-B	"	"	"	"	"	"	X					587		61.5	355	-0.01	

TABLE I (CONTINUED)

DETAILED FABRICATION DATA AND RESISTOR PARAMETERS

RESISTOR (SERIAL NO.)	SUB-STRATE (TYPE)	EVAPORATION PARAMETERS: SOURCE (TYPE)	EVAP-ORANT	SUB. T (°C)	DEP. PER. (MIN.)	P (TORR)	PROTECTION: NONE	SiO	BAKED PER. (HRS)	BAKED T (°C)	FILM PARAMETERS (1): COMPOSITION (2)	THICKNESS (Å)	RESISTANCE (OHMS)	RESISTIVITY R/SQ. (OHMS)	RESISTIVITY SPECIFIC (μΩ Cm.)	TCR (10^{-4}/°C)	REMARKS
						ZIRCONIUM (CONTINUED)											
Zr - 7A - B	GLASS MICRO-SCOPE SLIDE	7/40 15 W	Zr WIRE	450	10	4.3×10^{-6}	X							23,300		-16	
Zr - 7B - B	"	"	"	"	"	"	X							19,700		-12.8	
Zr - 7C - B	"	"	"	"	"	"	X							—		—	
Zr - 7D - B	"	"	"	"	"	"	X							—		—	
Zr - 8A - B	"	"	"	"	"	1×10^{-5}	X					730		40	282	+0.11	
Zr - 8B - B	"	"	"	"	"	"	X					786		49	385	-0.23	
Zr - 8C - B	"	"	"	"	"	"	X					—		79.8	—	-1.07	
Zr - 8D - B	"	"	"	"	"	"	X					520		160	832	-1.62	
						ZIRCONIUM EVAPORATED IN OXYGEN											
$Zr+O_2$ - 1 - B	"	"	"	"	6	$>1 \times 10^{-3}$	X							$>10^6$			FOR $Zr+O_2$ SPECIMENS,
$Zr+O_2$ - 2 - B	"	"	"	"	5	"	X							$>10^6$			GAS WAS ADMITTED TO
$Zr+O_2$ - 3A - B	"	"	"	"	1/2	1×10^{-5}	X					621		131	815	-2.64	BELL JAR TO INCREASE
$Zr+O_2$ - 3B - B	"	"	"	"	"	"	X					BROKE		195	—	-2.67	PRESSURE FROM $\frac{1}{2} \times 10^{-5}$
$Zr+O_2$ - 3C - B	"	"	"	"	"	"	X					—		297	—	-2.32	TORR TO INDICATED
$Zr+O_2$ - 3D - B	"	"	"	"	"	"	X					BROKE		511	—	-2.61	VALUE. THE BLEEDER
$Zr+O_2$ - 4A - B	"	"	"	"	5	5.3×10^{-4}	X					936		15.5	145	+3.6	LINE WAS NOT PURGED
$Zr+O_2$ - 4B - B	"	"	"	"	"	"	X					917		21.9	201	+2.07	PROPERLY FOR $Zr+O_2$ - 1-B
$Zr+O_2$ - 4C - B	"	"	"	"	"	"	X					BROKE		34.5	—	+0.53	THRU $Zr+O_2$ -18-B AND
$Zr+O_2$ - 4D - B	"	"	"	"	"	"	X					366		62.1	226	-0.44	A MIXTURE OF A & O_2
$Zr+O_2$ - 5 - B	"	"	"	"	5	5.5×10^{-5}	X					—		>106	—		WAS ADMITTED, THIS
$Zr+O_2$ - 6 - B	"	"	"	"	"	"	X					—		>106	—		MIXTURE CONSISTED
$Zr+O_2$ - 7A - B	"	"	"	"	5	8×10^{-6}	X					BROKE		958	—	-0.75	PRIMARILY OF ARGON IN
$Zr+O_2$ - 7B - B	"	"	"	"	"	"	X					—		107	—	-0.43	MOST INSTANCES. A
$Zr+O_2$ - 7C - B	"	"	"	"	"	"	X					392		193	757	+0.23	RELATIVELY HIGH RESISTIVITY
$Zr+O_2$ - 7D - B	"	"	"	"	"	"	X					BROKE		332	—	-0.61	WITH NEGATIVE TCR VALUE
$Zr+O_2$ - 8A - B	"	"	"	"	4	2×10^{-5}	X					726		83.8	604	+0.01	INDICATES A PREDOMINANCE OF O_2.

TABLE I (CONTINUED)

DETAILED FABRICATION DATA AND RESISTOR PARAMETERS

RESISTOR (SERIAL NO.)	SUB-STRATE (TYPE)	EVAPORATION PARAMETERS: SOURCE (TYPE)	EVAP-ORANT	SUB. T (°C)	DEP. PER. (MIN.)	P (TORR)	PROTECTION: NONE	SiO	BAKED: PER. (HRS)	BAKED: T (°C)	FILM PARAMETERS(1): COMPOSITION (2)	THICKNESS (Å)	RESISTANCE (OHMS)	RESISTIVITY: R/SQ. (OHMS)	RESISTIVITY: SPECIFIC (μΩ Cm.)	TCR (10⁻⁴/°C)	REMARKS
				ZIRCONIUM EVAPORATED IN OXYGEN (CONTINUED)													
$Zr+O_2-8B-B$	GLASS MICRO-SCOPE SLIDE	7/015 W	Zr WIRE	450	4	2×10^{-5}	X					544		107	582	+0.56	
$Zr+O_2-8C-B$	〃	〃	〃	〃	〃	〃	X					498		160	796	+1.8	
$Zr+O_2-8D-B$	〃	〃	〃	〃	〃	〃	X					–		346	–	-0.9	
$Zr+O_2-9-B$	〃	〃	〃	〃	5	$>4\times10^{-5}$	X							$>10^6$			
$Zr+O_2-10A-B$	〃	〃	〃	〃	12	2×10^{-5}		X						72.1	–	-0.37	
$Zr+O_2-10B-B$	〃	〃	〃	〃	〃	〃		X						86.8	–	-0.65	
$Zr+O_2-10C-B$	〃	〃	〃	〃	〃	〃		X						123.6	–	-0.43	
$Zr+O_2-10D-B$	〃	〃	〃	〃	〃	〃		X						187.2	–	-0.25	
$Zr+O_2-11A-B$	〃	〃	〃	〃	4	3.5×10^{-5}		X				–		19.3	–	+3.63	
$Zr+O_2-11B-B$	〃	〃	〃	〃	〃	〃		X				–		28.3	–	+0.97	
$Zr+O_2-11C-B$	〃	〃	〃	〃	〃	〃		X				–		44.1	–	+2.20	
$Zr+O_2-11D-B$	〃	〃	〃	〃	〃	〃		X				–		87.0	–	+0.88	
$Zr+O_2-12A-B$	〃	〃	〃	〃	10	2×10^{-5}	X					498		20.8	104	+6.04	
$Zr+O_2-12B-B$	〃	〃	〃	〃	〃	〃	X					655		28.3	185	+2.90	
$Zr+O_2-12C-B$	〃	〃	〃	〃	〃	〃	X					514		44.5	229	+0.50	
$Zr+O_2-12D-B$	〃	〃	〃	〃	〃	〃	X					BROKE		74.4	–	-0.15	
$Zr+O_2-13A-B$	〃	〃	〃	〃	〃	9×10^{-5}	X					761		32.6	248	+1.18	
$Zr+O_2-13B-B$	〃	〃	〃	〃	〃	〃	X					Est 850		26.1	221	+1.36	
$Zr+O_2-13C-B$	〃	〃	〃	〃	〃	〃	X					745		444	331	+0.21	
$Zr+O_2-13D-B$	〃	〃	〃	〃	〃	〃	X					–		≈ 57		-0.09	
$Zr+O_2-14A-B$	〃	〃	〃	〃	5	1×10^{-5}	X					708		46.6	330	+0.36	
$Zr+O_2-14B-B$	〃	〃	〃	〃	〃	〃	X					676		58	382	-0.51	
$Zr+O_2-14C-B$	〃	〃	〃	〃	〃	〃	X					437		83	363	-0.84	
$Zr+O_2-14D-B$	〃	〃	〃	〃	〃	〃	X					430		154	662	-1.47	
$Zr+O_2-15A-B$	〃	〃	〃	〃	10	1×10^{-4}	X					1230		120	1,480	-0.725	
$Zr+O_2-15B-B$	〃	〃	〃	〃	〃	〃	X					–		142	–	-0.136	
$Zr+O_2-15C-B$	〃	〃	〃	〃	〃	〃	X					1050		230	2,420	-0.88	
$Zr+O_2-15D-B$	〃	〃	〃	〃	〃	〃	X					–		488	—	-2.72	

TABLE I (CONTINUED)

DETAILED FABRICATION DATA AND RESISTOR PARAMETERS

RESISTOR (SERIAL NO.)	SUB-STRATE (TYPE)	EVAPORATION PARAMETERS: SOURCE (TYPE)	EVAP-ORANT	SUB. T (°C)	DEP. PER. (MIN.)	P (TORR)	PROTECTION: NONE	SiO	BAKED PER. (HRS)	BAKED T (°C)	FILM PARAMETERS(1): COMPOSITION (2)	THICKNESS (Å)	RESISTANCE (OHMS)	RESISTIVITY R/SQ. (OHMS)	RESISTIVITY SPECIFIC (μΩ Cm.)	TCR (10^{-4}/°C)	REMARKS
				ZICONIUM EVAPORATED IN OXYGEN (CONTINUED)													
Zr+O2-16A-B	GLASS MICRO-SCOPE SLIDE	7/8015 W	Zr WIRE	450	5	5×10^{-5}	X					1,300		57.1	742	+0.71	
Zr+O2-16B-B	"	"	"	"	"	"	X					–		64.5	–	+1.81	
Zr+O2-16C-B	"	"	"	"	"	"	X					1,040		88.5	920	+1.02	
Zr+O2-16D-B	"	"	"	"	"	"	X					–		157	–	-0.30	
Zr+O2-17A-B	"	"	"	"	"	1×10^{-4}	X					908		22.1	201	+3.3	
Zr+O2-17B-B	"	"	"	"	"	"	X					–		28.1	–	+2.05	
Zr+O2-17C-B	"	"	"	"	"	"	X					723		43.5	314	+0.95	
Zr+O2-17D-B	"	"	"	"	"	"	X					–		76.2	–	-0.12	
Zr+O2-18A-B	"	"	"	"	"	"	X					1,280		7.72	98.8	+17.9	
Zr+O2-18B-B	"	"	"	"	"	"	X					–		9.63	–	+18	
Zr+O2-18C-B	"	"	"	"	"	"	X					954		15	143	+13	
Zr+O2-18D-B	"	"	"	"	"	"	X					–		27.3	–	+13.2	
Zr+O2-19-B	"	"	"	"	"	1×10^{-3}	X							$>0.7\times10^{6}$	(POWDERY FILM)		BEGINNING WITH Zr+O2-19-B,
Zr+O2-20A-B	"	"	"	"	"	"	X					1,320		4.5×10^{6}	5.84×10^{7}	-62	O2 WAS ADMITTED TO THE
Zr+O2-20B-B	"	"	"	"	"	"	X					–		–		–	BELL JAR TO INCREASE
Zr+O2-20C-B	"	"	"	"	"	"	X					–		–		–	THE PRESSURE FROM
Zr+O2-20D-B	"	"	"	"	"	"	X					–		–		–	≈ 2×10^{-6} TORR TO THE
Zr+O2-21A-B	"	"	"	50	10	1×10^{-5}	X					1,915		11.1	2.12	+7.7	INDICATED VALUE.
Zr+O2-21B-B	"	"	"	"	"	"	X					–		11.1	–	+8.11	
Zr+O2-21C-B	"	"	"	"	"	"	X					1,218		–	–	–	
Zr+O2-21D-B	"	"	"	"	"	"	X					–		43.3	–	+1.79	
Zr+O2-22A-B	"	"	"	"	5	5×10^{-5}	X					2,020		152	3.07×10^{3}	-4.9	
Zr+O2-22B-B	"	"	"	"	"	"	X					–		316	–	-6.68	
Zr+O2-22C-B	"	"	"	"	"	"	X					1,846		736	1.35×10^{4}	-7.4	
Zr+O2-22D-B	"	"	"	"	"	"	X					1,280		4,790	6.13×10^{4}	-16.7	
Zr+O2-23A-B	"	"	"	"	"	"	X					1,562		5,819	9.1×10^{4}	-13.5	
Zr+O2-23B-B	"	"	"	"	"	"	X					1,249		9,100	1.13×10^{5}	-15.3	
Zr+O2-23C-B	"	"	"	"	"	"	X					–		—	—	—	

TABLE I (CONTINUED)

DETAILED FABRICATION DATA AND RESISTOR PARAMETERS

RESISTOR (SERIAL NO.)	SUBSTRATE (TYPE)	EVAPORATION PARAMETERS: SOURCE (TYPE)	EVAPORANT	SUB. T (°C)	DEP. PER. (MIN.)	P (TORR)	PROTECTION: NONE	SiO	BAKED PER. (HRS)	BAKED T (°C)	FILM PARAMETERS (1): COMPOSITION (2)	THICKNESS (Å)	RESISTANCE (OHMS)	RESISTIVITY R/SQ. (OHMS)	RESISTIVITY SPECIFIC (μΩ Cm.)	TCR (10^{-4}/°C)	REMARKS
							VANADIUM (CONTINUED)										
V-1A-B	GLASS	STRANDED Mo	V WIRE	400	3	5×10^{-6}	X					VERY THIN	4,016	378		-1.82	
V-1B-B	MICRO-	"	"	"	3	"	X					"	4,651	465		-3.2	
V-1C-B	SCOPE	"	"	"	3	"	X					"	1,283	685		-5.7	
V-1D-B	SLIDE	"	"	"	3	"	X					"	9,050	850		-6.6	
V-2A-B	"	"	"	"	3	$(1-10)10^{-6}$	X					"	32,950	3,295		-9.4	
V-3B-B	"	"	"	"	1/15	3.5×10^{-6}	X					"	2,588	259		+0.91	
V-3C-B	"	"	"	"	1/15	"	X					"	4,276	428		-0.8	
V-4A-B	"	"	"	"	5	$\approx1\times10^{-5}$	X					640	326	34.6	222	+1.67	
V-4B-B	"	"	"	"	5	"	X					550	338	33.8	186	+1.98	
V-4C-B	"	"	"	"	5	"	X					388	446	44.6	173	+2.56	
V-4D-B	"	"	"	"	5	"	X					505	741	74.1	374	+2.29	
V-1	CORNING #7059	E-BEAM @ 1 KW	"	"	2	1×10^{-5}			10	325			84.6	42.3	≈ 225	+2.23	
V-2	GLASS		"	"	"	"	X						91.7	45.8	≈ 225	+1.63	
V-3	"	Cu	"	"	"	"	X					284	167.8	83.9	238	+2.38	
V-4	"	CRUCIBLE	"	"	"	"			10	325			84	42	≈ 225	+2.36	
V-5	"	"	"	"	"	"	X						87.7	43.8	≈ 225	+1.59	
V-6	"	"	"	"	"	"	X					455	95.2	47.6	216	+1.67	
							VANADIUM EVAPORATED IN OXYGEN										
$V+O_2$-1A-A	GLASS	STRANDED W	"	450	≈2	5×10^{-5}	X					Est. 500	22.6	26.6	≈ 110	+4.43	FOR THE V+O2 SPECIMENS,
$V+O_2$-1B-A	MICRO-	"	"	"	≈2	"	X					Est 500	18.5	18.5	≈ 93	+4.87	PURE O2 WAS SUPPOSEDLY
$V+O_2$-1C-A	SCOPE	"	"	"	≈2	"	X					Est 500	26.4	26.4	≈ 130	+3.78	ADMITTED TO THE BELL JAR
$V+O_2$-2A-A	SLIDE	"	"	"	≈2	8×10^{-5}	X					480	22.1	22.1	106	+10.4	TO INCREASE THE PRESSURE
$V+O_2$-2B-A	"	"	"	"	≈2	"	X					450	20.2	20.2	91	+10.3	FROM ≈ 2X10⁻⁶ TORR TO
$V+O_2$-2C-A	"	"	"	"	≈2	"	X					400	27.1	27.1	108	+9.9	THE INDICATED VALUE.
$V+O_2$-3A-A	"	"	"	"	≈2	1×10^{-4}	X						25.5	25.5		+10.4	HOWEVER, INCOMPLETE
$V+O_2$-3B-A	"	"	"	"	≈2	"	X						23.8	23.8		+13.3	FLUSHING OF BLEEDER

TABLE I (CONTINUED)

DETAILED FABRICATION DATA AND RESISTOR PARAMETERS

RESISTOR (SERIAL NO.)	SUBSTRATE (TYPE)	EVAPORATION PARAMETERS: SOURCE (TYPE)	EVAPORANT	SUB. T (°C)	DEP. PER. (MIN.)	P (TORR)	PROTECTION: NONE	SiO	BAKED PER. (HRS)	BAKED T (°C)	FILM PARAMETERS (1): COMPOSITION (2)	THICKNESS (Å)	RESISTANCE (OHMS)	RESISTIVITY R/SQ. (OHMS)	RESISTIVITY SPECIFIC (μΩ Cm.)	TCR (10^{-4}/°C)	REMARKS
ZIRCONIUM EVAPORATED IN OXYGEN (CONTINUED)																	
$Zr + O_2$ - 23D-B	GLASS MICRO-	7/015 W	Zr WIRE	50	5	5×10^{-5}	X					—	—	—	—	—	
$Zr + O_2$ - 24A-B	SCOPE SLIDE	"	"	"	"	"	X					—		325.5	—	- 0.02	
$Zr + O_2$ - 24B-B	"	"	"	"	"	"	X					3,185		43.8	1,400	-0.47	
$Zr + O_2$ - 24C-B	"	"	"	"	"	"	X					—		185.5	—	- 2.7	
$Zr + O_2$ - 24D-B	"	"	"	"	"	"	X					—		1,034	—	- 10.8	
$Zr + O_2$ - 25A-B	"	"	"	250	"	"	X					(Too DULL		148.3	—	- 3.4	
$Zr + O_2$ - 25B-B	"	"	"	"	"	"	X					TO MEAS)		206.1	—	- 4.6	
$Zr + O_2$ - 25C-B	"	"	"	"	"	"	X					"		228.2	—	- 5.02	
$Zr + O_2$ - 25D-B	"	"	"	"	"	"	X					"		623	—	-14.9	
$Zr + O_2$ - 26A-B	"	"	"	"	"	3×10^{-5}	X					"		51.8	—	- 0.23	
$Zr + O_2$ - 26B-B	"	"	"	"	"	"	X					"		44.9	—	- 0.55	
$Zr + O_2$ - 26C-B	"	"	"	"	"	"	X					"		52.6	—	- 1.12	
ZIRCONIUM OXIDE																	
ZrO_2 - 1 - A	"	W BOAT	(ZrO_2 POWDER)	25		4×10^{-5}	X					11,500	$>10^7$ 2,375	2,375	2.73×10^5	- 12.5	VERY DIFFICULT TO EVAPORATE FROM W-BOAT DUE TO HIGH TEMPERATURE REQUIRED. EVAPORATIONS MADE AT AND SLIGHTLY ABOVE MELTING POINT OF ZrO_2 (2700°C). TCR VALUES NEAR ZERO WERE OBTAINED AT HIGHEST SOURCE TEMPERATURES USED.
ZrO_2 - 2A - A	"	"	"	450		5×10^{-6}	X					15,700	740	740	1.16×10^5	- 5.81	
ZrO_2 - 2B - A	"	"	"	"		"	X					—	3.8×10^6	3.8×10^6	—	-69.3	
ZrO_2 - 2C - A	"	"	"	"		"	X					—	860	860	—	- 5.50	
ZrO_2 - 3A - A	"	"	"	"		2×10^{-5}	X					15,000	225.5	225	3.82×10^4	- 2.91	
ZrO_2 - 3B - A	"	"	"	"		"	X					16,670	426.9	427	0.712×10^5	- 6.21	
ZrO_2 - 3C - A	"	"	"	"		"	X										

Note: ZrO_2 obtained from National Lead Co as C.P. Grade.

Mfg. Analysis: ZrO_2 - 99.12%, BaO - 0.01%, SiO_2 - 0.35%, CaO - 0.10%, TiO_2 - 0.16%, MgO - 0.15%, Fe_2O_3 - 0.05%, CuO - 0.001%, Al_2O_3 - 0.04%, Na_2O - 0.01%, S - 0.04%

GA. TECH SPECTOGRAPHIC TEST SHOWED: Si - Medium - 1.0 - 0.1%; Mg - TRACE - 0.05 - 0.005%; Pb - TRACE - 0.005 - 0.0005%; Fe - WEAK - 0.05 - 0.005%; Ti - WEAK - 0.1 - 0.01%; Ca - TRACE - 0.002 - 0.0002%; Zr - VERY STRONG

TABLE II-A

EFFECTS OF POST-DEPOSITION BAKING IN AIR
ON RESISTANCE AND TCR VALUES

Specimen (Code No.)	Resistivity ($10^{-6}\Omega$-cm)	ΔR (%)	TCR Before Baking (10^{-4}/°C)	TCR After Baking (10^{-4}/°C)	Δ TCR (10^{-4}/°)	Remarks
			Specimens baked at 200°C for 6 3/4 hours			
Mn + SiO-24-C	3.4×10^3	+ 14	- .223	- .472	- .249	Specimens placed on extended aging at 125°C in air after post-deposition bake in air.
Mn + SiO-25-C	2×10^2	+ 14		+ .268		
Mn + SiO-26-C	4×10^2	+ 15	+ 1.56	+ 1.36	- .20	
Mn + SiO-30-C	1.5×10^3	+ 12	+ 0.469	+ 1.55	+ 1.08	
			Specimens baked at 250°C for 6 1/2 hours			
Mn + SiO-28-C	3×10^2	+ 47	+ 1.76	+ 1.45	- .31	
Mn + SiO-29-C	1.4×10^3	+ 70	+ .67	+ 1.02	+ .35	
Mn + SiO-31-C	3.3×10^3	+ 66	- .358	- 0.186	+ .172	
Cr + SiO-18-C	3.1×10^4	- .04	- 4.12	- 4.13	- .01	
Cr + SiO-20-C	3.5×10^4	- 1.2	- 4.6	- 4.38	+ .12	
Cr + SiO-22-C	1.4×10^4	- .12	- 1.42	- 1.49	- .07	
			Specimens Baked at 250°C for 10 1/2 hours			
Cr + SiO-35-C	3.1×10^4	+ 22	- 4.08	- 3.75	+ 0.33	
Cr + SiO-38-C	1.6×10^3	+ 20	- 1.86	- 1.15	+ 0.71	
Cr + SiO-41-C	$\approx 1 \times 10^3$	+ 0.3	+ 2.04	+ 2.12	+ 0.08	
Cr + SiO-44-C	$\approx 1 \times 10^2$	+ 0.0	+ 2.81	+ 2.59	- 0.32	

(Continued)

TABLE II-A (Continued)

EFFECTS OF POST-DEPOSITION BAKING IN AIR
ON RESISTANCE AND TCR VALUES

Specimen (Code No.)	Resistivity ($10^{-6}\Omega$-cm)	ΔR (%)	TCR Before Baking (10^{-4}/°C)	TCR After Baking (10^{-4}/°C)	Δ TCR (10^{-4}/°C)	Remarks
			Specimens baked at 275°C for 16 hours			
Cr + SiO-23-C	2.2×10^6	- 0.8	- 27.6	- 27.8	- 0.2	
Cr + SiO-27-C	2.3×10^6	- 0.7	- 27.8	- 28.2	- 0.4	
Cr + SiO-30-C	1.8×10^6	+ 7.5	- 26.4	- 25.7	+ 0.7	
Cr + SiO-33-C	1.6×10^6	+ 13	- 25.3	- 38.8	- 13.5	
			Specimens baked at 300°C for 3 hours			
NbB_2-3	0.9×10^6	+ 82	- 49.9			
NbB_2-8	0.8×10^5	+170	- 32.6			
			Specimens baked at 300°C for 4 1/2 hours			
$CrSi_2$ + B_4Si-1	0.94×10^5	+ 0.71	- 25.2			
$CrSi_2$ + $TiSi_2$-6	1.2×10^3	+ 8.1	- 1.68			
$CrSi_2$ + $TiSi_2$-8	0.8×10^3	- 2.29	- 3.1			
			Specimens baked at 300°C for 5 hours			
$CrSi_2$-4	0.5×10^3	+ 4.2	+ 0.588			
$CrSi_2$-5	3.5×10^2	- 0.47	+ 1.25			
$CrSi_2$-6	1.5×10^3	+ 15	- 4.22			

(Continued)

TABLE II-A (Concluded)

EFFECTS OF POST-DEPOSITION BAKING IN AIR
ON RESISTANCE AND TCR VALUES

Specimen (Code No.)	Resistivity ($10^{-6}\Omega$-cm)	ΔR (%)	TCR Before Baking (10^{-4}/°C)	TCR After Baking (10^{-4}/°C)	Δ TCR (10^{-4}/°C)	Remarks
			Specimens baked at 300°C for 7 hours			
$TiSi_2$-11	2.6×10^3	+ 27	- 3.61			
$TiSi_2$-12	5×10^3	+ 29	- 5.13			
			Specimens baked at 325°C for 7 hours			
Cr + SiO-37-C	1.6×10^4	+ 25	- 1.73	- 0.92	+ 0.81	
Cr + SiO-40-C	3.3×10^4	+ 41	- 4.36	- 3.55	+ 0.81	
Cr + SiO-43-C	$\approx 1 \times 10^2$	0.0	+ 2.83	+ 2.83	0.00	
Cr + SiO-46-C	$\approx 0.9 \times 10^2$	+ 0.04	+ 2.16	+ 2.35	+ 0.19	
			Specimens baked at 325°C for 10 hours			
V-1	R/ = 42.3Ω	9,720.	+ 2.23	- 93.	- 95.	
V-4	R/ = 42 Ω	698.	+ 2.36	- 43.2	- 46.	

TABLE III

SUMMARY OF RESISTOR AGING AT 125 °C IN AIR

SPECIFIC RESISTIVITY (microhm-cm)	RESISTOR SERIES	DURING INITIAL TCR MEAS. ΔR [%] No.	Lo	Avg	Hi	AFTER 1000 HOURS ΔR [%] No.	Lo	Avg	Hi	ΔTCR [PPM/°C] Lo	Avg	Hi	REMARKS
				UNPROTECTED FILMS									ΔR OF 1000 HRS AGING INCLUDES ΔR OF INIT TCR MEAS. FOR UNPROTECTED FILMS
$(.2<1\leq 5)10^2$	$Al+SiO$	8	0.14	0.30	0.72								± ΔR
	Cr (FLASHED)	9	0	0.21	0.35								+ ΔR
	$Cr+SiO$ (FLASHED)	3	0.4	0.5	0.6								+ ΔR
	$Cr+SiO$	4	0	0.18	0.6								− ΔR
	$CrSi_2$	7	0	0.14	0.2	1		0.6	(NEG)				± ΔR
	$Cu+SiO$	7	0.35	21	130								MOSTLY + ΔR
	Gd	4	2.6	3.7	6.6		OXIDIZED COMPLETELY AFTER						+ ΔR
	$Gd+O_2$	2	1.1	1.2	1.3		FEW DAYS IN ROOM ATM.						+ ΔR
	$Mn+SiO$	2	0.14	0.37	0.6								± ΔR
	Ni_2B	2	0.06	0.17	0.29								+ ΔR
	$Ti+O_2$	6	0.1	0.7	1.4								+ ΔR
	TiN	1		0.9									+ ΔR
	$Tm, Tm+O_2$	14	0.06	0.5	1.6								+ ΔR
	V	13	0.5	2.4	31								+ ΔR
	$V+O_2) V+AIR$	22	0	1.4	4.3								+ ΔR
	Zr	6	0.02	0.14	0.4	6	2.1	5.2	10 (ONLY 7 HRS. AGING)				+ ΔR
	$Zr+O_2$	17	0	0.54	2.5	6	0.32	1.5	2.5 (ONLY 4 HRS. AGING)				+ ΔR
$(.5<1\leq 5)10^3$	$Cr+SiO$	5	0	0.22	0.85	2	0.23	0.32	0.42	4	13	22	MOSTLY + ΔR
	$CrSi_2$	5	0	0.24	0.57	1		1.9	(NEG)				MOSTLY NEG. ΔR
	$CrSi_2+TiSi_2$	7	0.11	0.21	0.32	1		0.15	(NEG)				+ ΔR
	$Cu+SiO$	3	7.7	27	49								+ ΔR
	$Gd+O_2$	2	0	0.65	1.3	OXIDIZED COMPLETELY AFTER FEW DAYS IN ROOM ATM. + ΔR							
	$Mn+SiO$	14	0.04	0.89	2.3	5	4.8	26	49	26	22	38	+ ΔR
	NbN	2	55	57	60								+ ΔR
	$Ti+O_2$	3	2.9	8.9	18								+ ΔR
	TiO	14	0	4.8	26								± ΔR
	TiO_2	6	0.36	3.2	8.8								+ ΔR
	TiN	7	0.3	4.1	6.6								+ ΔR
	$TiSi_2$	7	0.09	1.5	2.1	2	1.7	1.7	1.7				+ ΔR
	Zr	6	0.6	1.8	3.4	5	6.9	16	34	(ONLY 7 HOURS AGING)			+ ΔR
	$Zr+O_2$	11	0.6	3.1	9	4	5.8	17	38	(" " " ")			+ ΔR
$(.5<1\leq 5)10^4$	$Al+SiO$	2	0.13	0.18	0.24								± ΔR
	$Cr+SiO$	11	0.08	3.7	9.3	2	1.4	9.7	18.1	16	23	31	+ ΔR, − ΔTCR
	$Cu+SiO$	4	0.38	4.6	11								± ΔR
	$Mn+SiO$	1		.77									+ ΔR
	NbN	1		44									+ ΔR
	$Ti+O_2$	6	0.26	1.2	2.5								± ΔR
	TiO_2	1		7.1									+ ΔR
	TiB_2	3	5.5	11	19		(FILM WERE RETICULATED)						+ ΔR
	$TiSi_2$	2	1.7	11	20								+ ΔR
	Zr	4	1.7	2.9	4.7	4	32	68	108 (ONLY 5 HRS. AGING)				+ ΔR
	$Zr+O_2$	1		10.3									+ ΔR
	ZrO_2	2	2.3	2.4	2.5								+ ΔR
$(.5<1\leq 5)10^5$	$Cr+SiO$	5	0.11	2.8	11	2	1.1	14	27	23	24	25	+ ΔR, ± ΔTCR
	$CrSi_2+B_4Si$	3	0.5	0.57	0.61	1		0.8					+ ΔR
	$Cu+SiO$	2	12	19	25								+ ΔR
		1		3.1×10^4									+ ΔR
	$Mn+SiO$	3	023	4.5	11	2	18	27	37	138	178	218	+ ΔR, − ΔTC
	NbB_2	5	0	0.29	0.93	2	4	4	4	(+ ΔR FOR 1000 HRS)			− ΔR DURING TCR MEAS.
	Ta_2O_5	3	0.53	1.1	1.7								+ ΔR
	$Ti+O_2$	4	0.1	3.0	7.1								+ ΔR
	TiO_2	1		1.6									+ ΔR
	$Zr+O_2$	3	12	23	39								+ ΔR
$(.5<1\leq 5)10^6$	$Cr+SiO$	13	0	2.3	12.9	3	1.4	8.8	15	14	45	81	± ΔR DURING TCR MEAS, + ΔR DURING 1000 HRS AGING ± ΔTCR
	$Cu+SiO$	1		16									+ ΔR
	$Mn+SiO$	1		6.9				4.7			150		+ ΔR, + ΔTCR, PROBABLY THIN SiO OVERCOAT
	NbB_2	8	0	0.53	2.2	1		9	(+ ΔR FOR 1000 HRS AGING)				± ΔR DURING TCR MEAS.
	Ti_2C	1		13									+ ΔR
	$TiSi_2$	2	3.8	6.5	9.1								+ ΔR

(Continued)

TABLE III (Continued)

SUMMARY OF RESISTOR AGING AT 125 °C IN AIR

SPECIFIC RESISTIVITY (microhm-cm)	RESISTOR SERIES	DURING INITIAL TCR MEAS.				AFTER 1000 HOURS							REMARKS
			ΔR ‖%‖				ΔR ‖%‖			Δ TCR ‖PPM/°C‖			
		No.	Lo	Avg	Hi	No.	Lo	Avg	Hi	Lo	Avg	Hi	
			UNPROTECTED FILMS (CONTINUED)										ΔR OF 1000 HOURS AGING INCLUDES ΔR OF INIT. TCR MEAS. FOR UNPROTECTED FILMS.
$(.5<1\leq 5)10^7$	Al + SiO	2	1.1	1.7	2.3								$-\Delta R$
	Cu + SiO	1		34									$+\Delta R$
	Mn + SiO	1		4.6									$+\Delta R$
	Ta_2O_5	1		0.16									$+\Delta R$
	$TiSi_2$	2	5.2	5.7	6.1								$+\Delta R$
	$Zr + O_2$	1		230									$+\Delta R$
			FILMS BAKED IN AIR AT 200 °C										
$(.2<1\leq 5)10^2$	Mn + SiO					1		4.7			13		$+\Delta R$, $+\Delta TCR$
$(.5<1\leq 5)10^3$	Mn + SiO					3	3.3	4.3	5.5	2	8.2	18	$+\Delta R$, $+\Delta TCR$
			FILMS BAKED IN AIR AT 250 °C										
$(.2<1\leq 5)10^2$	Cr + SiO					1		0.05			22		$+\Delta R$, $+\Delta TCR$
	Mn + SiO					1		8.25			2		$+\Delta R$, $+\Delta TCR$
$(.5<1\leq 5)10^3$	Cr + SiO					1		0			4		$-\Delta TCR$
	Mn + SiO					2	2.1	2.2	2.4	7	7	7.3	$+\Delta R$, $-\Delta TCR$
$(.5<1\leq 5)10^4$	Cr + SiO					5	.0	0.18	0.3	4	17	35	$+\Delta R$, $\pm\Delta TCR$
			FILMS BAKED IN AIR AT 300 ± 25 °C										
$(.2<1\leq 5)10^2$	Cr + SiO					1		0			11		$+\Delta TCR$
	$CrSi_2$					1		0.15					$+\Delta R$
	V					2	3.2	32	60	20	47	74	$+\Delta R$, $\pm\Delta TCR$
$(.5<1\leq 5)10^3$	Cr + SiO					1		0			37		$+\Delta TCR$
	$CrSi_2$					2	0.2	0.36	0.55				$+\Delta R$
	$CrSi_2 + TiSi_2$					2	0.17	0.24	0.32				$-\Delta R$
	$TiSi_2$					2	0.3	0.35	0.4				$\pm\Delta R$
$(.5<1\leq 5)10^4$	Cr + SiO					2	0.08	0.14	0.2	0.8	4.9	9	$+\Delta R$, $\pm\Delta TCR$
$(.5<1\leq 5)10^5$	$CrSi_2 + B_4Si$					1		0.9					$+\Delta R$
	NbB_2					1		8					$+\Delta R$
$(.5<1\leq 5)10^6$	Cr + SiO					4	0.2	0.55	0.9	20	53	94	$\pm\Delta R$, $+\Delta TCR$
	NbB_2					1		7					$+\Delta R$
			FILMS OVERCOATED WITH SiO										
$(.2<1\leq 5)10^2$	Mn + SiO					2	0.1	0.4	0.7	5	20	39	$+\Delta R$, $-\Delta TCR$
$(.5<1\leq 5)10^3$	Mn + SiO					3	0.2	0.9	2.2	1	9	19	$+\Delta R$, $-\Delta TCR$
$(.5<1\leq 5)10^5$	Mn + SiO					1		36			86		$+\Delta R$, $-\Delta TCR$
$(.5<1\leq 5)10^6$	Cr + SiO					4	4.7	5.6	7.4	0	48	70	$+\Delta R$, $+\Delta TCR$
	Mn + SiO					1		29			430		$+\Delta R$, $+\Delta TCR$
$(.5<1\leq 5)10^7$	Mn + SiO					1		5			5		$+\Delta R$ $+\Delta TCR$
													FOR FILMS BAKED IN AIR AND OVERCOATED WITH SiO, THE ΔR & ΔTCR OF 1000 HRS. AGING ARE CHANGES IN R AND TCR AFTER THE PROTECTIVE MEASURES WERE TAKEN.

TABLE V

SUMMARIZED PARAMETERS OF RESISTIVE FILMS

MATERIAL EVAPORATED	NO. SPECIMENS	EVAPORATION TECHNIQUE	THICKNESS RANGE (Angstroms)	SPECIFIC RESISTANCE RANGE (microhm-cm)	TCR RANGE (10^{-4}/°C)	MAXIMUM SPECIFIC RESISTIVITY	
						WITHIN ± 500 PPM OF ZERO T.C.R. (microhm-cm)	WITHIN ± 300 PPM OF ZERO T.C.R. (microhm-cm)
Al + SiO	16	DUAL SOURCE EVAPORATION -- Al and SiO co-evaporated in high vacuum from independently heated BN crucibles.	500 to 6,000	40 to 4 X 10^7	-65 to + 10	2,000 at -500ppm	1,300 at -300ppm (600 at ZERO TCR)
Cu + SiO	25	DUAL SOURCE EVAPORATION -- Cu and SiO co-evaporated in high vacuun from independently heated W boats.	470 to 3,700	50 to 2 X 10^5	-99 to + 11		
	14	DUAL SOURCE EVAPORATION -- Cu and SiO co-evaporated in high vacuum from independently heated BN crucibles.	500 to 5,000	18 to 2 X 10^7	-36 to +6.1 (NOTHING OBTAINED BETWEEN -15 AND +4)	2 X 10^5 at + 400 ppm (OBTAINED LARGE VARIATION IN VALUES BETWEEN +300ppm & +1200ppm)	45 at +300ppm
Cr	12	Flash evaporated Cr powder from W boat in high vacuum.		R/Sq. = 1.3 to 15 ohms	+2.8 to + 14		
Cr + SiO	6	Flash evaporated Cr and SiO powders from W boat in high vacuum (approx. 1:1 volume mixture).	Approx. 850	Approx. 400	-1.5 to - 0.2		
Cr + SiO	45	COMMON SOURCE EVAPORATION: Cr and SiO co-evaporated from common source in high vacuum.	800 to 3,550 (Range for 17 specimens meas measured to determine specific resistivity vs. TCR)	100 to 1.2 X10^7	- 38 to + 2.8	4 X 10^4 at -500 ppm	2.3 X 10^4 at -300ppm (≈1 X10^5 at ZERO)
Cr + SiO	280 (for study of film uniformity over 2"X2" substrate area)	DUAL SOURCE EVAPORATION --Simultaneously evaporated Cr from 2 W-boats and SiO from graphite cloth source.	<500 to 5,000	100 to 2 X 10^8	-42 to + 6		
$CrSi_2$	9	$CrSi_2$ powder sublimated at temperatures near and slightly below its melting point from W boats.	300 to 2,000	240 to 2700	-7.4 to + 2.3	1,800 at -500ppm	1,200 at -300ppm (500 at ZERO)
	2	Evaporated with electron beam from $CrSi_2$ melt in Cu Crucible.	1320 ± 50	408 ± 10	+ 0.35 ± 0.05		
$CrSi_2$ +B_4Si	3	Evaporated with electron beam a powder mixture of mass ratio 2:1, $CrSi_2$:B_4Si from Cu crucible.	Approx. 6,600	Approx. 93,600	-25 ± 0.3		
	3	Electron beam on $CrSi_2$ melt on a bed of B_4Si powder in a Cu Cru.	Approx. 2,800	650 to 1,250	-0.63 to + 1.4		
$CrSi_2$ + $TiSi_2$	7	Electron beam evaporated 1:1 mass mixture of $CrSi_2$ and $TiSi_2$ powders from Cu crucible.	550 to 1,400	777 to 3,640	-4.4 to -1.06	3,640 at -440ppm (VARIES WITH TEMPERATURE OF EVAPORANT MIXTURE DURING FILM DEPOSITION.)	≈1,000 at -300ppm
Gd	4	Evaporated Gd turnings from Tantalum boat.	2,000 to 6,000	168 to 332	+5.03 to +7.6		
Gd + O_2	8	Evaporated Gd turnings from Tantalum boat in partial pressures of oxygen.	577 to 1,370	214 to 616	+3.9 to +6.2	≈ 300 at +500ppm	
Mn	4	Evaporated Mn (96%, carbon free) from tantalum grain box source.	Approx 700	74 to 210	-0.33 to +1.5		
Mn + SiO	30	COMMON SOURCE EVAPORATION: Mn and SiO co-evaporated from common grain box source (Ta) in high vac.	330 to 3,700	300 to 1.3 X 10^7	-33 to + 1.8	2.4 X 10^4 at - 500ppm	1.4 X 10^4 at -300ppm (3 X10^3 at ZERO)
NbB_2	15	Evaporated NbB_2 powder from Cu crucible with electron beam gun in high vacuum.	1,500 to 3,500	1 X 10^5 to 1 .1 X 10^6	-54 to -33		
NbN	3	Evaporated NbN powder from Ta boat in high vacuum.	300 to 520	2,900 to 6,600	-5.7 to -3.6	≈ 5 X 10^3 at - 500 ppm	

(Continued)

TABLE V (CONTINUED)

SUMMARIZED PARAMETERS OF RESISTIVE FILMS

MATERIAL EVAPORATED	NO. SPECIMENS	EVAPORATION TECHNIQUE	THICKNESS RANGE (Angstroms)	SPECIFIC RESISTANCE RANGE (microhm-cm)	TCR RANGE (10^{-4}/°C)	MAXIMUM SPECIFIC RESISTIVITY WITHIN ± 500 PPM OF ZERO T.C.R. (microhm-cm)	MAXIMUM SPECIFIC RESISTIVITY WITHIN ± 300 PPM OF ZERO T.C.R. (microhm-cm)
Ni_2B	3	Evaporated Ni_2B from W basket in high vacuum.	< 100 to 400	42 to < 3,000	-2.1 to +16.5		< 3,000 at -210ppm
Ta_2O_5	4	Evaporated Ta_2O_5 powder from Ta boat in high vacuum.	Approx. 650	Approx. 3.5×10^7	-80 to -71		
	4	Evaporated Ta_2O_5 powder from W boat in high vacuum.	Approx. 900	Approx. 4.9×10^5	-55 to - 49		
Ti	1	Evaporated Ti from stranded W fila.		R/Sq. = 13 ohms	+ 21		
Ti + O_2	21	Evaporated Ti from stranded W fila. in partial pressure of oxygen.	240 to 1230	200 to 279,000	-58 to +21	500 at -500ppm	400 at -300 ppm (250 at ZERO)
TiC	8	Evaporated TiC from W boat in high vacuum.	100 to 1,100	1,370 to 4,000	-14.9 to -3.5	≈2,000 at -500ppm	≈1,000 at -300ppm
	6	Evaporated TiC from Ta boat in high vacuum.	600 to 1300	687 to 943	-5.4 to -4.1	≈ 750 at -500ppm	≈ 500 at -300ppm
TiO_2	6	Evaporated TiC_2 from Ta boat in high vacuum.	Approx. 1,000	850 ± 100	-10 to -7		
	1	Evaporated TiO_2 from Mo boat in High vacuum (boat attacked severely).	< 100	< 1.05×10^4	-33.8		
	2	Evaporated TiO_2 from W boat in high vacuum	484 555	4.48×10^5 6.57×10^5	-64 -61		
TiB_2	5	Evaporated TiB_2 powder with electron beam gun from Cu crucible in high vacuum.	Est. 1,500 (films reticulated)	Est. > 1×10^4	-4.3 to -1.7		
TiN	9	Evaporated Titanium Nitride powder from W boat in high vac.	350 to 770	340 to 2,670	-7.4 to -0.3	1,000 at -500ppm	600 at -300ppm (350 at Zero TCR)
$TiSi_2$	12	Evaporated $TiSi_2$ powder from W boat in high vacuum	250 to 1,060	1,000 to 3.1×10^7	-65 to -4	1,000 at -500ppm	≈ 400 at -300ppm
Tm	4	Evaporated Tm from Ta boat in high vacuum.		R/Sq. = 4.4 to 8.2 ohms	+11.8 to +13.8		
Tm + O_2	10	Evaporated Tm from W basket in partial pressure of oxygen (Argon - O_2 Mix., mostly Argon).	743 (one)	235 R/Sq. = 16 to 32 ohms	+9.5 +8.5 to +11		
V	3	Evaporated V from stranded W. in high vacuum.	740 to 925	90.2 to 102	+8.6 to +9.3		
	11	Evaporated V from stranded Mo. in high vacuum.	388 to 640 (four) very thin (Five)	173 to 374 R/Sq.= 259 to 3,295 ohms	+1.7 to +2.6 -9.4 to +0.9		
	6	Evaporated V with electron beam gun from Cu crucible in high vac.	≈250 to 455	216 to 238	+1.6 to +2.4		
V + O_2	11	Evaporated V from stranded W fila. in partial pressures of Argon - oxygen mixture.	330 to 500 (Nine) (Two)	81 to 297 R/Sq=23.8 &25.5 ohms.	+3.8 to +15.5 +10.4 & +13.3		(270 at ZERO) 352 at -170
	11	Evaporated V from stranded Mo fila. in partial pressure of Argon- O_2.	237 to 603 (four) very thin (Seven)	174 to 352 R/Sq=3,060 to 340K ohms	-1.7 to +0.44 -236 to -10		
V + Air	9	Evaporated V from stranded W fila. in partial pressure of Argon-air.	330 to 718 (Seven)	109 to 210	+3 to +10.4		
V_2O_5	4	Evaporated V_2O_5 powder from W boat in high vacuum.	(One) Approx. 4,000 (Two)	R/Sq=1,572 ohms Approx. 2.5×10^7	-47.2 - 87		
Zr	29	Evaporated Zr from stranded W fila. in high vacuum	330 to 1,182(16) (Eleven)	174 to 18,3000 R/Sq=226 to 23,300 ohms	-5.1 to +5 -16 to -1.47		
Zr + O_2	85	Evaporated Zr from stranded W fila in partial pressure of Argon - O_2.	366 to 3,185 (34) (Forty-eight)	99 to 5.8×10^7 R/Sq=9.6 to 1,034 ohms	-62 to +18 -16 to +18	8,500 at -500ppm	3,500 at -300ppm (500 ± 300 at Zero @ 100 ppm)
ZrC_2	7	Evaporated ZrC_2 from W boat in high vacuum.	11,500 to 16,640 (Four) (Two)	3.82×10^4 to 2.73×10^5 R/Sq=660 and 3.8×10^6	-12.5 to -2.9 -5.5 -69.3	6.5×10^4 at -500ppm	3.8×10^4 at -300ppm (Est. 1×10^4 at Zero)
TOTAL	= 758						